Post-stroke rehabilitation of hand function based on Electromyography biofeedback

Doctoral Dissertation
Doctoral Program in Electronic Engineering (30th Cycle)

Post-stroke rehabilitation of hand function based on Electromyography biofeedback

By

Michela Di Girolamo

Supervisor (s):
Prof. C. F. Pirri
Prof. M. G. Ajmone
Dr. P. Ariano

Doctoral Examination Committee:
Dr. A. Turolla, Referee, Fondazione Ospedale San Camillo IRCCS, Venezia
Dr. J. H. Villafañe, Referee, IRCCS Fondazione Don Gnocchi, Milano

Politecnico di Torino

2018

Declaration

I hereby declare that, the contents and organization of this dissertation constitute my own original work and does not compromise in any way the rights of third parties, including those relating to the security of personal data.

Michela Di Girolamo

2018

* This dissertation is presented in partial fulfillment of the requirements for **Ph.D. degree** in the Graduate School of Politecnico di Torino (ScuDo).

Acknowledgments

This research has been developed in the Artificial Physiology (AP) Lab, at the Italian Institute of Technology (IIT- Center for sustainable Future Technologies CSFT@Polito). First of all, I would like to express my gratitude to Prof. Fabrizio Pirri for having given the opportunity to work on this interesting subject. Moreover, I would like to address my sincere thanks to my advisor Paolo Ariano for the constant help and support. All the members of the AP Lab have been a valuable source of collaboration and confrontation and I would to thank all of them: Alain Favetto, Marco Paleari, Nicolò Celadon, Andrea Lince, Alessandro Battezzato and Silvia Appendino.

A special thank goes to my family.

Their courage inspires me every day.

Abstract

The aim of my thesis work is the application and validation of an electromyographic biofeedback (EMG-BF) system in post-stroke rehabilitation setting. The absolute number of strokes is expected to dramatically increase in coming years, thus suggesting a need for strategies to improve post-stroke assistance and rehabilitation. The electromyogram (EMG) signal has shown good perspectives in the analysis of movements and motor impairment and the introduction of closed loop rehabilitation strategies revealed an increase of patient self-consciousness and motivation. Results are promising but a lack in the optimization of the devices for the application in the clinical context has been revealed. The device and the related software employed in the present research have been specifically conceived with this purpose. The device has been optimized during a clinical pilot study and then, a complete clinical trial has been started to investigate the characteristics of post stroke patients eligible for a rehabilitation therapy with the device, and the short-term clinical effect of the therapy on the recovery of the hand functionality. A statistical analysis has been performed on the dataset collected for 3 months. The data analysis included both clinical data and data collected from patients with the device during the execution of the experimental protocol. The preliminary results of the data analysis have confirmed the suitability of the system for its intended use and highlighted that the patient ability of controlling the EMG-BF based device is related to the degree of impairment with minimum p-value<0.001, depending on the patient clinical picture and on the exercise performed. Moreover, according preliminary results observed on four patients that received a 15 hours therapy for 3 weeks, the improvement of the parameters related to the hand and fingers motor function, suggests the efficacy of the therapy. Finally, aspects related to the analysis of continuous motions of the wrist performed during the therapy have been investigated and the relevance of the temporal information in the interpretation of this type of movements has been revealed ($p<<0.01$).

Contents

List of Figures

List of Tables

Summary

The motor control of voluntary movements is a complex mechanism that primarily involves the areas of the primary motor cortex with function of planning and initiation of the movement. The control signal is then integrated with somatosensory and visual feedback and reaches muscles fiber through the axons that exit the spinal cord and progressively traverse smaller branches of peripheral nerves. These circuits are the base of an independent and high-quality life for human beings and can be damaged as a result of neuromuscular injuries or diseases, such as stroke. The absolute number of strokes is expected to dramatically increase in coming years, therefore the restoration of limb functions is becoming a goal that needs enhanced and optimized strategies. In this scenario, technology solutions have good perspectives since they allow the decrease of the time a therapist needs to consume with each single patient and can guarantee high quality therapy also after the discharge of the patient from the hospital. Moreover, the introduction of new parameters to evaluate and monitor the degree of motor impairment is advisable. It is well known that the electromyogram (EMG) signal contains a large amount of information related to limb movements and functionality, so it can be usefully applied for this purpose. The present research is devoted to the application of an electromyographic biofeedback (EMG-BF) system in the post-stroke rehabilitation context. The device and the related Graphical User Interface (GUI) have been specifically conceived and optimized, following development criteria requested from new emerging needs of the clinical context. Moreover, a study about the analysis of the EMG signal of continuous movements performed during hand and wrist rehabilitation protocols has been performed with the aim of identifying the relevance of the temporal information in the interpretation of the movements.

The first chapter summarizes muscle physiology concepts and provides an overview of motor control mechanisms from the initialization of voluntary actions to muscle contraction. Moreover, the basic concepts of the recording and processing of the surface EMG are shown.

The second chapter presents the effects of stroke and the role of technology applications in rehabilitation therapies. Moreover, the use of EMG biofeedback in hemiplegic patients is analyzed.

The third chapter presents the main concepts about medical devices and clinical trials performed on patients in order to assess security and efficacy.

The fourth chapter presents the hypothesis and the aims of the thesis.

The fifth chapter is focused on the criteria that the EMG-BF system employed in the present thesis aims to meet and describes the definition process of the clinical trial that has been planned to validate the device. The chapter also presents quantitative results of the analysis performed on the dataset collected during the clinical trial, available at the time of writing.

The sixth chapter presents the study focused on continuous movements of the hand and wrist that has been performed in order to optimize the analysis of motor patterns during rehabilitation activities.

Finally, in the seventh chapter, the conclusions of the thesis are described.

1 Muscle physiology

The present chapter summarizes muscle physiology concepts which are relevant to understand the generation of the electromyographic signal. Moreover, an overview of motor control mechanisms has been presented from the initialization of voluntary actions by the cortical premotor areas to muscle contraction. Finally, the basic concepts regarding the recording and processing of the surface EMG have been shown.

1.1 Structure and organization of muscle

The structural unit of the skeletal muscle is the muscle fiber (muscles cell), with a range in thickness from approximately 10 to 100 μm and in length from 1 to 30 cm [1]. Sets of myofilaments (*myofibrils*) that compose fibers are surrounded by an excitable cell membrane of about 7.5 nm of thickness which is known as *sarcolemma*. The fluid enclosed within the fiber by the sarcolemma is named *sarcoplasm*, it contains fuel sources, organelles, enzymes and an extensive system functionally linked to the sarcolemma surface which contribute to the conduction of signals from the nervous system (*sarcoplasmatic reticulum, lateral sacs and traverse (T) tubules*) [2].

Myofibrils consist of longitudinally repeated cylindrical units, called *sarcomeres*. The sarcomere is the basic contractile unit of muscle, it contains proteins organized in a regular matrix of thick and thin filaments bounded by Z discs [3]. Thin filament (approximately 5 nm diameter) is mainly constituted by polymerized actin monomers arranged as a helix, thick filament (approximately 15 nm diameter) is constituted by myosin: a long, two chains, helical structure that terminates in two large globular heads.

The sarcolemma is innervated by the *motor neurons*, whose axons exit the spinal cord and traverse progressively smaller branches of peripheral nerves until they enter fibers they control. A motor neuron can innervate from 100 to 1000 fibers and each muscle fiber is normally innervated by only one motor neuron in only one place (*end-plate*), usually near its midpoint [3]. The ensemble of the motor neuron and muscle fibers it innervates is called a *motor unit*. The activation of the muscle fiber by the motor neuron occurs when the axon terminal end of one neuron, in response to an electrical impulse, release the neurotransmitter acetylcholine (ACh), which travels towards the receptors on the

end-plate of muscle membrane: the nicotinic type of ACh receptor [2]. Activation of the ACh receptors results in the depolarization of the end-plate (*end-plate potential*), the end-plate potential is converted in a potential, which propagates along the muscle fiber with a mechanism that will be described in the following paragraph.

The most widely held theory of muscle contraction is the "sliding filament hypothesis", developed by A.F. Huxley and colleagues in the 1950s [4]. According to this theory, the relative movement of the actin and myosin filaments past one another causes the active shortening of the sarcomere, and hence of the muscle. When the muscle fiber is activated, changes in the transmembrane charge determine the passive diffusion of Ca^{2+} among the myofilaments. The result is a conformational change in the thin filament that exposes actin-binding sites, allowing the myosin heads to attach and form cross bridges between the thick and thin filaments. Each globular myosin head contains an ATPase that converts the chemical energy of the adenosine triphosphate (ATP) into mechanical energy that pulls the thick and thin filaments into greater overlap, shortening the muscle fiber. After the sliding motion of about 0.06 μm, the stress in the cross bridge is completely relieved and it can detach, then the head can attach to another binding site [3].

1.2 Action potential

Electrical potentials are generated from the electrochemical activity of cells from the nervous and the muscular tissue. These cells have a resting membrane potential of 70/90 mV, which is negative inside the cell with respect to the extracellular environment [5]. This potential difference results from two factors: the unequal distribution of ions over the membrane, in particular the positively charged Sodium (Na+) and Potassium (K+) ions and the negatively charged amino acids and proteins and the selective permeability of the cell membrane to just K+ [3].

The unequal distribution of positively charged ions on either side of the cell membrane depends on the activity of a membrane protein called *Sodium-Potassium pumps* working against the concentration gradients of ions flowing through the membrane. These proteins keep the Na+ ion concentration in the cell low (about 10 times lower than that outside the cell) and the K+ ion concentration high (about 20 times higher than that outside the cell) [6]. The cell membrane also contains *ion channels* highly permeable to K+ but less permeable to Na+, when the cell is at rest they are opened and K+ ions tend to leak out down their chemical concentration gradient. As a result, the

outside of the membrane accumulates a positive charge (excess of K+) and the inside a negative charge (excess of anions) [3].

Conditions change when the membrane is depolarized over a threshold and an action potential is generated: if the membrane potential reaches -40 mV, the membrane permeability to Na+ increases due to rapid opening of voltage-gated Na+ channels. Voltage-gated ion channels have the remarkable properties of opening, closing and inactivation (soon after opening they close spontaneously) in response to changes in the membrane potential, moreover they are highly specific for ions that will permeate and those that will not [7]. The net influx of positive charge (Na+ influx exceeds the K+ efflux) causes further depolarization. As the depolarization increases, more voltage-gated Na+ channels get opened resulting in a greater influx of Na+, which accelerates the depolarization even further. The membrane potential reaches the saturation value of 30-40 mV, in the meanwhile two processes contribute to limit and finally divert the depolarization. First, the process of inactivation closes Na+ channels; second, the opening of the voltage-gated K+ channels gradually increases the efflux of K+. Ion fluxes continue across the membrane toward the cell repolarization. K+ channels are slightly display so a period of hyperpolarization occurs while the K+ channels are open. Eventually all voltage-gated K+ and Na+ channels close. The only open channels are the non-voltage-gated K+ channels that generate the inside-negative potential characteristic of the resting state; as a result, the membrane potential returns to its resting value [8].

1.3 Motor System Control

The human motor system controls force, posture and movements of the body, according to a variety of internal and external demands and constraints [9]. The motor system comprises three main levels of control: the spinal cord, the descending system of the brain stems and the motor areas of the cerebral cortex. The interactions among these three levels are extensive and no action involves exclusively one level [10]. The most intensively studied areas of the cerebral motor cortex are the premotor area (PMA), the supplementary motor area (SMA), and the primary motor cortex (MI), which appear to have different roles in movement [11]. Voluntary actions are initiated and controlled by the cortical premotor areas and by the supplementary motor area. The brain stem integrates information provided by the vestibular apparatus, the sensory receptors in the neck region and the input from the cerebral cortex and the cerebellum. Moreover, it has four motor centers that send

efferent fibers to the spinal cord and give rise to dedicated pathways which are under the control of the sensorimotor cortex and the cerebellum [2].

The largest part of the cerebral cortex consists of the neocortex, which is of the outer shell of each cerebral hemisphere and is involved in higher-order brain functions such as sensory perception, cognition, generation of motor commands, spatial reasoning and language. The specific inputs and outputs vary across the neocortex and involve the processing of visual, auditory, somatosensory and motor information. The motor cortex sends outputs to the basal ganglia, the cerebellum, the brain stem and the spinal cord.

The primary motor cortex has a somatotopic organization which has been widely investigated and mapped. In the early 20th century, Sherrington and colleagues [12] collaborated to the meticulous mapping of the cerebral cortex in nonhuman primates using electrical stimuli and observing the related peripheral motor response. Experiments revealed a histologically unique area, with the lowest stimulation threshold for evoking a contralateral limb response, in front of the central sulcus which has been variously called *precentral gyrus*, *Brodmann's area 4*, *Rizzolatti's F1* and *primary motor cortex* (M1). These results was the foundation for similar motor mapping experiments on humans performed by Wilder Penfield during neurosurgical procedures [13]. In the 1940s and 50s, Penfield and his team developed the iconic motor homunculus (Figure 1), a distorted representation of the human body within the brain. From left to right, his visualization showed toes and feet extending to the body's trunk, then a very large hand equipped with a particularly prominent thumb, followed by the head, face and a dangling tongue beneath it all. More recent studies have improved this understanding of somatotopic arrangement using techniques such as functional magnetic resonance imaging [14] [15][16], but the Penfield model has been widely reproduced.

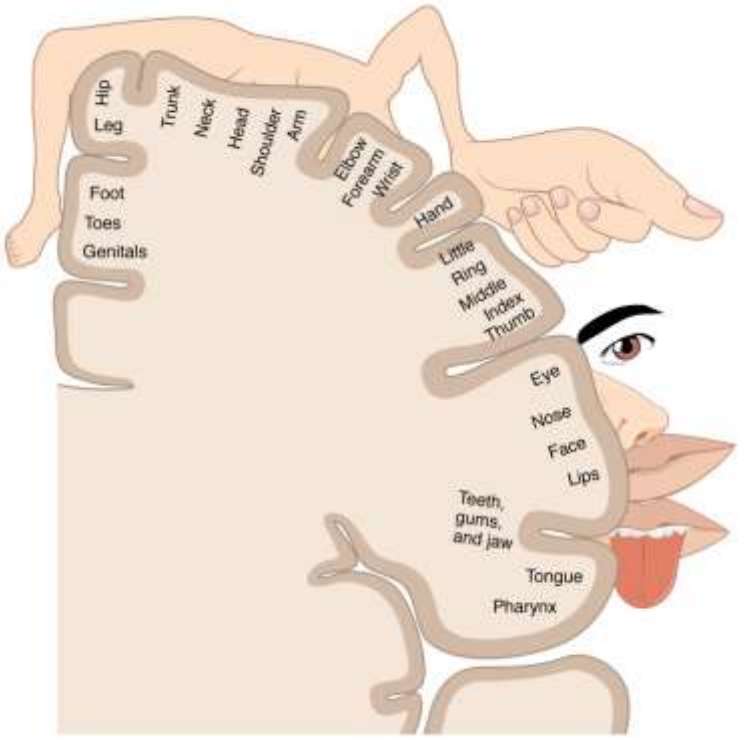

Figure 1. "Penfield motor homunculus" by "Carl Fredrik" is licensed by CC BY 3.0. The areas specializing in different parts of the body are arranged in approximately top-to-bottom order. The amount of cortex devoted to any given body region is not proportional to that body region's surface area or volume, but rather to how rich and complex the motor connection system is.

The spinal cord transmits nerve signals from the motor cortex to the body, and from the afferent fibers of the sensory neurons to the sensory cortex. The projections from the primary motor cortex to the spinal cord are mainly constituted by the corticospinal tract. The link between the corticospinal tract and the alpha (α) - motoneurons that innervate muscle fibers provides direct cortical control of muscle activity.

Many studies have demonstrated that the recruitment strategy of the motoneurons from the central nervous system is sized-based. This “size principle” of Henneman et al. [17] was based on results from cat motoneurons and is supported by strong evidence that in muscle contraction there is a specific sequence of recruitment in order of increasing motoneuron and motor unit (MU) size. The factors that influence the motor unit recruitment and firing frequency (rate coding) are primarily the level of force and the speed of contraction.

The premotor cortex and the supplementary cortex also project to the spinal cord as parallel outputs often referred as *central command* or *motor command*. A copy of this outgoing command (the *corollary discharge*), is returned to the cortical centers and compared with incoming sensory

information to determine differences between the intended and the actual performance of a movement.

The corticospinal tract is also constituted by the axons of the primary somatosensory cortex (S1) and other parietal lobe areas (roughly 24%). The function of S1 is processing the afferent information received from mechanoreceptors in the skin, muscle and joints and giving rise to a sense of touch, position and movement. S1 is also responsible for detecting the presence and magnitude of a sensory stimulus but also localization on the body surface. The control of voluntary movements by the motor system is graphically resumed in the following scheme.

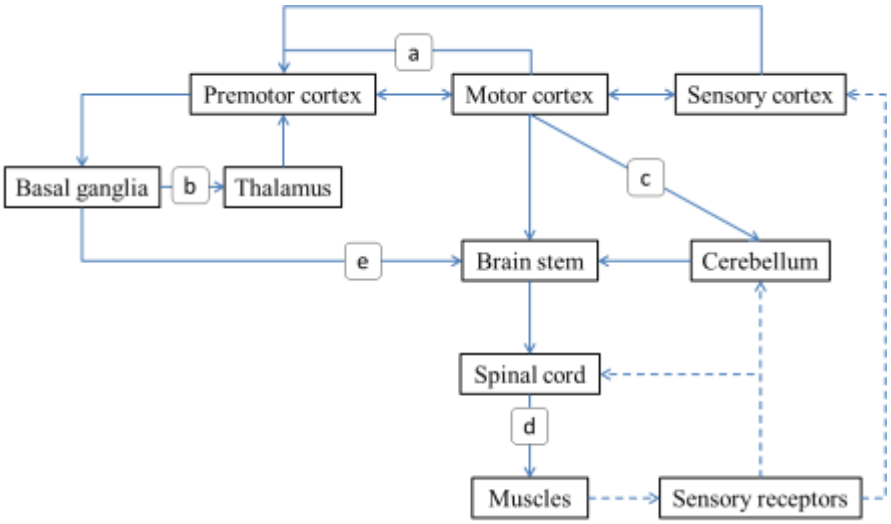

Figure 2. a. The sensory cortex provides information about the position of the body in the environment; b. Basal ganglia receive information from several different regions of the cerebral cortex, process information and return it to the motor cortex via the thalamus; c. Regulation of the sequence and duration of the elementary movements of all body segments are elaborated by the cerebellum to obtain smooth movements; d. The axons of the neurons of the motor cortex descend all the way into the spinal cord, where they make the final relay of information to the motor neurons. These neurons are connected directly to the muscles and cause them to contract; e. The basal ganglia–brainstem system contributes to automatic control of movements and adjustment of postural muscle tone during locomotion, occurs in conjunction with voluntary control processes; f. Sensory receptors continuously provide feedback to the system to refine the movement.

1.4 Electromyographic signal recording and processing

A single action potential in a motor neuron activates hundreds of muscle fibers in synchrony, the resulting currents generate an electrical signal that is readily detectable outside the muscle itself. Furthermore, many motor neurons generate an asynchronous barrage of overlapping action potentials arising in each muscle unit when more than minimal force is required. The result is a

complex pattern of electrical potentials (typically on the order of 100 μV in amplitude) that can be recorded as an electromyogram [3].

A physiological and mathematical model related to the EMG detection has been created: signals generated by the motor system reach the α-motoneuron through the spinal cord, firing pattern can be described by a train of impulses (Dirac Delta functions). As a rule, neural spikes do not occur regularly, in particular each specific spike train is a realization of a random process [18]. Each motor unit innervated by the motor neuron axon generates a motor unit action potential train (MUAPT, s(t)) which is the convolution of the motor unit impulse response (motor unit action potential - MUAP) and the Delta function train [19], [20]. This relation is mathematically described by the following equation:

$$s(t) = \sum_{i=1}^{M} \sum_{j=+\infty}^{-\infty} h_i(t)\delta(t - t_{ij}) \quad (1)$$

where h_i is the temporal waveform of the MUAP of the *i*-th motor unit, t_{ij} the timing of the *i*-th motor neuron action potential, and δ(t) is the unit impulse function.

MUAP waveform is a function of the geometrical properties of the motor unit, muscle tissue, and location of the recording site with respect to the active motor units [21]. The superimposition of generated MUAPT defines m_p *(t, F)*. The notation underline that in this model, the sum of MUAP trains is considered to be only a function of time (t) and force (F) [22], [23]. At the recording site, an electrical noise (*n(t)*) is introduced by the environment and by the recording system. Moreover, the signal is affected by the filtering properties of the recording electrode (*r(t)*) [21]. The observed EMG signal can be represented as:

$$\mathrm{m(t,F)} = [\mathrm{m_n\,(t,F)} + (\mathrm{n(t)})] \otimes (\mathrm{r(t)}) \quad (2)$$

The electrical noise *n(t)* which affects EMG signals, can be categorized into the 4 types: the inherent noise in electronics equipment, electromagnetic radiation to which our bodies are exposed and which may have an amplitude that is one to three orders of magnitude greater than the EMG signal, motion artifact caused by the electrode interface and the electrode cable and the inherent instability of the EMG affected by the firing rate of the motor units (0 to 20 Hz) [24].

1.4.1 Data collection

The EMG signal can be detected using electrodes inside of a muscle (intramuscular EMG) or on the skin surface over the muscle (surface EMG) [2]. Only the aspects related to surface EMG (sEMG) will be deepened since this thesis deals with this type of EMG signals.

sEMG is more practical in clinical, research and commercial fields than the needle electrode techniques but some measures are required to guarantee high-quality signals, due to the larger distance between the recording site and the signal source and to the signal attenuation and distortion introduced by the underlying tissue. In fact, the skin-electrode interface can be considered a boundary between two media: a multilayer, nonhomogeneous, and anisotropic conductive media (skin, subcutaneous tissue, and muscle) that contains the sources of the electrical field, and an isotropic media (the electrode itself) [25]. The electrode–skin interface is very complex with highly non-linear behavior, with a capacitive impedance whose R and C components are current and frequency dependent. Moreover, it incorporates a DC generator accounting for the half cell potential of the metal-electrolyte interface [20]. Figure 3 shows the correspondence between the skin-electrode (wet electrodes) interface layers and a simplified but effective electrical model which has been proposed in 1978 by Neuman [26].

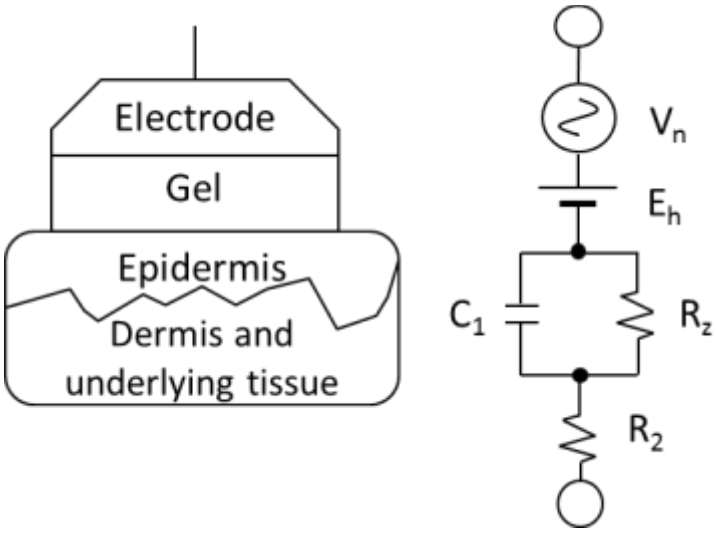

Figure 3. Electrical model of electrode-skin interface [26].

Two types of electrodes are commonly used: wet electrodes which use a conductive gel to improve chemical and electrical properties of the interface between the skin and the metallic part of the electrode, and dry electrodes: in direct contact with skin. Wet electrodes are conventionally realized in silver/silver chloride (Ag/AgCl), they have lower skin-electrode impedance and lower susceptibility

to motion artifact with respect to dry electrodes, however they have some disadvantages: allergic reactions to electrolyte gel may occur and in case of long-term monitoring, the electrolyte gel may dry out, leading to a significant decrease in signal quality [27]. Dry electrodes are designed to operate without the electrolyte. From a practical point of view, they are preferable but enabling high quality and low-noise recording of bioelectrical events with small amplitudes requires surface optimization from a chemical, electrical and mechanical point of view. Different materials has been tested, from noble metal [9] to micro-fabricated silicon structures and ceramic [28], and several methods have been applied to obtain the lower and most resistive impedance in the EMG frequency range [29], [30].

Electrodes can be used in a monopolar configuration or in differential configurations. The monopolar configuration (with an additional reference electrode, placed on an electrically inactive area) is mainly applied in the research field, because it contains the entire information available from the detected signal nevertheless, the high sensitivity to common mode signals prevents its application when recording condition are not strictly monitored. The differential configurations exploit electrodes in pairs and one additional electrode to compute the difference between the two electrodes respect to the reference. Allowing a better signal-to-noise ratio, cross-talk reduction and an increase in spatial selectivity, it is the most widely used configuration [9]. Surface electrodes can be also combined in mono- and bi-dimensional arrays (also referred as *arrays* or *matrixes*), providing multichannel information for advanced EMG applications and research purposes [31]–[33].

1.4.2 Filtering and amplification

EMG signals detected by electrodes require voltage and current amplification to change low voltage signals into optimized signals suitable for digital conversion and additional processing. Front-end amplifiers need some important characteristics related to the specific circuit configuration adopted. High common mode rejection ratio (CMRR) is required to maximize the suppression of correlated signals common to both recording sites in bipolar electrodes arrangement (signals from power sources, electromagnetic devices, more distant muscles) [30]. The CMRR is defined as CMRR = 20Log10 (Ad/Ac), where Ad and Ac are, respectively, the amplifier's differential and common mode gains. The best CMRR that can be achieved with commonly used technology is about 105 to 106 (100–120 dB), which is considered sufficient to limit the equivalent input voltage to a value negligible with respect to EMG [34], [35]. In order to avoid attenuation and distortion of the detected signal, the

input impedance of the amplifier must be at least two orders of magnitude greater than the largest expected electrode–skin impedance of 1 MΩ however, values just higher than 100MΩ are usually considered acceptable [9]. One drawback with high input impedance is the increasing of power line and radiofrequency noise and movement artifacts introduced in the lead wires by means of capacitive coupling. A solution to reduce this effect is to place the amplifier as close as possible to or directly on the detection surfaces of the electrode [36], [37]. Another advantage of this configuration is the reduction of the output impedance of the amplifier can be made on the order of 10 Ω.

Even with the aforementioned considerations, the EMG signal will be affected by some noise: the signal to noise ratio can be further increased by suitable filtering. Movement artifacts and instability of the skin-electrode interface determine slow variations with harmonics in the frequency range of 0 to 20 Hz, a high-pass filter is therefore designed with a cut-off frequency in the 25 to 30 Hz range. If the recording application concerns the firing rates of the active motor units, whose frequency range is between 20 and 30 Hz, the cut-off frequency may be lower (15-20 Hz). Other low frequency unwanted fluctuations, may be attenuated but not removed (i.e. artifacts due to sliding of the innervation zone below the electrodes, fluctuations in the electrode impedance, half-cell potentials) [9]. The 50 or 60 Hz interference has been often managed with notch filters, this practice is not recommended in some applications since it considerably changes the signal waveform, moreover it removes power from EMG in a high-power density frequency band [38]. Digital adaptive noise cancellation filters may be used to remove power line interference avoiding unwanted attenuation and distortion [39], [40]. Low-pass filters with a cut-off frequency near 450–500 Hz and a roll-off slope of 40 dB/decade are included in the system to avoid signal aliasing without removing harmonic of interest from the sEMG signal [9].

1.4.3 Sampling and conversion

As the Nyquist theorem requires, sEMG signals are sampled at least 1 kHz. The following analog to digital (A/D) conversion transforms the sampled voltages into “levels” represented in binary code. An important specification is the minimum acceptable signal resolution. A/D converter resolution is defined as the ratio between the input range and the number of quantization levels. With a specific baseline noise, it is necessary to digitize the signal with enough bits so that noise can be resolved with a suitable number of bits and even the faintest EMG activity can be appreciably quantified. It is common practice to select the resolution of the system somewhat below the noise level of the system

(1-5 μV), and the range somewhat above the maximum expected peak-to-peak amplitude of the signal at the output of the conditioning amplifier-filter (±20 mV to ±2 V). Thus, 16-bit A/D converters with a ±5V input range are commonly used, the gain of the amplifier is often 1000. If the desired resolution cannot be matched, the amplifier must be designed with adjustable gain in order to obtain the desired [9].

2 Stroke and motor rehabilitation

In the present chapter the aspects related to the effects of stroke and to the rehabilitation therapies are presented. The use of EMG biofeedback in hemiplegic patients is analyzed from the earliest studies to more recent task-oriented rehabilitation therapies. The overview is focused on the role of technology applications and on the criteria that should be met for a wider applicability in rehabilitation protocols.

2.1 Epidemiology and pathophysiology

Stroke is characterized as a neurological deficit attributed to an acute focal injury of the central nervous system (CNS) by a vascular cause, including cerebral infarction (ischemic stroke), intracerebral hemorrhage and subarachnoid hemorrhage (hemorrhagic stroke) [41]. Stroke diagnosis tools include clinical diagnosis, radiographic diagnosis, serum Biomarkers and pathology.

According to Béjot et al. [42], approximately 1.1 million inhabitants of Europe suffered a stroke each year. Moreover, rates observed in young adults are on the rise, thus suggesting a need for strategies to improve prevention. In addition, since incidence rates increase by a factor of 100 between the age of forty and eighty and because of the ageing population, the absolute number of stroke is expected to dramatically increase in coming years: by 2025, 1.5 million European people will suffer a stroke each year [42]. At the beginning of the 21st century, one-month case-fatality rates in population-based studies ranged from 13 to 35%. Huge variations were observed according to the subtype of stroke. Intracerebral hemorrhage, accounting for 10 to 25% of overall cases, was associated with the highest one-month case-fatality rates ranging from 25 to 61%, better prognosis was noted in patients with ischemic stroke, accounted for 0.5 to 5%, with case-fatality rates ranging from 9 to 19%.

Approximately one third of the patients who survive the stroke suffer from long-term disabilities, many of them requiring permanent care. As the third leading cause of death and the number one cause of adult physical disability in the developed world, stroke is a major public health burden.

Depending on which region of the brain is damaged, different disorders can arise:

- Hemiplegia
- Visual deficits
- Aphasia (loss of the ability to speak or understand a known language)
- Agnosia (inability to process sensory information)

The hemiplegia involves the 75% of post-stroke patients and affects facial, trunk, lower and upper limb muscles [43]. Loss of upper limb motor control is characterized by weakness of specific muscles, abnormal muscle tone, lack of mobility, abnormal movement synergies, loss of inter-joint coordination and loss of sensation.

Upper limbs, and especially the hand, strongly influence the human interaction with the environment. Reducing the independence of the subject in Activities of Daily Living (ADL), the impairment in the functional use of the hand may lead to a decrease in the life quality and social integration. ADL require fine motor control of the hand and fingers, in terms of regulation of the magnitude of muscle activity, integration of sensorimotor information and synchronization of temporal and spatial recruitment of relevant muscles [44], [45]. Therefore, the restoration of the functional use of the hand after a neurological injury appears as much challenging as relevant.

Clinically, the most successful therapy to promote functional recovery is the rehabilitative training. The World Health Organization (WHO) defined rehabilitation as a term “to reach and maintain optimal functioning in physical, intellectual, psychological and/or social domains” [46]. Understanding of biological basis of neural recovery has been accompanied by a better understanding of rehabilitation mechanisms. Patients may be classified as being in an acute (<2 weeks), subacute (2 to 12 weeks) or chronic (>12 weeks) stage after stroke [47]. Although several and different restorative processes can occur together in different stages after stroke, it can be said that spontaneous recovery begins in the very early stages after stroke but lasts several weeks until it reaches a plateau and represents a stable but still modifiable chronic phase [48]. In true recovery, the same muscles as before the injury are recruited through neuroplasticity strategies such as changes in interhemispheric lateralization, activity of association cortices linked to injured zones and organization of cortical representational maps. In compensation strategies, alternative muscle coalitions are used for skill performance. Clinical manifestations of maladaptive plasticity may occur in some cases [49]. To date, the influence of different therapy modalities on true recovery and compensation have not been

clarified. In any case, learning is a necessary condition [50] and can be stimulated and shaped by rehabilitation therapies [51].

2.2 Rehabilitation approaches

The aim of a rehabilitative training is the recovery of the functional use of the paretic limb through impairment reduction or compensatory strategies. Hatem et al. [52] have recently published a systematic review focused on standard treatment methods and innovating rehabilitation techniques. The twenty-six rehabilitation treatments that have been analyzed, have been classified in six categories:

- Neurofacilitatory approaches/multiple exercising approaches
- Isolated concepts
- Motor learning
- Interventions based on the hypothesis of mirror neurons and motor imagery
- Adjuvant therapies
- Technology-supported training

Neurofacilitatory approaches/multiple exercising approaches. Since the motor system learns by repetition and training, stroke rehabilitation massively applies exercise therapy [48]. Exercises may differ for their objective or technical characteristics (duration, training load, type of feedback) and involve both the patient and the therapist. The aim of the therapy is facilitating voluntary movements, normalizing of muscle tone or improving the patient perception of the joint position thus including cognitive sensory-motor training.

Isolated concepts. Isolated rehabilitation techniques are sometimes included in multiple exercising protocols and are focused on specific objectives such as Muscle Strengthening [53][54]. Other techniques are based on the interaction between the paretic and the non-paretic upper limb requiring repetitive movements of the upper extremities in a symmetric or asymmetric design [55], or completely restraining the non-paretic limb without specific training protocols.

Motor skill learning - Constraint-induced movement therapy (CIMT). In stroke, motor learning refers to the re-learning of a previously acquired movement pattern. CIMT is a high intensity protocol of repetitive task-oriented practice, constraint of the non-paretic upper extremity during 90% of the

waking hours and with translation of the achieved clinical setting in to the patient's daily real-world environment [56]–[58] .

Interventions based on the hypothesis of mirror neurons and motor imagery. The mirror neuron system is activated during the execution, as well as during the only observation of actions. Thus, these approaches are based on the re-assembling of the injured neural circuits associated with the execution of movements, through active (movement imitation) or passive (observation) involvement of the patient [59].

Adjuvant therapies. Different adjuvant therapies could be integrated with previously cited concepts to increase their efficacy. Electrical stimulation can be applied as somatosensory stimulation of peripheral nerves [60], to directly elicit muscles contraction [61] or to manipulate the membrane potential and modulate spontaneous firing rates of neurons [62]. Moreover, drugs can be used to influence neurotransmission or reduce spasticity [63][64].

Technology-supported training. Technological solutions participate to rehabilitation therapies in the forms of active (actuators moving limbs) or passive (stabilizing limbs) robotic systems, performance-related visual and auditory feedback in virtual environment and multimodal devices. The aim of technology-supported training is to close the sensory-motor loop to increase patient self-consciousness and motivation [65].

2.3 Technology-supported training

Scientific evidence [52] individuates some recommended rehabilitation approaches: muscle strengthening exercises, constraint-induced movement therapy, mirror therapy and botulinum toxin. Moreover, according to the stage of stroke, some rehabilitation concepts may be more appropriate than others. Technological approaches give promising outcome prognosis but further RCTs are needed to ascertain treatment effects.

For the last few decades, rehabilitation evolution has conferred an important role to technology and its applications. Stroke incidence in Europe in 2025 is expected to increase to 1.5 million causing a general increase in the amount of therapy. Furthermore, it is well documented [66], [67] that functional and task-oriented approaches are more beneficial for skill acquisition than passive or impairment-oriented modalities.

In this scenario, the introduction of technology in the rehabilitation has good perspectives since it allows the decrease of the time a therapist needs to consume with each single patient. Moreover, the quality of the therapy can be guaranteed also after the discharge of the patient from the hospital and the automatically recorded training data can be retrieved by clinicians for subsequent analysis. There is scientific evidence that guided home rehabilitation helps patients in preserving their ability to undertake activities of daily living and may lead to further functional improvement [68] [69]. Training of skills that are meaningful to the stroke patient, are efficiently supported by three-dimensional graphical environments provided by technological rehabilitation systems and immediate biofeedback increases patient motivation, self-management and social interaction [70]–[74].

2.3.1 Biofeedback

Biofeedback is the real-time recording of a biomedical variable providing information about the activity of the related system.

The improvement of patient's motor control supported by biofeedback consists of re-educating the patient in that control by providing visual or audio feedback about the measured biomedical variable.

Feedback can be categorized as either "intrinsic" or "extrinsic". Intrinsic feedback is provided to a person who performed the task and refers to his/her sensory-perceptual information. Extrinsic (or "augmented") feedback is provided from an outside source and includes verbal encouragement from the therapist, video camera materials, charts, performance reports [75]. Extrinsic feedback can be further categorized in knowledge of results (KR) and knowledge of performance (KP). KR provides information about the outcome of performing a skill, KP gives information about characteristics of the movement performed in order to complete the task. Although extrinsic feedback is not necessary for the recovery of motor skills, the use of KR and KP in therapy has shown better motor outcomes [76][77]. Moreover, brain damages can impair a patient capability to understand intrinsic feedback, in these cases information about performance can be presented through alternative channels and tools [78].

Intrinsic feedback can be directly provided as a numerical value of the measured variable (i.e. Heart Rate displayed on a wearable device during treadmill exercise) or it can be used to control an adaptive auditory signal, visual display or tactile feedback. Giggins et al. [79] have categorized biofeedback in Biomechanical biofeedback, involving measurements of movement, postural control and force and Physiological biofeedback, which derived from measurement of specific physiological systems.

Biomechanical biofeedback

Biomechanical biofeedback estimates 3-D kinematic information of a body segment with a variety of sensors. Inertial sensors measure orientation, velocity and gravitational force [80][81], gyroscope is used to measure angular velocity [82][83]. Joint kinematics measurement during functional tasks could be performed by electrogoniometery [84], while optical motion capture systems use a network of cameras and a series of markers placed on anatomical landmarks on the subject's body [85]. Gait, movement and balance analysis can also exploit measurements of the ground reaction forces generated by the body and quantified by force plate systems [86][87].

Physiological biofeedback

Physiological biofeedback is related to the physiological system which is monitored. Cardiovascular biofeedback measure Heart Rate and Heart Rate Variability using a heart rate monitor or an electrocardiogram and provide it to the user as a numerical value. Electrodes and sensors attached to the abdomen are used to teach patients with respiratory diseases by converting breathing to auditory and visual signals. EMG biofeedback converts EMG signals, usually recorded with surface electrodes, into visual and auditory signals and are applied in both musculo-skeletal and neurological rehabilitation.

Electromyography (EMG) biofeedback in hemiplegic patients

EMG biofeedback was first introduced in the literature more than 40 years ago as a training tool used in rehabilitation therapies to facilitate the recovery of movement patterns after injury [88]. In earliest studies, the feedback was indicated in a relatively simple format through visual display of analog, digital or binary values, auditory pitch or volume, or mechanical tactile stimulation. Cues were ultimately proportional to the EMG signal recorded above electrodes located on specific muscles [89]–[95]. Patients usually worked in static positions and practiced to control a specific parameter however, performed movements were unrelated with ADL [92]–[94]. Traditional EMG biofeedback studies showed improvements in the control of trained muscles [91], [96], [97], increased range of joint motion [96], [98], [99] and positive trends in outcome measures used for physical and psychological assessment [89], [90], [100]. On the other hand, most reviews of static biofeedback therapy failed in demonstrating a significant motor recovery [101][102] showed that the effects are limited to specific muscles and joints. For example, functional walking does not benefit from static EMG biofeedback training to LE in hemiplegic patients [89][101].

Contemporary approach to rehabilitation therapy is more focused on promoting independent life of the patient, this requires the ability to complete functional tasks related to specific ADL performed in a real-word environment. Many studies have demonstrated that task-oriented biofeedback therapies are beneficial for the improvement in the recovery of functional activities [66], [67]. Thus, more recent studies about the efficacy of EMG-BF in neuromotor rehabilitation have applied this concept.
Park et al. [103] have introduced EMG-BF in their task-oriented training to increase motivation and to reach maximum muscle contraction during kinetic chain exercises (KCE) and have revealed that closed KCE overtook open KCE in increasing the balance ability and lower extremity muscle activation of vastus lateralis and vastus medialis. In the field of the recovery of the walking capacity of stroke patients, continuous repetition of movements allowed by cycling exercises in condition of a reduced lower physical load and therapist's engagement has shown good perspectives. This task-oriented locomotor training has shown good results with a more efficient contraction of the flexor muscles of the paretic leg and in the inhibition of hypertonicity in the extensor [104], [105]. Jonsdottir et al. have revealed that task-oriented BF treatment was effective in increasing peak ankle power, gait velocity, and stride length in a population with hemiparesis [106]. A randomized pilot clinical study was conducted with stroke patients to compare the effect of EMG-BF in combination with conventional occupational therapy for performing basic activities of daily living [107]. Results show that the group that underwent the combined therapy showed a significantly better performance in all assessments.

2.3.2 Closed loop rehabilitation technologies

In the last decade, a variety of technological opportunities have been created for patients and therapists to close the sensory motor loop during rehabilitation therapies. A variety of solutions based on different control strategies are available on the market of medical devices. **Riablo** (CoRehab, Trento, Italy) and **Sword** (SWORD Health, Porto, Portugal) provide biomechanical feedback through wearable inertial sensors and continuous movement analysis of body segments. Movements and posture of the patient are monitored, and a real-time visual, auditory and vibratory feedback is provided about the execution of the exercises. **VRRS** (Khymeia, Padova, Italy) supplies virtual and augmented reality environments for the rehabilitation therapy. Patient movements are monitored using a magnetic kinematic acquisition system or infrared cameras. This is the case of VRRS Handbox, the system dedicated to wrist, hand and fingers rehabilitation. Virtual reality is often associated with devices based on motion capture and 3D tracking systems: **SeeMe** and **VAST.REHAB** (Brontes

Processing, Gliwice, Poland) use Kinect technology (Microsoft, Redmond, Washington), whereas **GRAIL** (Motekforce Link, Amsterdam, The Netherlands) combines data from 3 video cameras to reconstruct movements. **RAFAEL Smart Glove** (NEOFECT, Burlingame, California) is a haptic glove based on inertial and magnetic sensors. Wrist and single finger movements are monitored and visual and auditory feedback in virtual reality are provided to the patient. In the robot-assisted rehabilitation field, physiological or motor parameters (e.g. force and EMG signals) can be used to trigger the assistance supplied by the robot. **Hand of Hope** (Rehab-Robotics, Hong Kong, China) is an EMG driven hand exoskeleton. Signals are recorded by single cabled electrodes positioned by the therapist on patient forearm. A similar control strategy is performed by **Amadeo** (Tyromotion, Graz, Austria), a rehabilitation robot that can use force measurements or EMG signals recorded with single cable electrodes to trigger the robot assistance. Both these systems support patients in performing finger flexion and extension and provide a visual feedback during the execution of the rehabilitation therapy.

Most of the above cited systems are based on the kinematic and force data produced by the patient during the movement execution. Both aspects are the result of a process that origins in the cortical areas dedicated to motor control and reaches motor neurons, whose axons exit the spinal cord and traverse progressively smaller branches of peripheral nerves until they enter the muscle they control. In some cases, the high level of motor impairment of a post-stroke patient prevents the subject from developing a movement or producing a level of force that biomechanical sensors can reveal. In case of highly impaired patient who are unable to produce movement, the produced EMG signal can quantify muscular activity and interpret user's intentions. Moreover, a biofeedback based rehabilitation system that exploits the analysis of muscular activation patterns, can reveal unwanted compensation strategies that the patient could use to perform the correct movement [108].

Many studies have been performed to assess the effect of the introduction of EMG-BF based systems in hand rehabilitation protocols. Results are promising but the focus is on the rehabilitation approach and a lack in the optimization of the devices for the application in the clinical context can be revealed: single cabled electrodes have been used and a non-portable acquisition system has been applied to process EMG signals. Such a configuration increases the application time, reduces usability in a clinical context and can introduce variability in electrodes location and thus in the control of the system by the patients across different rehabilitation sessions. Moreover, in most of the cases, the recognition

of the performed movement is threshold based which can be a practical strategy when the device is applied in protocols that include only movements that require the activation of antagonist muscles but is no more robust when the rehabilitation protocol becomes more structured.

In recent years, **Myo** armband (Thalmic Labs, Ontario, Canada) has been commercialized. It recognizes arm, hand and finger gestures using a set of EMG sensors, combined with a gyroscope, accelerometer and magnetometer. It has been conceived as a device to control video games, presentations, music and visual entertainment. Several hand rehabilitation studies applied Myo armband as an EMG acquisition system since it represents a good trade-off between performance and wearability.

2.3.1 Implementation criteria

A vast spectrum of technological solutions are available for closed loop rehabilitation protocols however, widespread application of the devices in clinical field remains low [67]. Reasons for this phenomenon should be individuated and solved for the technology to be more applied in rehabilitation protocols.

Hochstenbach et al. [110] have acquired information by a vast literature review and a semi-structured interview with therapists of post-stroke patients rehabilitation, they have identified two series of criteria and conditions that technology should meet. The result is a guidance, from a therapist's perspective, that could facilitate successful implementation of technology assisting rehabilitation devices in clinical environment.

Therapy-related criteria

WHO classifies health and disease at three levels: 1) Function level (aimed at body structures and functions), 2) Activity level (aimed at skills, task execution and activity completion) and 3) Participation level (focused on how a person takes up his/her role in society) [46].

Current therapy strategies are widely influenced by the growing awareness that healthcare goes further than mere function level, as has been the case until the middle of the last decade. Therefore, training should be oriented to the specific task the patient need to recover and should be applied in a meaningful context with methods supporting a practical translation in the real-world environment [111]. Therapies should be patient-tailored considering any cognitive impairment and proposing challenging but achievable objectives. The inclusion of gaming elements, variability in the exercises and feedback has been found to increase patient attention and participation and offers a good

compensation to training hardship [72]. Finally, training intensity and frequency need to be determined individually, according to the degree of impairment and to the rehabilitation stage.

Software- and hardware-related criteria

From the therapists point of view, most software- and hardware-related criteria concerns the usability of the system which should require little time for the setup, should adapt to the individual patient, to patient progression over time and to various tasks [110]. The patient perception of the system is also relevant: it should not represent a constraint or disturb to the interaction of the patient with the environment and the therapists; restrained size, lightweight and portability could support the compliance of the device, especially in home-therapy protocols. With this perspective, clear instructions and feedback during and after exercises promote the patient independence for the use, making possible a continued rehabilitation in chronic patients [20]. Moreover, therapists need to observe some performance parameters to monitor patient progression and to tailor therapy to the specific patient needs and abilities over time, these parameters should be also provided by technological solutions. Some examples of measurable variables are strength, speed in task completion, coordination, deviation from the intended trajectory. Moreover, new systems should be able to register the exercise history of the patient. Some relevant exercise parameters are: type of exercise, number of repetitions, speed of motion, range of motion, force of resistance and period of training.

3 Medical devices and closed loop rehabilitation technology

The present chapter presents main concepts about medical devices and clinical trials performed on patients in order to assess their security and efficacy.

Medical devices refer to any device, instrument, apparatus, software or material intended to be used in diagnosis, prevention, monitoring, treatment, or alleviation of a disease. In 2010, the World Health Organization (WHO), has estimated that there are around 1.5 million different medical devices, with a variety of products ranging from needles to engineered tissues, defibrillators or prosthesis. Despite the mixture of products, some characteristics are common such as the development process, the standards that must be complied, the regulatory framework, the classification, the pathway to market, and the post-market reporting process. Clinical trials in humans are generally required for a medical device to be commercialized and allow the assessment of the quality and the efficacy of the device. Trials in clinical context involving medical devices, must meet specific safety and ethic requirements which include aspects related to technical, legal, and social fields.

Since the device used in the present thesis was developed and tested in Italy, these aspects will be evaluated in accordance with the European Community (EU) Law. In order for the requirements in the European Directives to be mandatory in each member state, the directives were transposed to each state's legislation. Moreover, to ensure a uniform application, the MEDDEV guidelines (Directorate General Health & Consumers 2010) were created. Albeit, they are legally non-binding documents, they are widely used as reference for the procedures involving new medical devices.

Finally, the device is devoid of the CE mark (abbreviation of French "Conformité Européenne" meaning "European Conformity"), which is the required mark for medical devices to be commercialized in EU. Thus, the following paragraphs will be focused on clinical trials performed in EU with non-marked medical devices.

3.1 Main Directives

Nowadays, clinical trials with medical devices in Italy are regulated by the following laws:

- Legislative Decree 46/97 (transposition in National Law of the European Council Directive 93/42/EEC which covers most of the medical devices) modified by the Legislative Decree 25/01/2010 n. 37;
- Legislative Decree 507/92 (transposition in National Law of the European Council Directive 90/385/EEC on active implantable medical devices) modified by the Legislative Decree 25/01/2010 n. 37;
- Health Ministry, Decree of 2 August 2005: "Modalità di presentazione della documentazione per notifica di indagine clinica con dispositivi medici";
- Circular 2 August 2011: "Chiarimenti sulle modalità di presentazione della documentazione per notifica di indagine clinica con dispositivi medici";
- Health Ministry, Decree of 08 February 2013: "Criteri per la composizione e il funzionamento dei comitati etici";
- Health Ministry, Decree of 12 March 2013: "Limiti, condizioni e strutture presso cui è possibile effettuare indagini cliniche di dispositivi medici, ai sensi dell'articolo 14 del decreto legislativo 24 febbraio 1997, numero 46 e successive modificazioni";
- Health Ministry, Decree of 25 June 2014: "Modalità, procedure e condizioni per lo svolgimento delle indagini cliniche con dispositivi medici impiantabili attivi ai sensi dell'articolo 7, comma 6, del decreto legislativo 14 dicembre 1992, n. 507 e successive modificazioni".

3.2 Clinical trial with medical devices devoid of CE mark

Most clinical trials on medical devices devoid of CE mark are promoted by the device manufacturer in order to verify the device safety and performance and obtain the CE mark (pre-market trial). In other cases, universities, research centers, hospitals or Institutions not qualified as the manufacturer perform clinical investigations for the purpose of research or analysis (no-profit trials). Regardless the aim of the clinical trial, it has to be notified to the Health Department and obtain the authorization of a Research Ethics Committee.

3.2.1 Classification

The first step of the procedure is the definition of the risk class of the device according to Annex IX of the Legislative Decree 46/97. The classification mainly depends on the following aspects:

- duration of the contact with the body and degree of invasiveness;
- whether the device is active or not;
- whether special rules are applicable to the device.

The risk class has to be based on the intended use of the device. If multiple applications are planned, the classification has to be performed according to the most critical use. Accessories are classified separately from the device moreover, any software for the device proper functioning automatically acquires the same risk class of the device itself. The following table summarizes characteristics of medical devices for every risk class.

Table I. Summary of medical devices characteristics according to the risk class.

Risk Class	Type	Description
I	Invasive	Devices invasive in stoma or body orifice for transient use or short-term use in oral or nasal cavity or ear canal; reusable surgical instruments
	Non-invasive	Devices that either do not touch patient or contact only intact skin; devices in contact with injured skin (only mechanical barrier - absorb exudates)
	Active	All active devices not included in the other classes
	Special Rules	Special rules are not applicable
IIa	Invasive	Devices intended for short term use in stoma or body orifice or long-term use in oral or nasal cavity or ear canal; devices connected to a device of Class IIa or higher
	Non-invasive	Devices for channeling or storing for use with body fluids, organs, tissues and/or connected to an active medical device
	Active	Devices intended to administer or exchange energy and medicines with the body; device for diagnosis; applications with low risk
	Special Rules	Devices to record X-ray diagnostic images; substances for disinfecting medical devices (no contact lenses) other than by physical action
IIb	Invasive	Devices for long term or mainly absorbed; short term devices which undergo chemical change in body (NOT in teeth) or supply energy/ionizing radiation
	Non-invasive	Devices for biochemical modification of anybody liquids intended for infusion; devices intended for wounds which breach dermis

	Active	Devices intended to exchange energy or administer medicine in a potentially hazardous way; devices to monitor vital processes where variations could result in immediate danger; blood bags
	Special rules	Short term devices used for contraception or prevention of sexually transmitted diseases; devices emitting ionizing radiation and related monitors in medical procedure
III	Invasive	Devices for diagnose/control of or in direct contact with heart, central circulation system or central nervous system; Long-term use and implantable devices; devices for short-term use mainly absorbed; long term devices which undergo chemical change in body - or administer medicines (NOT in teeth)
	Non-invasive	Special rules are not applicable
	Active	Special rules are not applicable
	Special rules	Devices used for contraception or prevention of sexually transmitted diseases if implantable or long-term invasive

3.2.2 Clinical Trial Notification

The notification of clinical trials requires the following type of documents:

- information and responsibility statements of the persons responsible for the trial;
- device related documents;
- protocol related documents.

Information and responsibility statements

The sponsor of the clinical trial has to assume the responsibility of the investigation according to the Directives 90/385/EEC and 93/42/EEC and declare that the clinical protocol has been specifically conceived to definitely prove or deny the expectation formulated for the device. Moreover, the sponsor has to declare that the investigation will be conducted according to the Annex VIII and X of the Legislative Decree 24 February 1997, n.46 and to the Annex VI and VII of Legislative Decree 14 December 1992, n. 507 that regulate devices for particular intended use and implantable active devices respectively. Moreover, the sponsor undertakes to notify every adverse event occurred during the investigation. The study must be in accordance with the Helsinki Declaration [112] and with the UNI EN ISO 14155-2012 about the Good Clinical Practice (GCP), participant data have to be treated according to the Legislative Decree n. 196/03 about Protection of Personal Data. The sponsor

must provide the authorization for the investigation obtained by an Ethical Committee that further guarantee protection of patients from a legal, ethical and insurance point of view.

The sponsor also assumes the responsibility for the device, which has to be compliant with the essential requirements provided by for law, a risk assessment has to be performed on the device according the EN ISO 14971:2012 or to other harmonized international standards. All the costs associated to the investigation have to be paid by the sponsor and however, neither the public health nor patients must be involved in the expenses.

Finally, all the documents about the clinical protocol and the device have to be kept at the disposal of the Health Department.

Device related documents

The device has to be univocally identified by document information such as name, model number and name and address of manufacturer. Full description of device, including a list of accessories and user manual is required, moreover principal design drawings and circuit diagrams including descriptions and explanations necessary to understand the aforementioned drawings/diagrams must be provided. Material selection has to be documented to fully characterize the identity and chemical composition of all materials coming into patient contact, including name and address of manufacturer, trade name/code. Detailed description of how biocompatibility and biological safety have been addressed must be included in the documentation. The application of harmonized standards is not mandatory and alternative methods can be chose to demonstrate compliance with the essential requirements, which should be supported by a risk assessment, preferably to EN ISO 14971. It should be apparent from the risk assessment, how hazards were identified and characterized and how the risks arising from the identified hazards were estimated and justified in relation to anticipated benefits.

Protocol related documents

The Ministerial Decrees 12 March and 25 June 2014 define limits and conditions for the evaluation of the eligibility of Institutions to the execution of the clinical trials. Clinical structures where the investigation take place and the clinical investigator of the study have to demonstrate expertise in the specific field of the investigation under the experiment and support it by scientific publications or patents. A copy of the Ethics Committee opinion of the structure has to be provided to ensure that

the health, safety and human rights of the participating patients are protected. Moreover, for the same purpose, a copy of informed consent, of the patient information sheet and of the insurance of subjects must be attached to the documentation. All investigation parameters and design features have to be communicated: aims and objectives, type of investigation (i.e. whether the use of a controlled group of patients is planned), number of patients, duration of study, inclusion and exclusion criteria for patient enrollment. Moreover, a description of data recording is required, with a justification of statistical design, method and analytical procedures.

3.2.3 Clinical trial approval

The Notification has to be presented to the Health Department within 60 days prior to the intended clinical investigation. If the Health Department raises grounds for objection or need some integrative documentation it will notify the sponsor of the decision and the assessment period is suspended. The sponsor of the clinical investigation has 90 days to provide the requested documentation or clarifications. The approval of the clinical trial is notified to the sponsor through a formal acceptance. However, if within 60 days the Health Department has not given written notice of objection, the clinical investigation may proceed.

3.2.4 Clinical trial conclusion

The sponsors are required to notify the Health Department when a clinical investigation comes to an end (Annex X of the Legislative Decree 24 February 1997, n. 46). A final report of the trial had to be redacted and make public. Risk assessment has to be revised according to data collected during the investigation. The final report includes a resume of all clinical and technical aspects of the investigation. Adverse events and device deficiencies have to be reported and corrective actions taken in order to solve encountered problems documented. The conclusion section of the report includes a critical evaluation of results from the point of view of security, performance and efficacy of the device under study.

4 Hypotheses and aims

Drawing on the analysis of the state of the art and on the consultation of rehabilitation therapists, the following hypotheses were made:

- Hypothesis 1 - The optimization of an EMG-BF system in a real clinical context can lead to the implementation of a device which shows both high usability from the point of view of the therapist and the patient, and high efficacy in the rehabilitation process;
- Hypothesis 2 - The temporal relation between the activation of the muscles involved in continuous movements performed during motor rehabilitation therapies could provide an important support to the study of this type of movement.

The overall aim of this thesis work was, therefore, the optimization and the validation of an EMG-BF system in the post-stroke rehabilitation setting. In this context, a further aim was to broaden the understanding of the relevance of the EMG temporal information in the interpretation of continuous motions.

These objectives were pursued by means of two activities: a clinical trial that employs the proposed system and the analysis of the clinical and instrumental patient data collected during the therapy (described in detail in Chapter 5), and an experimental protocol specifically conceived to investigate the contribution of temporal information and to quantitatively evaluate its relevance in the interpretation of the sEMG signals recorded during continuous movements (described in detail in Chapter 6).

5 The clinical trial

The following chapter describes the developed EMG-BF system and the clinical pilot study that was conducted in order to gain useful information for the definition of the clinical trial. Moreover, the clinical trial and the results of the analysis performed on the available dataset are presented. The goal of the clinical trial was to investigate the characteristics of sub-acute post stroke patients that are eligible for a rehabilitation therapy with the device and the short-term clinical effect of the therapy on the recovery of the hand functionality.

5.1 The EMG-BF system

5.1.1 Hardware

Myo armband (described in Paragraph 2.3.2) has been considered for the present study, nevertheless, some technical requirements have not been met. In fact, Myo transmits a downsampled sEMG signal (sampling frequency 200 Hz) digitalized with low resolution (8 bit) that may cause information loss. Furthermore, the minimum forearm circumference that the armband can support is 19 cm. The muscular hypotonia that may occur in the acute phase of stroke, could prevent some patients from using the device as reported by the therapists of the Cerebrovascular Disease Unit of the San Camillo Hospital (Venezia, Italy), who contributed from a clinical point of view to the realization of the device applied in the present study.

A wearable EMG-BF device was developed by the Artificial Physiology group of the Istituto Italiano di Tecnologia (IIT), Torino. The system was conceived for the application in a clinical environment following principles of electrical and mechanical safety. The system comprises two components: a flexible and stretchable electrode array (Figure 4.A) and an elaboration module (Figure 4.B), the two components are connected through a USB Type-C (Figure 4.C).

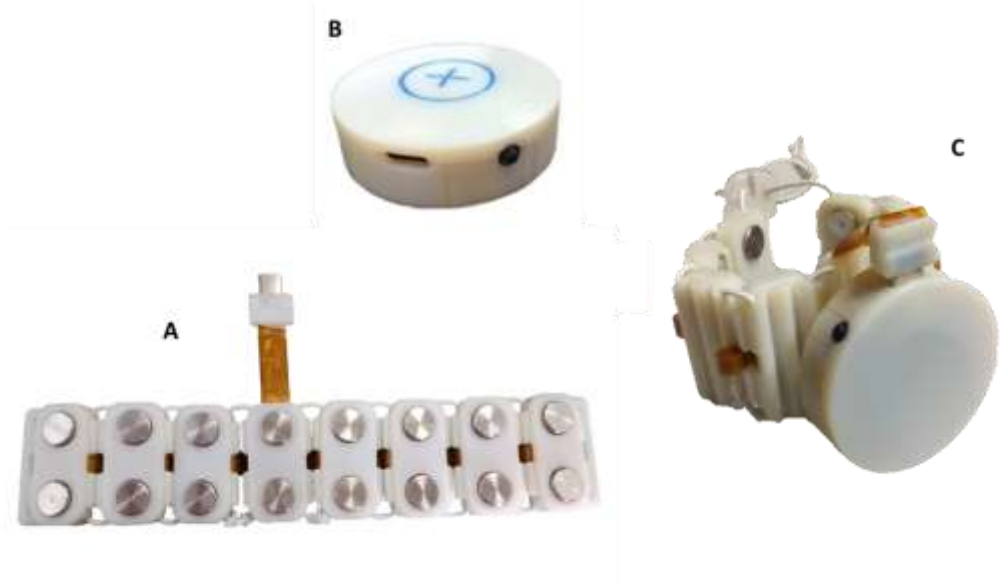

Figure 4. A. Electrode array with USB-C connector. B. Elaboration module with USB-C port and on/off switch. C. Complete set up

The electrode array includes 8 bipolar stainless steel dry electrodes embedded in a biocompatible shell. The electrode diameter is 10 mm with an interelectrode distance ranging from 2 to 3 cm depending on the degree of stretch of the array. This configuration is in line with literature related to movement analysis based on sEMG signals [113], [114]. Several studies have revealed that the classification accuracy of movements based on sEMG improves by increasing the number of electrodes, up to a limit beyond which a plateau is reached. In fact, studies about the optimal number of electrodes needed to analyze hand and finger movements, suggested that 8 electrodes could be a good compromise between classification performance and reduction in the electrode number for practical myoelectric control applications [33], [83], [113]–[117]. The electrode array has been conceived to be placed around the proximal portion of the forearm as shown in Figure 5, over the apex of the muscle bulge (3-5 cm distal to the elbow crease), in order to record signals from muscles physiologically related to wrist and hand movements [118].

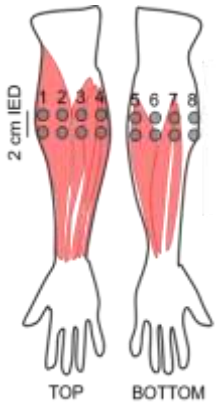

Figure 5. Scheme of electrode positioning on the forearm.

The length of the electrode array ranges between 17 to 27 cm, these values were determined mixing several information related to anatomical forearm percentile of man, woman, old and young people. The system design allows a practical electrode placement from the point of view of the physiotherapist and an efficient adaptation to different upper limb rehabilitation protocols.

The elaboration module (weight [gr]: 40, size [mm]: 50x50x15) integrated an analog front-end for bio-electrical signal acquisition and inertial measurement unit (IMU). Here the signals were band-pass filtered (10-500 Hz), sampled at 1000 Hz and digitally converted (24-bit A/D converter) with a resolution per least significant bit of 0.28 µV. Input impedance is > 90MΩ on the whole bandwidth, the Common Mode Rejection Rate (CMRR) is > 96dB. Furthermore, the elaboration module calculates the Root Mean Square (RMS) of the digitalized signal on a window of 64 ms and transmitted it to a host PC via Bluetooth 4.1 by the included ARM R processor. The elaboration module is powered by a rechargeable 3.7 V integrated battery which lasts around 8 hours of continued use on one charge.

5.1.1 Device classification and compliance aspects

The device is noninvasive, it is an active device intended to not administer or exchange energy and medicines with the body and it is not a diagnosis device. Thus, according to Annex IX of the Legislative Decree 46/97 the class of risk of the device is I.

The conformity of the device with the requirements of the European Community Directives “Electromagnetic Compatibility (EMC) Directive 2014/30/UE” (implemented in Italy by Legislative Decree 80/16) and the compliance with Community Directives “Medical Equipment Directive CEE 93/42, and CE 2007/47” have been verified by an accredited laboratory, with reference to the EN 60601-1-2 and EN 60601-2-40 standards. Safety requirements from the point of view of the

biocompatibility of the device parts that contact with the patient skin are met using certified bipolar stainless-steel electrodes embedded in a biocompatible shell of a polyjet photopolymer, specifically intended for medical purposes including prolonged skin contact and short term mucosal-membrane contact.

5.1.2 Software

A Graphical User Interface (GUI) has been developed with Matlab and provided to the therapists for the clinical trial. The GUI provides a step-by-step guide for positioning the electrode array on the patient forearm, exploiting signals from the accelerometers and gyroscopes integrated in the elaboration module. The RMS signal received from the device is visualized on a radar graph, where each spoke represented one of the channels (Figure 6**Error! Reference source not found.**).

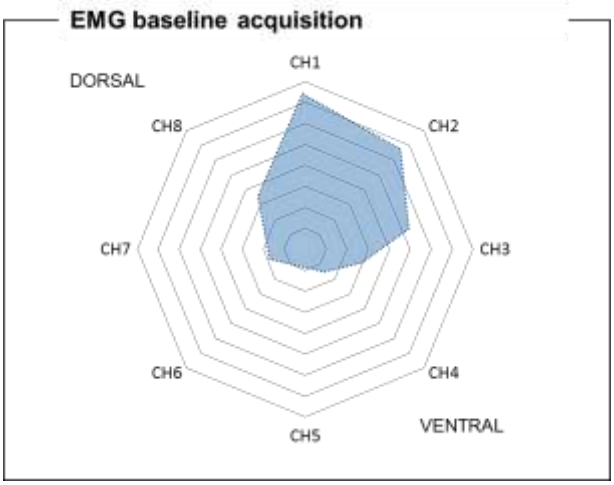

Figure 6. Radargraph of signals recorded from each channel

Thanks to the positioning guide provided by the GUI, the graph shows some anatomical references that allow the evaluation of the EMG patterns associated to each movement. The GUI supports therapists also during the calibration of the device and the execution of the exercises of the therapeutic protocol. The real-time biofeedback is represented by a marker displayed on the PC screen, whose position is related to the RMS signal recorded by the device. The biofeedback control strategy is based on two concurrent aspects: the repeatability of the sEMG patterns that the patient produces during the execution of a specific movement of the hand and/or wrist and the muscular force of the contraction during the movement.

The sEMG patterns repeatability is assessed by a movement recognition algorithm. Since the muscle force and the EMG amplitude depend on the same physiological mechanisms [29], the estimation of

muscle force is performed evaluating the amplitude of the RMS signal. Moreover, the GUI has been optimized to obtain a controller delay <200 ms in order to avoid that the processing delay could be perceivable for the user [119].

The GUI allows local storage of relevant information such as demographic patient data and therapy-related data. For every therapeutic session, type of exercises performed with related parameters and patient's performance (e.g. exercises completion and time requested to complete exercises) are saved. Moreover, all signals recorded and calculated by the device and the GUI during each movement calibration and exercise are stored: RMS signals, control signals generated by the patient (i.e. signals resulting from the RMS processing performed by the pattern recognition algorithm), target signals (i.e. true control signals that the patient should generate to complete the exercise). The complete data set about the rehabilitation session can be post-processed with the aim of monitor patient performance and to tailor the therapy to the specific patient needs.

5.2 Clinical pilot study

In order to evaluate the feasibility of using the aforementioned system in a clinical context on a group of post-stroke patients with different levels of impairment, a pilot study was conducted. The system evaluation was conducted considering the device setup time, the duration of the calibration procedure, and the patients' capability to understand and complete the proposed EMG-BF exercises. Furthermore, two therapy outcomes were calculated with the aim of quantifying the capability to modulate the muscle contraction from patients. Also a group of healthy subjects were involved in the pilot study, in order to assess if the calculated outcomes were able to reveal some differences between neurological patients and healthy subjects.

Subjects were informed about the protocol and signed informed consent form prior to enrollment. Experiments were approved by the Ethics Committee of the Provincia di Venezia and IRCCS San Camillo. The study was carried out in accordance with the ethical standards of the Declaration of Helsinki and participant data have been treated according to the Organic Law of Protection of Personal Data.

Demographics of the participants

Three patients (see Table II for demographic data) were recruited from the Cerebrovascular Disease Unit of the San Camillo Hospital. Inclusion criteria were: age between 18-90 years, mild to severe post-stroke upper limb impairment (0 <FMA-UE< 66) and ability to understand instructions. Exclusion criteria were: epilepsy without a pharmacologic treatment, severe aphasia (Token Test score < 58) and upper limb pain. Table III shows demographic data of 5 healthy subjects that were recruited.

Table II. Demographic data of recruited patients

Patient	***1***	***2***	***3***
Age	60	45	43
Gender	M	M	M
Paretic side	Left	Right	Right
Nature of stroke	Hemorrhage	Hemorrhage	Infarct
Time since stroke (mths)	73	10	8
Time since evaluation (mths)	1	1	1
MAS-UE score	6	0	2
FMA-UE	38	65	52

FMA-UE: Fugl-Meyer Assessment [120] for the upper extremity (maximum score=66)
MAS-UE: Modified Ashworth Scale [121] for the upper extremity (maximum score=20)

Table III. Demographic data of healthy subjects

Subject	***1***	***2***	***3***	***4***	***5***
Age	21	35	27	23	22
Gender	F	M	M	F	F

Experimental setup and protocol

Subjects' forearm length was measured. Thus, the 25% of the forearm length was calculated and used as reference from the elbow crease to position the device. The electrode configuration allowed the acquisition of the sEMG activity of extensor and flexor muscles of the forearm, that make a fundamental contribution to the movement and to the dexterity of the human hand and wrist and to their motor functionalities [118] (Figure 7.A-C).

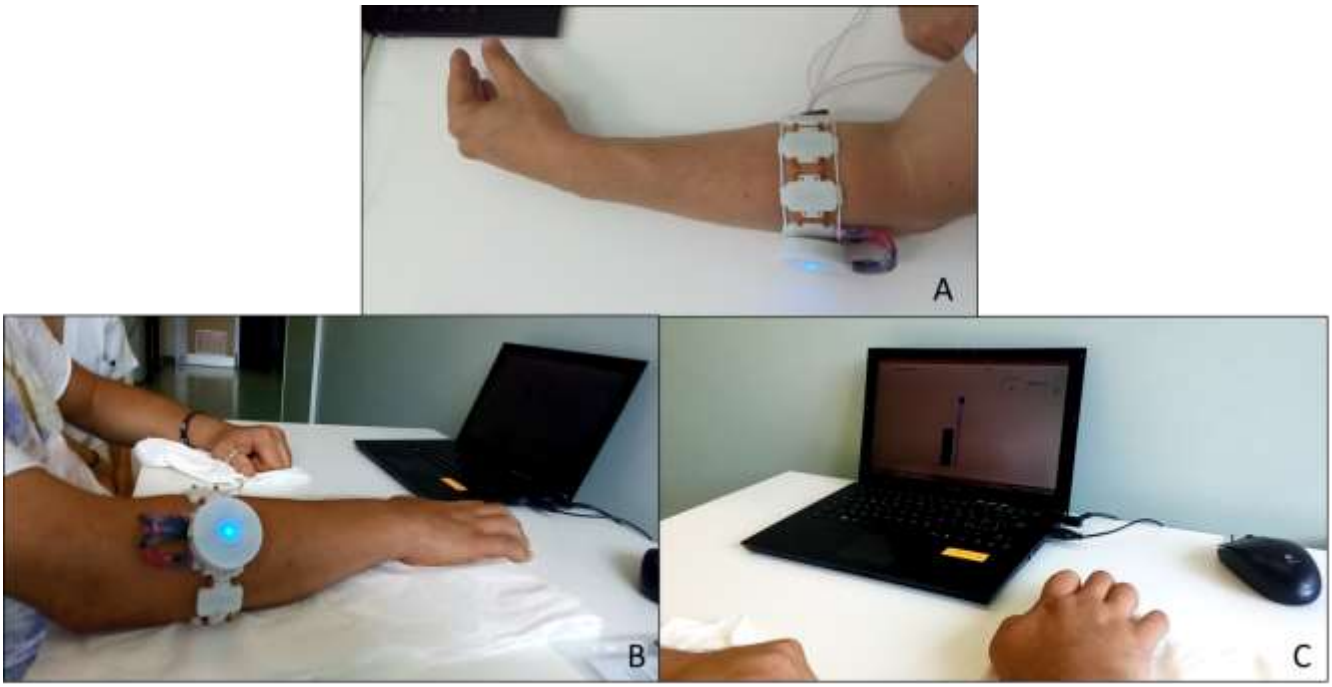

Figure 7. Experimental setup for the pilot study. A) The device positioned on the left forearm of a healthy subject, the stretchable electrode array complies with different forearm circumferences. B) The wireless device positioned on the forearm of a patient impaired side and the PC used to receive EMG data and display the GUI. C) Detail of an exercise displayed during the experimental protocol.

No skin preparation was required. The subject comfortably sat in front of a PC screen with the elbow and the forearm resting on a horizontal surface and with the arm forming a 45° angle with it.

This configuration was maintained during the entire experimental protocol, providing proper corrections during exercises that required a forearm support.

Subjects performed each of the following task:

1. Thumb extension (prone hand) - The thumb moved to the most extended position.
2. Fingers extension (prone hand) - Fingers were extended avoiding involvement of the wrist.

3. Wrist flexion and extension (lateral hand) - Fingers were relaxed during both flexion and extension movements.
4. Hand cupping and fingers extension (prone hand) - During the cupping of the hand, the subject slid the tips of its fingers along the table towards his palm, without fingers flexion and with wrist and forearm in their stationary position. For fingers extension see task number 2.

Calibration

The RMS were visualized on a radar graph, where each spoke represented one of the channels. The EMG background activity (EMG baseline) was firstly acquired in relaxed condition. Afterwards, during the subject-specific calibration phase, EMG activation patterns of each movement included in the task were acquired: users were asked to maintain each target movement for 3 seconds. According to the recorded calibration signals, most active channels were automatically selected as the channels with maximum relative amplitude. The relative amplitude was calculated after removing the baseline activity recorded during the previous phase.

Online test

During the online test, the subject was able to proportionally control the vertical position of a marker modulating the contraction intensity of calibrated movements. Tasks including two movements were managed through a classification algorithm allowing the marker movement in two different directions depending on the performed movement. Two types of exercises have been performed: Reach a target (R-ex) and Jump an obstacle (J-ex) following a trapezoidal profile. Both the exercises are outlined in Figure 8. Tasks comprised 10 cyclic repetitions in which the reference marker or the obstacle changed the vertical position from 50% to 70% of the maximum voluntary contraction (MCV) in a random order. The entire experimental protocol lasted approximately 30 minutes.

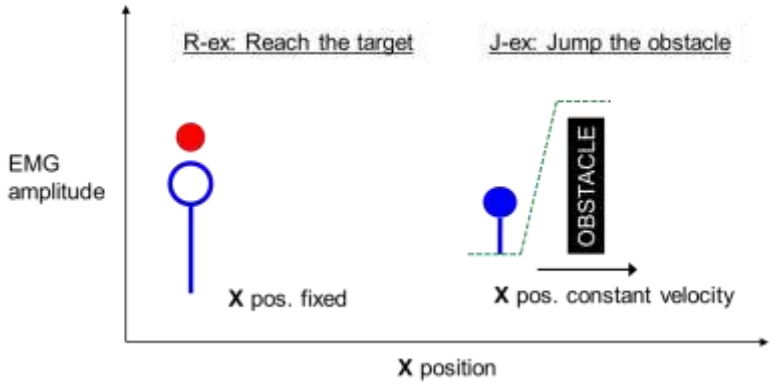

Figure 8. In R-ex the subject had to maintain a large blue marker, indicating the estimated activation level superimposed on a smaller target red circle, representing the desired activation. An auditory signal indicated when the subject succeeded to maintain the correspondence for 0.4 s and the exercise proceeded to the next repetition. In J-ex the user produced a controlled and sustained contraction following a trapezoidal target profile (green dashed line) and without intersecting the obstacle. The marker was controlled in its vertical position and the background with target references moved at a proper constant speed. The obstacle required a constant contraction of 1 s.

Data analysis

The root mean square error (RMSE) between the control signal and the target signal during J-ex was calculated. The parameter was evaluated only during each sustained contraction at required level and not during the entire trapezoidal profile. Values were averaged across all repetitions related to each task.

During each R-ex, the time that the subject took to complete each task repetition was saved. The average needed time across repetitions of each task were evaluated.

RMS signals related to samples during which subjects successfully completed R-ex repetitions, were applied to calculate the ratio between RMS amplitude on selected channels and the mean of RMS amplitude of channels not supposed to be active.

Results of eight subjects were statistically analyzed with the statistics software GraphPad Prism 5 using non-parametric tests. The Friedman test was applied to assess the statistically significant difference at the group level. If the Friedman test determined the difference, the conditions were compared pairwise using the Wilcoxon signed-rank tests with Bonferroni correction. A level of $p<0.05$ was selected as the threshold for the statistical significance.

Results

All subjects succeeded to complete the entire experimental protocol. The setup time lasted less than 3 minutes and the calibration of the movements described in section II-B lasted approximately 10 minutes. These timings are consistent with guidelines for post-stroke rehabilitation technology design.

Figure 9 shows the EMG-BF signal (blue line) generated by one representative patient during a J-ex of wrist flexion and extension. The patient was able to produce a contraction higher than the obstacle (constant phase of the trapezoidal profile) with both movements, accomplishing the exercise 10 repetitions. Nevertheless, the blue signal presents fast rising/falling edges, suggesting a poor muscular contraction modulation.

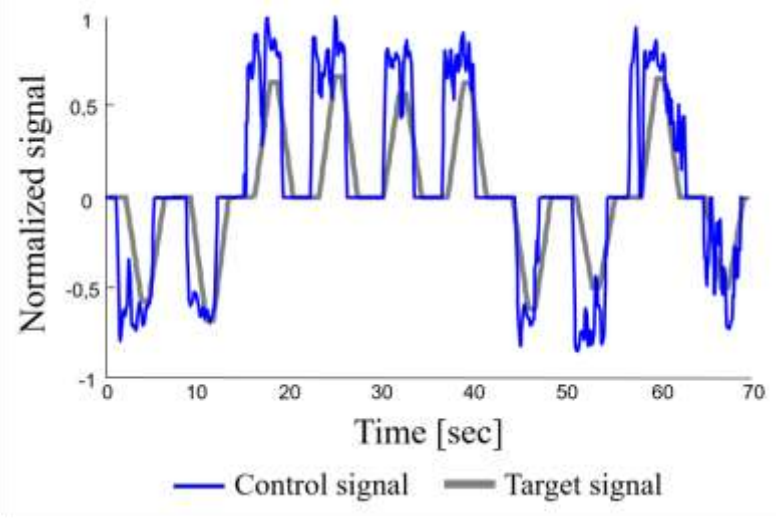

Figure 9. EMG-BF produced by a representative patient (p1) during the J-ex of wrist flexion and extension.

The patient lack of modulation is underlined in Figure 10, that shows the RMSE (median and interquartile range - IQR 25% - 75%) between control signal and target signal calculated for all the J-ex. It can be observed that patients' data have a considerably higher median values (0.4-0.82 for patients vs 0.18-0.2 for healthy subjects) and a higher IQR if compared with healthy subjects data. Specifically (as shown in Figure 10), the Mann-Whitney test performed to reveal the statistically significant difference between not normally distributed groups, shows that there is no difference between accuracy reached by healthy subjects (s1, s2, s3, s4, s5), who consistently differs from p1 and p2 ($p<0.01$).

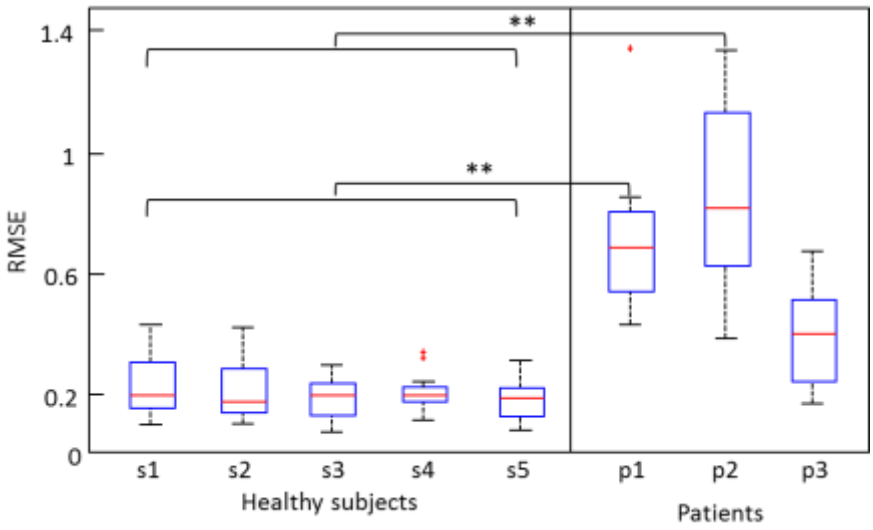

Figure 10. RMSE (median and interquartile range - IQR 25% - 75%) between control signal and target signal calculated during the constant sustained contraction of J-ex. Results of the Mann-Whitney reveal statistically significant differences between the group of healthy subjects and p1 and p2, with p-value<0.01.

During the R-ex, an outcome of the exercise was the time that the subject needed to complete a task repetition. As shown in Figure 11, patient timings have median values from 2.6 s to 3.8 s while healthy subjects data ranges between 1.7 s and 2.6 s. Also in this case healthy subjects perform similarly without statistical difference within the group, according to the Mann-Whitney test. Median and IQR of the patients are distributed in a wide range of values, and specifically p1 statistically differs from s1, s2, s3, s4 and s5 ($p<0.01$).

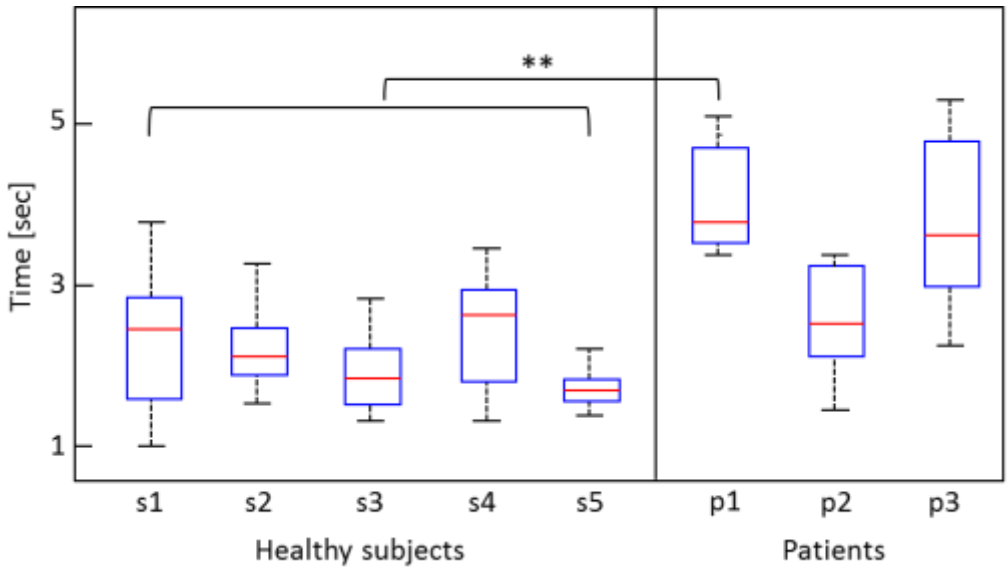

Figure 11. Time required to reach a target (median and interquartile range - IQR 25% - 75%) during R-ex. Results of the Mann-Whitney reveal statistically significant differences between the group of healthy subjects and p1, with p-value<0.01.

Although post-stroke patients had a less accurate modulation of the intensity of the contraction, their timings in concluding a repetition are not extremely higher if compared to those of healthy subjects because the trained movement and the intensity of the requested contraction were personalized during the training phase of the algorithm.

During the calibration phase, the maximum RMS value and most active channels were selected. An additional outcome of the training session was the ratio between the RMS amplitude recorded on the selected channels and the mean RMS amplitude of all other channels during Reach tasks. As shown in Figure 12, for all the subjects the activity related to the selected channels is higher than the mean activity over channels not supposed to be active.

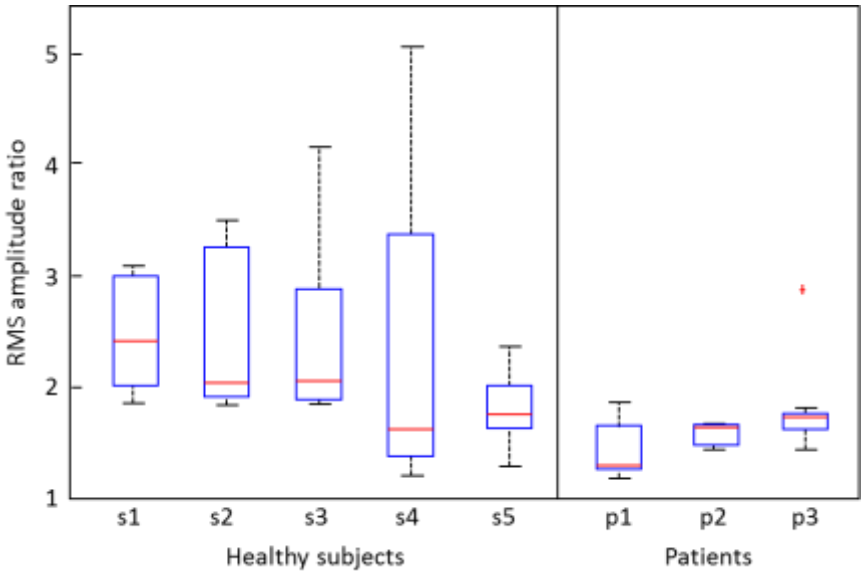

Figure 12. Ratio between RMS value of selected channels and channels not supposed to be active (median and interquartile range - IQR 25% - 75%) during R-ex. The Mann-Whitney reveals no statistically significant differences between groups ($\chi 2=11$, $p=0.13$).

The median values of the ratio are slightly higher in healthy subjects (selected channels activity is from 1.6 to 2.4 times left over channels) with respect to patients (the ratio is from 1.34 to 1.7), nevertheless the Mann-Whitney test shows that there is no statistical difference between subjects ($\chi 2=11$, $p=0.13$). According to this results the device configuration and the channel selection strategy was effective to recognize movements included in the training protocol.

Conclusions from the pilot study

The aim of the pilot study was to preliminarily test the system which was conceived to address the main recommendation for rehabilitation technology design according to the ICF [46]. These criteria

are related to the comfortability of the sensor system and to the use of intuitive and clear feedback to avoid possible attention-capacity overload.

The electrode application, which did not require skin preparation and the flexible bracelet allowed quick configuration of the acquisition system by the therapists and a good adaptability to different forearm sizes. The graphical interface drove the execution of repetitive hand rehabilitation tasks, providing feedback proportional to the exerted force and allowing the complete execution of the protocol by all patients. Moreover, the subject-specific calibration made it possible to personalize tests according to the muscular activity and to the degree of impairment of each subject. The patients reported that the movement of the marker was synchronized and congruent with the type and the intensity of contraction they were trying to perform. The therapy outcomes related to contraction strength and degree of motor control were able to revealed the pathological condition of stroke patients with respect to healthy subjects.

In conclusion, the application of the system to a clinical environment showed promising perspectives and the experience gained from this pilot study has been applied to improve the definite EMG-BF protocol. The specific observations are both therapy, and software- and hardware- related:

Therapy-related criteria

- The system should promote patient-tailored therapies: training intensity and frequency need to be parametrized and the therapist should be able to set parameters according to the degree of impairment and to the rehabilitation stage. The aim is to provide to each patient and at every therapy stage a challenging but not frustrating set of exercises.
- Spasticity following a stroke occurs in about 30% of patients [122], thus the system should give a feedback about the relaxed condition before and after each repetition of the exercise;
- The sensitivity of the control signal (i.e. the minimum variation of EMG signals that determines a variation in the control signal) need to be adapted to the rehabilitation context and adjustable according to the patient degree of impairment.
- The therapy should stimulate patient attention and participation through a greater variability in the exercises and feedback.
- Patients enrolled to a further clinical trial should have a minimum cognitive function in order to understand the cognitive task (study inclusion/exclusion criteria).

Software- and hardware-related criteria

- More audio feedback should be added to give clearer instructions to the patient.
- The use of images is preferable to make the GUI instructions more intuitive.
- The intervention of the therapist in the exercise session (prematurely ending the session or modifying some parameters of the exercise) should be minimum but always feasible and it should not entail loss of data.
- Data recorded during the therapy should be managed and organized in order to provide both KR and KP biofeedback, thus a complete set of parameters related to the patient and the therapy should be save for further elaboration.

5.3 Study protocol design

The clinical trial planned for the device was approved by the Ethics Committee of the Provincia di Venezia and IRCCS San Camillo on 21/03/2017, obtained the approval of the Health Department and started on 15/10/2017.

The study duration is two years and consists of two potentially concomitant phases. The first phase is a cross-sectional study (named *Screening*). The control of the device by patients is appropriate if the subject succeeds in the calibration of the protocol movements and in addition, if he/she is able to manage the visual feedback through the calibrated movements. In addition, during the Screening phase, the patients that are enrolled for the second phase of the study are selected. The second phase is a longitudinal pilot study (named *Therapy*) for the evaluation of the clinical effect and safety of a rehabilitation therapy performed with the device.

For the cross-sectional study, clinical outcome measures are evaluated once, before the beginning of this phase. The longitudinal study provides for three evaluation phases:

1. Initial evaluation: before the beginning of the therapy (T0);
2. Final evaluation: at the end of the therapy (T1);
3. Follow-up assessment: after one month (T2).

Clinical assessments are detailed in Table IV.

Table IV. Clinical assessment scales measuring motor and sensory deficits

Assessment scale	Measuring	Scoring
FMA-WH: Fugl-Meyer Assessment scale of wrist and hand [120]	Motor impairment of the wrist and hand	0-24 points (lower scores indicate greater impairment)
FMA-UE-SPJM: Fugl-Meyer Assessment scale of range of motion of joints and Joint pain (upper limb) [120]	Range of motion and joint pain of the upper limb	0-48 points (lower scores indicate greater pain and lower range of motion)
FMA-UE-SF: Fugl-Meyer Assessment scale of upper limb sensory function [120]	Sensory function of the upper limb	0-24 points (lower scores indicate lower sensory function)
RPS: Reaching performance scale [123]	Compensatory movements used during the transport phase of reaching	0-36 points (higher scores indicate less compensatory strategies)
BBT: Box and Block Test [124]	Functional level in dexterity	Number of transported blocks in one minute (larger scores indicate better dexterity)
NHPT: Nine Hole Pegboard Test	Functional level in fine dexterity	Ratio between the number of transported pegs and time interval (50 s) (larger scores indicate better fine dexterity)
MAS-UE*: Modified Ashworth Scale of upper extremity [125].	Spasticity level of the upper limb muscles	Sum of all five joints: 0-25 points (lower scores indicate less spasticity)
FIM: Functional Independence Measure	Level of disability in ADL	0-126 points (lower scores indicate lower independence)

*Only values related to Flexor carpi, Flexor digitorum profundus, Flexor digitorum superficialis have been considered for the present study

The clinical assessment scales will be employed to evaluate the therapy efficacy. The FMA-UE scale will be monitored and in accordance with literature [126], an improvement of 5 points from T0 to T1 is representative of clinically important changes. Moreover, clinical assessments will be applied to evaluate the treatment effect size and to quantify the sample size of a randomized controlled study (RCT) [127], expected for the next stage of the research.

5.3.1 Experimental setup

The experimental setup of the pilot study has been replicated since it allowed the acquisition of the sEMG activity of extensor and flexor muscles of the hand. A rigid forearm support has been provided during all exercises to increase patient comfortability and ergonomics (Figure 13).

Figure 13. The patient sat on a wheelchair or on a chair depending on his/her trunk control level. The PC and the forearm support (size [cm]: 54x26x9) located on a height adjustable mobile table.

5.3.2 Experimental protocol

The exercises proposed during the therapy involve coarse movements of the wrist and fine motions of the fingers. These exercises are typically proposed during upper limb rehabilitation sessions:

- Wrist pronation
- Wrist supination
- Wrist flexion
- Wrist extension
- Wrist abduction
- Wrist adduction
- Finger flexion
- Finger extension
- Thumb abduction
- Pinch

As suggested by the notion that repetition of identical movements is the basis of motor learning and as highlighted by some studies that applied the same concept to rehabilitation protocols [128]–[130], the therapy is based on the repetitive training of each movement. Moreover, the patient is required to relax forearm muscles to successfully complete a movement repetition. The feedback about the relaxed condition before and after each repetition of the exercise has been included with the aim of monitoring also the degree of inability to fully relax as a result of impaired motor control.

5.3.2.1 Screening protocol

The cross-sectional study procedure is performed once for each patient and consists of two phases: the calibration of each movement and the control of the visual feedback performing calibrated movements. During the calibration phase, the patient is asked to perform each movement and to maintain the contraction for 3 seconds. A movement is successfully calibrated if the amplitude of the RMS signal recorded during a Maximum Voluntary Contraction (MVC), exceeds a threshold proportional to the baseline signal recorded during the rest position. Then, for each calibrated movement, the patient ability to control the device with the specific movement is investigated: the patient performs 6 repetitions of *reach a target* exercise described in paragraph 5.2 of the present thesis, and consists in proportionally controlling the vertical position of a marker modulating the contraction intensity of the movement. The reference marker has a constant position that corresponds to the range 20%-40% of the MCV. The maximum time to perform each repetition is 10 seconds, if the patient successfully completed at least 1 repetition, it is able to control the device with the specific movement. The maximum duration of the test is 30 seconds for each movement. Thus, the entire procedure can last approximately from 15 to 30 minutes.

5.3.2.2 Therapy protocol

During the longitudinal pilot study, the rehabilitation therapy is administered to patients who successfully control the device and have been enrolled in the *Therapy* phase. Before each session, the calibration of all movements is repeated to reveal if the patient spontaneously recovers the control of new movements with respect to the previous session. The duration of the entire EMG-BF therapy is 15 hours as suggested by the literature evidence [131], [132], that investigated the minimum time required for a therapy with augmentative technologies (i.e. Robot, Virtual Reality Environments, Biofeedback supported therapy) to be clinically effective. Patients receive one-hour session per day, five days a week for three consecutive weeks. Missed sessions are made up as early as possible.

Four types of exercises are available for the therapy protocol and are presented in the following paragraphs. Figures show the GUI screen associated, an illustrative description is presented for the first exercise and is valid for the structure of all the other cases.

1. **Exercise Bar**: in this exercise the patient has to maintain the top of a bar (the marker) on a grey square which becomes green if the marker is in the right position, representing the range of the desired activation level, for a minimum amount of time. Then, the patient has to take

back the marker under a threshold level. The marker is controlled through the intensity of the contraction. The bar top can be moved in a maximum of 4 directions, each direction is associated to a different movement according therapist settings. Figure 14 shows the GUI visualized during this exercise, three main sections are included:

- A *settings panel* (sections B and C) for the selection of the movements and related directions and for the exercise parameter selection, moreover it allows to turn on/off the sound signal (section E);
- Play/Pause and Stop *buttons* (section F), so that the therapist can manage the exercise if it is necessary;
- Sections for the *feedback* that the GUI provides to the user about the exercise type (sections A), the progress of the exercise (sections D) and the performed muscular activity (section G).

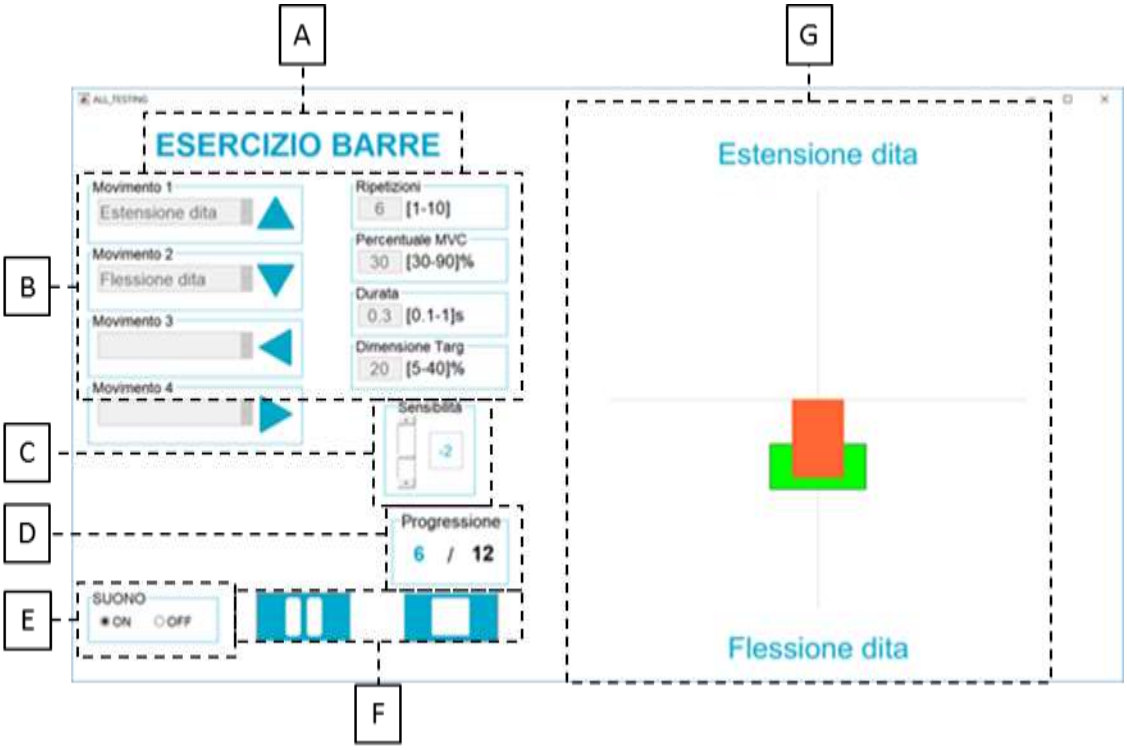

Figure 14. User interface visualization during the exercise *Bar*

2. **Exercise Ball**: in this exercise, the patient has to move a ball from its initial position to its target position, represented by a grey circle. The ball can be moved in a maximum of 4 directions by means of likewise movements. The association between directions and movements is set by the therapist.

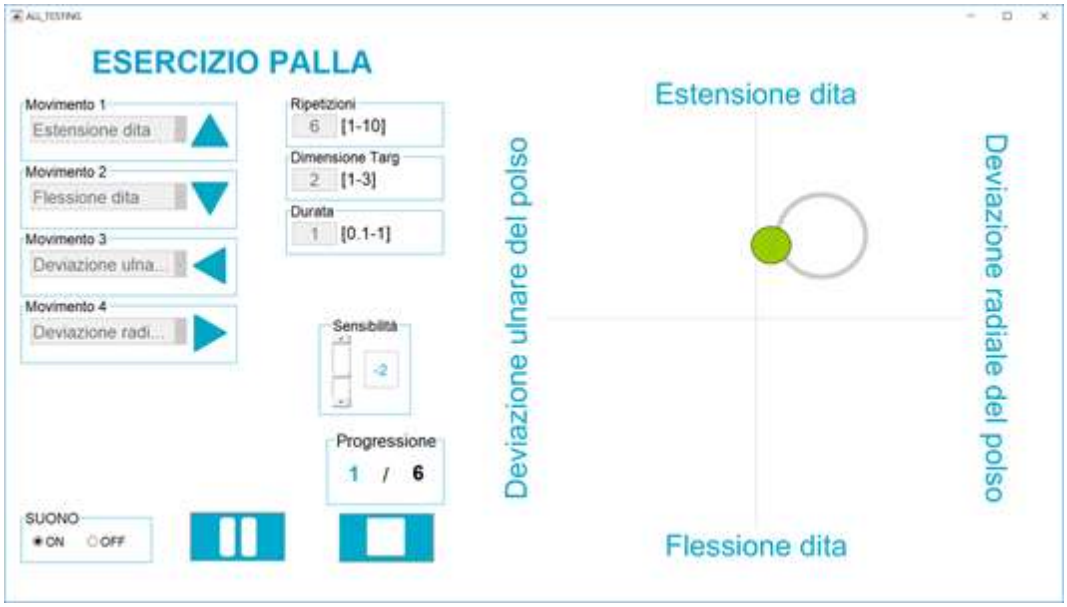

Figure 15**.** User interface visualization during the exercise Ball

3. **Exercise Jump**: a ball is controlled in its vertical position and the background, with target references, moves at a constant speed. The patient produces a controlled and sustained contraction avoiding the obstacle. The marker can be moved in a maximum of two directions.

Figure 16. User interface visualization during the exercise *Jump*

4. **Exercise Arrow**: this exercise is a variation of the jump exercise. The marker can be moved in a maximum of two directions. The arrow movement in each direction is controlled by different movements and the target position moves at a constant speed.

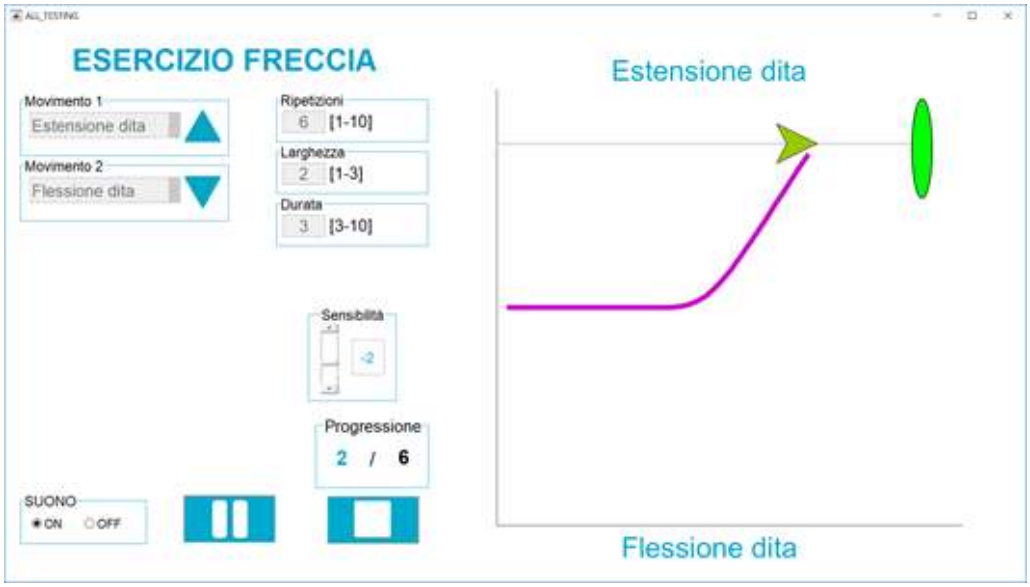

Figure 17. User interface visualization during the exercise *Arrow*

Exercises can be grouped according to two aspects: the real-time feedback strategy control and if the movement execution timing is constrained by the GUI or not.

With regard to the biofeedback control strategy, in exercises *Bar* and *Jump* the position of the marker is proportional to the intensity of the muscular contraction: whenever the RMS amplitude increases, also the marker distance from the initial position increases and the marker accelerates, when the RMS amplitude decreases, the marker distance also decreases, and the marker gets slower. In exercises *Ball* and *Arrow*, only the marker speed is proportional to the contraction intensity and if the RMS amplitude decreases and tends to the baseline, the speed decreases until the marker stops in the position reached at that moment. This type of exercises had been introduced to remove, from the BF control strategy, the aspect related to muscular force and to concentrate on the repeatability of the sEMG patterns. This control strategy could be applied if the therapeutic exercise is focused on the execution of the right movement or if the impairment level of the patient in modulating the muscular contraction prevents the execution of exercises *Bar* and *Jump.*

Regarding the constrained or not timing of the movement execution, in exercise *Jump* and *Arrow*, the background of the GUI screen moves at a constant speed, requiring that the muscle contraction is performed at a specific moment.

In accordance with the therapy-related criteria that technological solutions for rehabilitation should meet which have been individuated by Hochstenbach et al. [110], the GUI allows the therapist to perform a patient-tailored therapy. With this aim, the therapy is modular, and each exercise can be associated with different movements according the type of patient motor impairment. Moreover, the degree of difficulty of the therapy can be modulated through a series of parameters: the number of movement repetitions to successfully complete an exercise, the required muscular contraction force (calculated as percentage of the MVC recorded during the calibration phase), the duration of an exercise repetition and the dimension of the target. The following table presents the range of the parameters for each exercise.

Table V. Summary of exercise parameters

Exercise	Repetition number	%MVC [%]	Repetition duration [s]	Target dimension
Bar	1-10	30-90	0.1 - 1	5-40%
Ball		N.A.		1-3
Jump		10-90	3 - 10	5-50%
Arrow		N.A.		1-3

For exercises *Bar* and *Ball*, the duration of a repetition is the maximum waiting time for the exercise to move forward to the next repetition, while for exercises *Jump* and *Arrow* it is proportional to the target speed. Moreover, the target dimension parameter for exercise *Bar* is the percentage variation of the target vertical size with respect to the selected MVC, while for exercises *Ball* and *Arrow* it is the multiplier factor between the dimension of the target and the dimension of the ball, finally for exercise *Jump* it is the percentage width of the obstacle calculated with respect to the repetition duration.

5.3.3 Participants

The stroke patients are recruited from the Cerebrovascular Disease Unit of the San Camillo Hospital. All these patients are hospitalized and identified according to the recommendation of the Italian guidelines “The Stroke Prevention and Educational Awareness Diffusion” (SPREAD) [133] for stroke

prevention. The confirmation of the diagnosis of stroke and the location of the side affected are obtained following the criteria of the Oxford Community Stroke Project (OCSP) and the results of Computerized Axial Tomography (CAT) or Magnetic Resonance Tomography (MRT).
Prior to being enrolled, all patients are informed about the study and gave written consent.

Study inclusion and exclusion criteria

Eligible patients have to receive a clinical diagnosis of hemorrhage or ischemic stroke with a score in the Functional Independence Measure (FIM) [134] ≤100. There is no age limit. Exclusion criteria include: depression diagnosis, head injury, epilepsy without a pharmacologic treatment, apraxia or severe aphasia (Token Test score < 58). These criteria guarantee the enrollment of a stroke population which needs for intensive rehabilitation therapy, without cognitive impairment which could impair their capacity to take part in the research.

Sample size

The expectation for the cross-sectional study is that at least the 90% of enrolled patients succeeds in efficiently interacting with the EMG-BF device, with a level of confidence of 90% and precision of 5%. Thus, the sample size estimated is 97.4 patients [135]. The enrollment of 100 patients is suitable to the statistical analysis that will be performed on data. The sample size of 40, for the longitudinal pilot study is determined according previous pilot studies for robotic treatments [136], [137].

5.3.4 Statistical analysis

Statistical analysis is performed on the data from the longitudinal study, with the aim of designing a randomized control study. Depending on the results of the Shapiro-Wilk normality test, the two-sample t-test (parametric test) or the Wilcoxon test for paired data (non parametric test) is used to compare patient clinical assessments across different evaluation phases (T0, T1 and T2).
Logistic regression is used to estimate the probability that a patient can receive the EMG-BF based therapy. Clinical assessment scales (i.e. Fugl-Meyer Upper Extremity, Reaching Performance Scale, Modified Ashworth Scale, Nine Hole Pegboard Test, Box and Block Test, see paragraph 5.3) are used as the covariates of the model. The Cohen's *d* effect size is calculated for all clinical outcomes. The effect size is then applied to determine the sample size of the randomized controlled study that will be performed in the future.

5.4 Preliminary study of results

The clinical trial presented in the previous paragraphs was still ongoing when the dataset analyzed in the present thesis was acquired. The cross-sectional study and the longitudinal study have been simultaneously performed and twenty-eight and four patients have been respectively recruited. Since the two phases of the clinical trial differ in protocols, main objectives and sample size, the related datasets have been separately studied. The performed analysis partially differed from the statistical analysis planned for the clinical trial, because the number of recruited patients was lower than the sample size estimated for the complete study. The preliminary dataset has been assessed with the aim of investigating the relation between data recorded with the EMG-BF device and patient clinical data. A level of $p<0.05$ was selected as the threshold for the statistical significance.

5.4.1 Cross-sectional study

5.4.1.1 Participants

Twenty-eight post-stroke patients (eleven females and seventeen males, 65±12 years old (mean±std)), recruited from the San Camillo Hospital, were considered for the analysis of the cross-sectional study data. Based on the FMA-UE, patients are stratified into different severity levels: severe (0-20), moderate (21-50), mild (51-66) [120]. Each category of motor impairment was represented as follow: 39.28% of patients showed severe, 21.42% showed moderate and 39.28% showed mild upper limb impairment. Most patients (75%) suffered from ischemic strokes, the populations were comparable from the point of view of affected side (46% suffered from right-side stroke, 54% from left-side stroke). Table VI details patients' demographics.

Patients have been divided in two groups depending on their capability in controlling the device with the entire set of movements included in the experimental protocol: patients who succeeded in completing the protocol have been included in the group called Complete Group (CG), patients who failed in controlling the device with one or more movements or needed support by the therapists, have been included in the group called Not Complete Group (NCG).

Table VI. Demographic data of patients enrolled in the cross-sectional study. FMA-UE (-WH): Fugl-Meyer Assessment of Upper Extremity (Wrist and Hand); FMA-UE SPJM: FMA-UE Scale of Pain and range of Joint Motion; FMA-UE SF: FMA-UE Sensory Function; RPS: Reaching Performance Scale; BBT: Box and Blocks Test; NHPT: Nine Hole Pegboard Test; MAS-UE: Modified Ashworth Scale of Upper Extremity ; FIM: Functional Independence Measure; Severity: based on the FMA-UE - severe (0-20), moderate (21-50), mild (51-66)*[115]

Patient	Age	Gender	Paretic side	Nature of stroke	Time since stroke	FMA-UE (-WH)	FMA-UE SPJM	FMA-UE SF	RPS	BBT	NHPT	MAS-UE	FIM	SEVERITY*
P1	77	F	R	Isc.	1.8	66(24)	48	24	34	57	0.6	0	121	mild
P2	75	M	L	Isc.	3.7	4(0)	44	13	0	0	0.00	0	68	severe
P3	45	M	R	Hemod.	37.3	4(0)	39	11	0	0	0.00	4(211)	70	severe
P4	83	F	R	Isc.	1.8	58(21)	46	19	36	59	0.56	0(000)	103	mild
P5	59	M	R	Isc.	11.4	10(0)	41	13	0	0	0.00	4(400)	96	severe
P6	49	M	R	Hemod.	3.3	5(0)	34	2	0	0	0.00	4(211)	45	severe
P7	73	F	L	Isc.	0.5	2(0)	45	18	0	28	0.00	3(111)	37	severe
P8	82	M	R	Isc.	1.6	66(24)	48	24	36	57	0.69	0	112	mild
P9	76	M	L	Isc.	0.9	63(23)	46	19	34	32	0.26	0	71	mild
P10	83	M	R	Isc.	69.5	18(6)	33	16	13	0	0.00	0	80	severe
P11	67	M	L	Isc.	10.6	42(9)	46	22	24	9	0.02	1(100)	114	moderate
P12	71	M	R	Isc.	4.0	33(8)	38	23	17	0	0.00	1(100)	113	moderate
P13	57	F	L	Isc.	0.4	51(17)	41	22	27	29	0.29	0	103	mild
P14	61	F	R	Isc.	0.4	58(23)	48	24	36	27	0.39	0(000)	116	mild
P15	75	F	L	Isc.	1.3	42(11)	48	12	31	30	0.00	1(100)	62	moderate
P16	55	F	L	Isc.	0.7	54(17)	48	24	29	33	0.04	0	118	mild
P17	45	F	L	Hemod.	29.6	11(0)	33	20	3	0	0.00	7(432)	104	severe
P18	52	F	L	Hemod.	2.5	63(24)	44	24	36	65	0.69	0	99	mild
P19	48	M	L	Hemod.	45.3	2(0)	42	6	0	0	0.00	12(001)	56	severe
P20	66	M	L	Isc.	0.6	57(24)	46	23	34	53	0.5	0	106	mild
P21	71	F	R	Isc.	4.6	7(0)	34	23	0	0	0.00	2(200)	75	severe
P22	78	M	L	Hemod.	1.2	45(18)	45	19	31	16	0.10	0(000)	63	moderate
P23	74	M	R	Isc.	0.9	65(24)	48	12	35	48	0.45	0	36	mild
P24	62	M	R	Isc.	1.5	59(15)	45	24	36	52	0.45	0(000)	116	mild
P25	73	M	L	Isc.	0.6	4(2)	46	22	0	0	0.00	0	46	severe
P26	67	M	R	Hemod.	7.8	9(5)	34	14	0	0	0.00	0(000)	65	severe
P27	63	F	L	Isc.	44.03	36(8)	45	22	18	16	0.02	3	112	moderate
P28	45	M	R	Isc.	23	34(11)	48	24	13	6	0	3	119	moderate

5.4.1.2 Statistical analysis

Clinical data

The statistical analysis of clinical data of the cross-sectional study has been performed with the statistics software GraphPad Prism 5 and included 3 phases. After a univariate analysis of patient clinical outcomes (phase 1), a bivariate analysis (phase 2) was performed to evaluate the differences between the group of patients that were able to successfully control the device with all the proposed movements and the patient group that failed in controlling the device with one or more movements. During the third phase, clinical outcomes that had statistically significant differences between the two groups of patients, were further analyzed and cut-off values able to discriminate patients were calculated.

The following paragraph shows the results of the univariate analysis of variables.

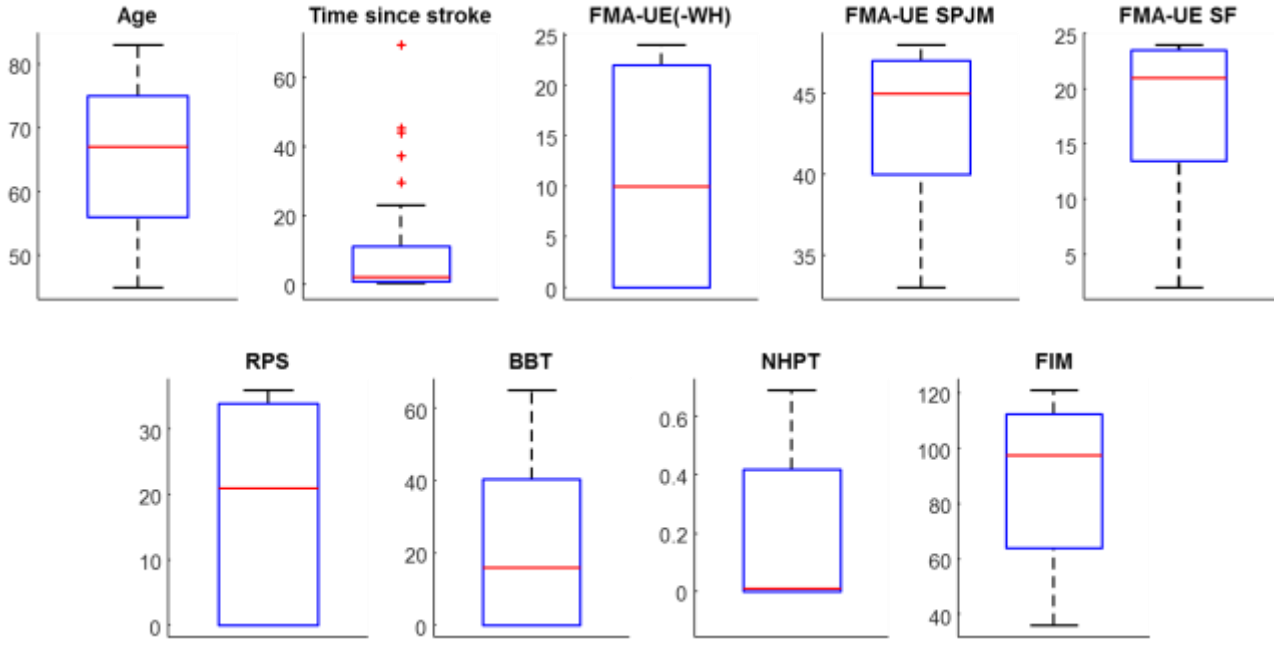

Figure 18. Boxplots of quantitative clinical variables.

The boxplot of each quantitative variable of the population is shown in Figure 18. Results show that Age has a symmetrical distribution, Time since stroke, BBT and NPHT are positively skewed, which means that the bulk of observations shows higher frequency of high valued scores for the related variables, while FMA-UE SJM, FMA-UE SF and FIM are negatively skewed. The only data set that contains outliers is the Time since stroke variable set, with 5 patients with anomalous values.

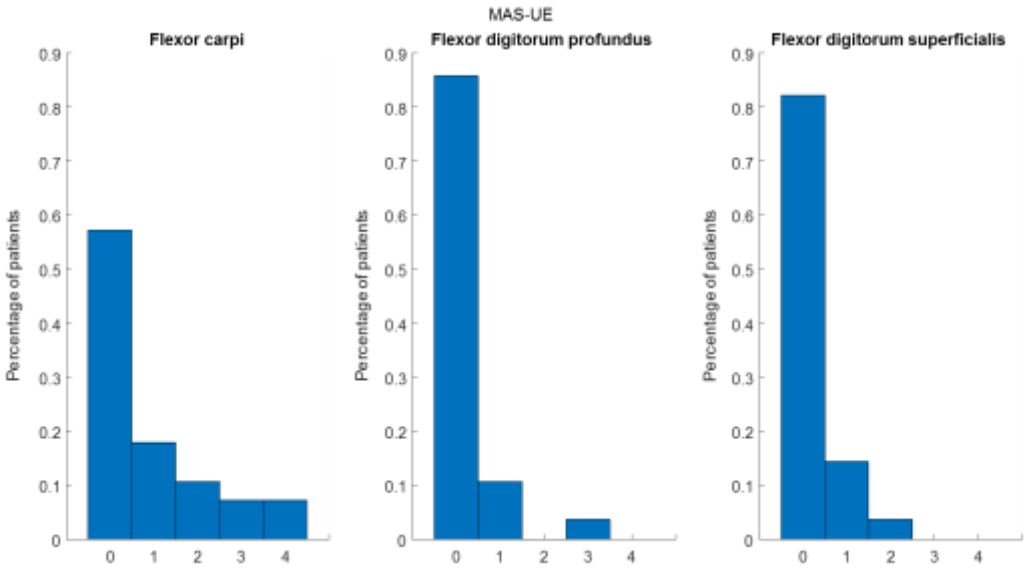

Figure 19. Histograms representing the percentage of patients for each degree of muscle spasticity of the MAS

Figure 19 shows the percentage of patients with regard to the muscular spasticity of hand muscles measured whit the MAS. Most patients show no increase of muscle tone in the investigated muscles.

A bivariate analysis has been performed to reveal a statistically significant difference between patients included in the CG or in the NCG. Normality of quantitative variables of patient groups has been verified by the Shapiro-Wilk test with a significance level of 0.05. Normality has been verified in both groups only for Age, thus the t-test was applied to investigate the statistical statistically significant difference between the two groups for this variable. All other variables were compared through the Mann-Whitney test.

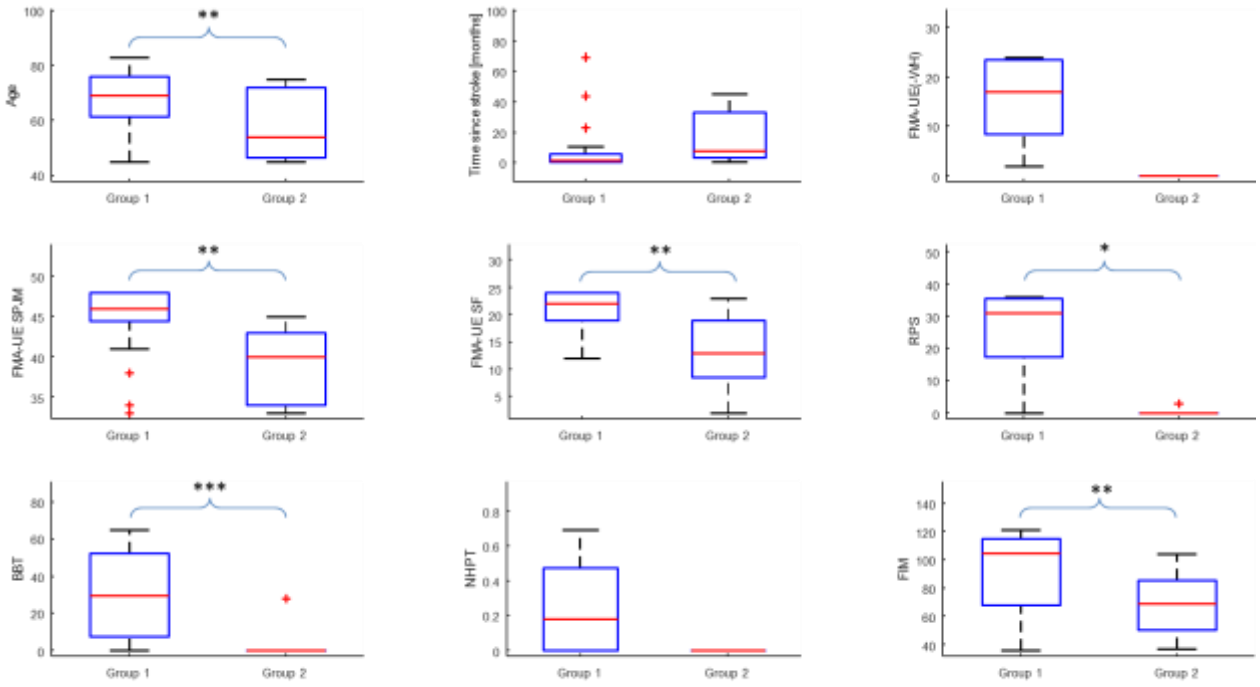

Figure 20. Boxplots of the bivariate analysis performed to compare the clinical data of patients of Complete Group and Not Complete Group. * ($p<0.05$). ** ($p<0.01$). *** ($p<0.001$).

Figure 20 shows the boxplots of the quantitative variables, separately for CG and NCG and reports the statistical significance of the difference between the groups. Median values of CG and NCG are similar only for Time since stroke variable, all other variables show higher median values for patients in CG. FMA-UE and NHPT for patients who failed in completing the entire protocol are equal to 0, thus the Mann-Whitney couldn't be performed. RPS and BB distributions contain one outlier with respect to the rest of the values which are equal to 0. CG presents some outliers for Time since stroke and FMA-UE-SPJM with three values respectively higher than 10 and lower than 41. The variability is similar for every variable, except for FMA-UE-SF with a standard deviation, for NCG, which is twice than the standard deviation of CG.

The percentage of patients included in CG and NCG and related qualitative variables have been calculated and are shown in Table VII.

Table VII. Distributions of Complete Group (CG) and Not Complete Group (NCG) regarding the qualitative clinical variables

	Gender		Affected UE		Nature of stroke		Flexor carpi		Flexor digitorum profundus		Flexor digitorum superficialis	
	M	F	R	L	Isc	Hemod	0	1-4	0	1-4	0	1-4
CG	60	40	50	50	75	25	75	25	85	15	85	15
NCG	60	40	50	50	50	50	25	75	63	38	38	63

The percentage values for Gender and Affected UE are equal for CG and NCG. Most patients who completed the protocol with the entire set of movements suffered from Ischemic stroke while patients who failed are equally distributed. Flexor carpi and Flexor digitorum superficialis MAS values reveal a higher spasticity level in patients of NCG, with most patients showing MAS values between 1 and 4. Instead, the distribution of patients in regard to the Flexor digitorum profundus MAS value has no difference between the groups.

The Fisher's exact test has been applied to assess the significance of categorical (Gender, Nature of stroke and Affected UE) and ordinal variables (Flexor carpi, Flexor digitorum profundus, Flexor digitorum superficialis values of the MAS) in determining if a patient belongs to Complete Group or to Not Complete Group. MAS values from 1 to 4 have been aggregated as the related percentage of patients was considerably lower with respect to the percentage of patients with MAS values equal to 0 (see Figure 19). The Fisher's exact test rejected the null hypothesis of independence for Flexor carpi (p-value = 0.0283) and Flexor digitorum superficialis (p-value = 0.0114). All other tested variables proved to be independent from the Group.

The bivariate analysis highlights that some clinical data can reveal if a patient is able to manage to EMG-BF system and be involved in a rehabilitation protocol based on the system. Nevertheless, it could be of interest to determine the threshold values of these parameters. With this aim, the clinical outcomes that had statistically significant differences between the two groups of patients, have been further analyzed and cut-off values able to discriminate patients have been calculated. The study was based on the Receiver Operating Characteristic (ROC) curve analysis. The Area under the ROC Curve (AUC) has been calculated for each variable and a threshold of 0.7 has been selected to highlight variables that sufficiently discriminate patients. All variables have been found suitable ($0.7344<AUC<0.8438$). Cut-off values have been individuated with the aim of guarantee the best

compromise between the sensitivity and the specificity of the test [138]: the point on the ROC curve closest to the 0.1 has been selected. Results are detailed in Table VIII.

Table VIII. Results obtain from the study of the ROC curve about the cut-off values of clinical outcomes

	Age	FM-UE (-WH)	FMA-UE-SPJM	FMA-UE-SF	RPS	BBT	FIM
AUC*	0.7344	1	0.8438	0.8313	0.9125	0.7938	0.7688
Cut-off value	< 50.50	< 1.020	< 45,5	< 18.50	< 8.000	< 3.015	< 105.0
Sensitivity	50	100	100	75	100	87.5	100
Specificity	95	100	60	80	90	80	50

*AUC: Area Under Curve

The Specificity of the cut-off values is higher than 80% for all variables except for FMA-UE-SPJM and FIM that respectively obtained 60% and 50%. The Sensitivity has slightly lower values for Age, FMA-UE-SF and BBT but is higher than 75% for all other outcomes.

Instrumental data

As mentioned in paragraph 5.1.2, the GUI locally stores some therapy-related data. All signals recorded during the therapeutic protocol and related to each movement repetition were automatically segmented. Recorded data are post-processed with the aim of extracting some relevant information about task performance.

No patients of Not Complete Group succeeded in performing movements of finger extension, thumb abduction and pinch. Seven patients successfully performed wrist supination, while wrist pronation, flexion, adduction and finger flexion has been managed by six patients. The device has been controlled thought wrist extension and adduction by 5 patients only.

Since only patients of Complete Group succeeded in completing the entire protocol, instrumental data from this group have been analyzed.

Studies on the effects of stroke on motor control in the human upper extremity suggest that stroke alters the normal muscle patterns [139], [140]. Prior studies have reported that during voluntary wrist flexion and extension [141] and during contraction of the finger extensors [142], stroke patients exhibit weakness and impersistence of muscle contraction. Recent studies showed the capability of EMG amplitude in highlighting motor control impairment of different stroke group patient when compared to healthy subjects [143], [144]. Thus, in the present study, the RMS amplitude has been assessed and correlated with clinical outcomes related to the upper limb motor impairment. The RMS

amplitude has been evaluated on the 3 channels that recorded the highest signals calculated as the mean value during the entire task execution.

For each movement of the experimental protocol, the Spearman's correlation analysis has been applied to evaluate the correlation between clinical assessments and instrumental data. Results of the analysis are summarized in Table IX.

Table IX. Correlation between RMS values and clinical assessments

	Age	Time since stroke	FM-UE (-WH)	FMA-UE SPJM	FMA-UE SF	RPS	BBT	NHPT	FIM
Wrist pronation	0,06933	-0,2328	0,4225	-0,05888	0,3675	-0,03175	0,2714	0,2757	0,2465
Wrist supination	0,3537	0,02293	**0,563***	-0,1223	**0,4819***	-0,1922	0,2489	0,4207	0,4435
Wrist flexion	0,05968	0,02646	**0,5923****	0,1839	**0,4558***	0,2346	**0,4589***	**0,5957****	**0,6281****
Wrist extension	0,2606	-0,01764	0,2126	-0,3161	0,327	-0,142	0,3066	0,1909	0,212
Wrist abduction	0,1181	-0,2054	**0,7288*****	0,1499	**0,5107***	0,02266	**0,5564***	**0,654****	**0,6333****
Wrist adduction	0,2121	-0,05967	0,2564	0,0007728	0,3169	0,0506	0,2312	0,2347	0,2217
Finger flexion	0,1571	-0,3386	**0,4954***	-0,05435	0,3973	-0,1878	0,1749	0,2881	0,2447
Finger extension	0,2799	-0,2205	**0,7569*****	0,1069	0,4315	-0,03439	**0,6366****	**0,7468*****	**0,75*****
Thumb abduction	0,2354	-0,105	**0,5729****	0,04946	**0,4686***	0,05967	**0,518***	**0,5872****	**0,609****
Pinch	0,3746	-0,2545	**0,6786****	0,09273	**0,5709****	0,05363	**0,6273****	**0,6388****	**0,612****

* ($p<0.05$). ** ($p<0.01$). *** ($p<0.001$).

RMS values are significantly correlated with FM-UE(-WH), FMA-UE SF, BBT, NHPT and FIM for Wrist flexion and abduction and for Thumb adbuction and Pinch. A correlation is revealed for Wrist supination in case of FM-UE(-WH) and FMA-UE SF and for Finger flexion when FM-UE(-WH) values are evaluated. All statistically significant results show a positive correlation.

Li et al. [145] recorded EMG signals and movement kinematics in patients and control subjects while performing arm reaching tasks. They found that the patient group showed a longer duration of each task. Therefore, the time that the patient took to complete each task repetition has been assessed. It has been calculated as the period from the GUI trigger and the end of the period during which the patient was required to maintain the marker on the target, normalized to the selected duration of the contraction.

Table X shows the Spearman's correlation analysis results between the time that the patient took to complete each task repetition and clinical assessments.

Table X. Correlation between the time to complete task repetition and clinical assessments

	Age	Time since stroke	FM-UE (-WH)	FMA-UE SPJM	FMA-UE SF	RPS	BBT	NHPT	FIM
Wrist pronation	0,2406	-0,002646	-0,01512	0,05855	-0,2998	-0,1271	-0,1643	-0,1529	-0,2443
Wrist supination	**0,4715***	-0,08113	0,4349	0,2144	0,02446	0,3093	0,4187	0,449	-0,07231
Wrist flexion	**0,4612***	-0,01284	-0,01826	0,2955	0,05023	0,127	0,08353	0,1253	0,2273
Wrist extension	**0,62****	0,1397	0,1164	0,007694	**-0,4498***	-0,08082	0,2179	0,1572	**-0,5453***
Wrist abduction	0,2643	0,08378	-0,04002	0,1549	-0,05254	0,04148	-0,06272	-0,009722	-0,172
Wrist adduction	0,2859	0,01279	0,08898	0,2163	-0,1124	0,1741	0,1193	0,1578	-0,341
Finger flexion	0,3529	0,3376	-0,3279	0,04999	-0,4397	-0,1125	-0,2377	-0,2081	-0,2183
Finger extension	0,2954	-0,001511	-0,2546	-0,03155	-0,4144	-0,03855	-0,1869	-0,1592	-0,368
Thumb abduction	0,2846	0,2554	-0,3332	-0,164	-0,2692	-0,07036	-0,09987	-0,1331	-0,3361
Pinch	0,3898	0,05291	-0,1601	0,03153	-0,2536	0,02705	0,007067	0,01149	-0,2954

* ($p<0.05$). ** ($p<0.01$). *** ($p<0.001$).

Results show that time significantly correlates with Age for Wrist supination, flexion and extension. Moreover, for Wrist extension, significant negative correlations are revealed with FMA-UE SF and FIM.

5.4.1.3 Conclusions

Summarizing key results, the analysis of the dataset recorded during the cross-sectional study reveals some relevant aspects. All patients who failed in completing the entire protocol (Not Complete Group), have severe upper limb impairment and represent the 72% of patients that show this level of impairment. Moreover, all the quantitative clinical outcomes show higher median values for patients in Complete Group, showing that the ability of controlling the device is related to the patient clinical picture. The Fisher's exact test highlights a significant association also with spasticity of Flexor carpi and Flexor digitorum superficialis muscles measured with MAS. These results are confirmed by the study performed on the cut-off values. The promising sensibility and specificity levels obtained with the calculted cut-off values, have prospects for a preventive evaluation of patients that could successfully perform the EMG-BF based rehabilation therapy on the complete set of movements. An optimization could be performed in order to improve the discriminant power of the procedure: since consequences of a wrong classification of a patient as a subject that can control the device has a low criticity, specificity could be increased in the face of a slight reduction of the sensitivy value.

Evidence about the analysis on instrumental data recorded from patients included in the Complete Group is also promising. The correlation with the RMS amplitude of the EMG signal has statistical significance for a subset of movements and outcomes. Results are in line with baseline studies [143], [144] and, actually, the conclusions are confirmed on finest movements of the wrist and fingers, monitored with the only EMG signal. The positive correlation suggests that higher RMS amplitude can be related to lower levels of motor impairment for stroke patients. The correlation of clinical outcomes with the time that patients need to complete exercises is rarely verified and revealed lower precision levels. The significant correlations that have been found, however, are plausible: time values are higher for older patients and for patients with reduced sensory functions and a lower independence level.

In conclusion, it is evident that the degree of control of the device is related with the patient's motor impairment and data recorded during exercise execution are promising as performance parameters to monitor patient progression and to tailor therapy to the specific needs and abilities over time. Further work should be done in order to confirm the relevance and reliability of proposed parameters and to identify other efficient performance measures.

5.4.2 Longitudinal study

5.4.2.1 Participants

Four patients (P11, P12, P14, P15; 63±11 years old) were selected for the longitudinal study. Table XI shows patients' demographic and clinical data. They have been treated as mentioned in Paragraph 5.3.2.2 of the present thesis: 1 hour per day, 5 days a week for 3 weeks. The therapy has been patient-tailored considering the specific degree and the type of motor impairment and has been administered by the therapists according the rehabilitation stage from the point of view of intensity and frequency of the proposed tasks. Moreover, each session included different exercises with the aim of focusing on muscular force or on the repeatability of the sEMG patterns and in order to increase patient attention and participation.

5.4.2.2 Data analysis

Clinical data

Preliminary assessments have been done on the comparison between initial (before the beginning of the therapy) and final evaluation (at the end of the therapy). Table XI shows clinical assessments of each patient, mean and standard deviation values have been calculated for each outcome. Moreover, the percent variation of quantitative clinical data has been calculated as the ratio between mean values before and after the therapy.

Table XI. Before and after-therapy clinical assessments.

Variable		Patient 1	2	3	4	Mean	Standard deviation	Percent variation [%]
FMA-WH	PRE	8	23	11	9	12.75	6.02	13.73
	POST	11	21	15	11	14.50	4.09	
FMA-UE-SPJM	PRE	38	48	48	46	45.00	4.12	-6.11
	POST	36	43	46	44	42.25	3.77	
FMA-UE-SF	PRE	23	24	12	22	20.25	4.82	-7.41
	POST	22	24	7	22	18.75	6.83	
RPS	PRE	17	36	31	24	27.00	7.18	8.33
	POST	19	36	36	26	29.25	7.19	
BBT	PRE	0	27	30	9	16.50	12.46	42.42
	POST	10	40	29	15	23.50	11.80	
NHPT	PRE	0	0.39	0.00	0.02	0.10	0.17	-7.61
	POST	0.00	0.36	0.00	0.02	0.10	0.15	
FIM	PRE	113	116	62	114	101.25	22.69	10.86
	POST	113	124	98	114	112.25	9.28	
MAS-UE	PRE	2	1	2	1	/	/	/
	POST	3	1	2	1	/	/	

Mean values of FMA-WH, RPS, BBT and FIM show a positive percent variation ranged between 10.86% and 42.42%, a maximum decrease of 7.61% is calculated for the other parameters.

Instrumental data

As above mentioned, the GUI locally saves some relevant information about exercise performance. For each exercise, a significant output variable has been individuated which allowed the quantitative assessment of patient performance during the execution of the therapy. Moreover, the exercise parameters that have been modified by the therapists during the therapy protocol have been

individuated. Data recorded during different therapy sessions and with different parameters have been separately analyzed for each exercise in order to reveal two aspects: the existence of any trends in the variations of the output variable across therapy sessions and the influence of exercise parameters on patient performance. In order to evaluate the first aspect, the mean value of the output variable has been calculated for each patient. The second aspect has been analyzed calculating the mean value of data recorded for all patients during the entire rehabilitation protocol. Movements have been firstly compared to reveal if specific movements were more difficult to perform then, the output variable has been studied for each specific movement, in order to assess the influence of parameters variation on the output variable values. Data have been pre-processed to remove outliers from the data set. The statistical analysis has been performed with the statistics software GraphPad Prism 5.

Exercise: Bar

The output variable of this exercise is the time that the patient took to complete each task repetition, this parameter has been assessed as the period from the GUI trigger and the end of the period during which the patient was required to maintain the marker on the target, normalized to the selected duration of the contraction. Parameters that have been varied during the therapy were the percentage of the MVC required to manage the control signal and the duration of the required contraction (Hold Time), three combinations of these parameters have been applied and analyzed:

1. %MVC (M): 30% - Hold Time (H): 0.3 s;
2. %MVC (M): 60% - Hold Time (H): 0.3 s;
3. %MVC (M): 60% - Hold Time (H): 0.4 s.

Following figures (Figure 21-Figure 24) show the variation of the mean time across therapy sessions and the respective exercise parameters.

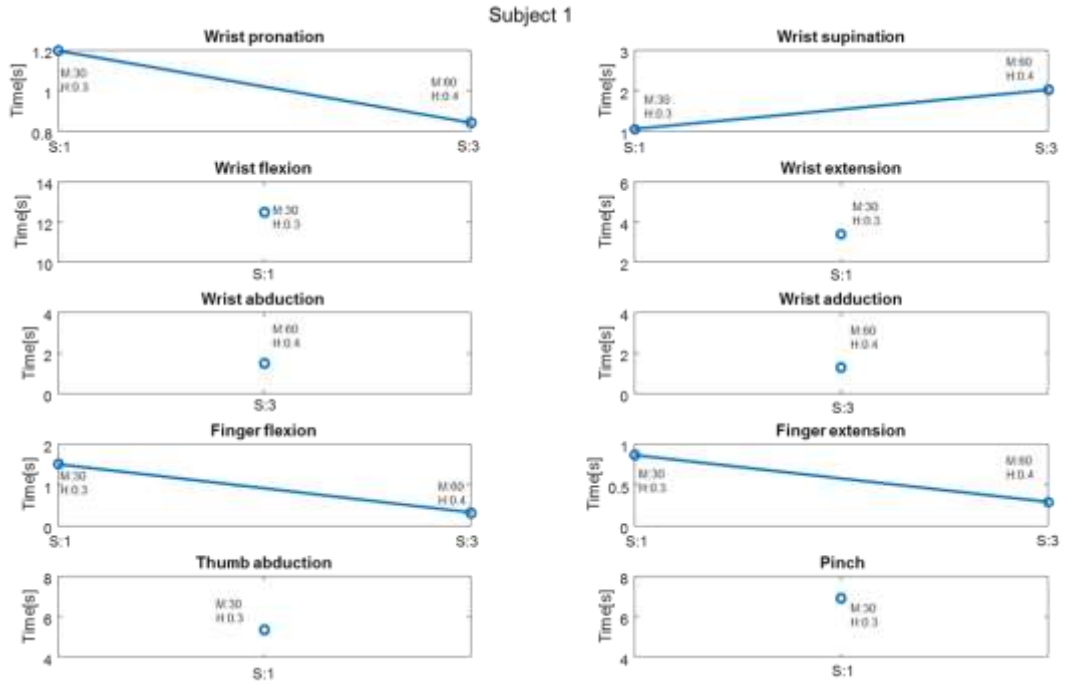

Figure 21. Mean values of the output value and related parameters across sections for patient 1.

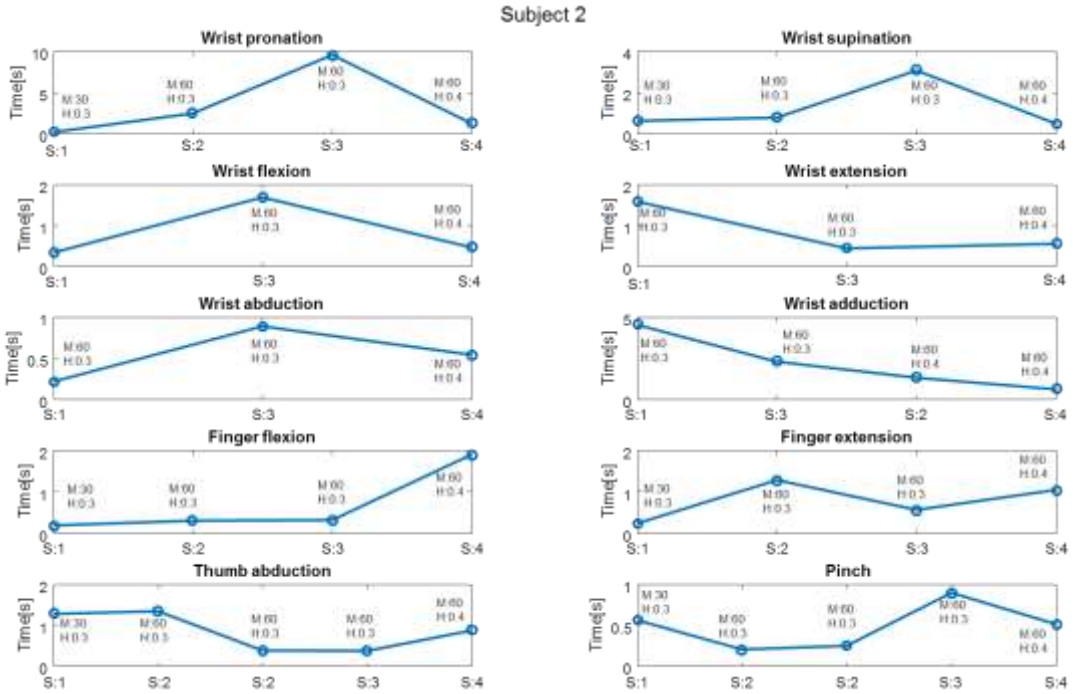

Figure 22. Mean values of the output value and related parameters across sections for patient 2.

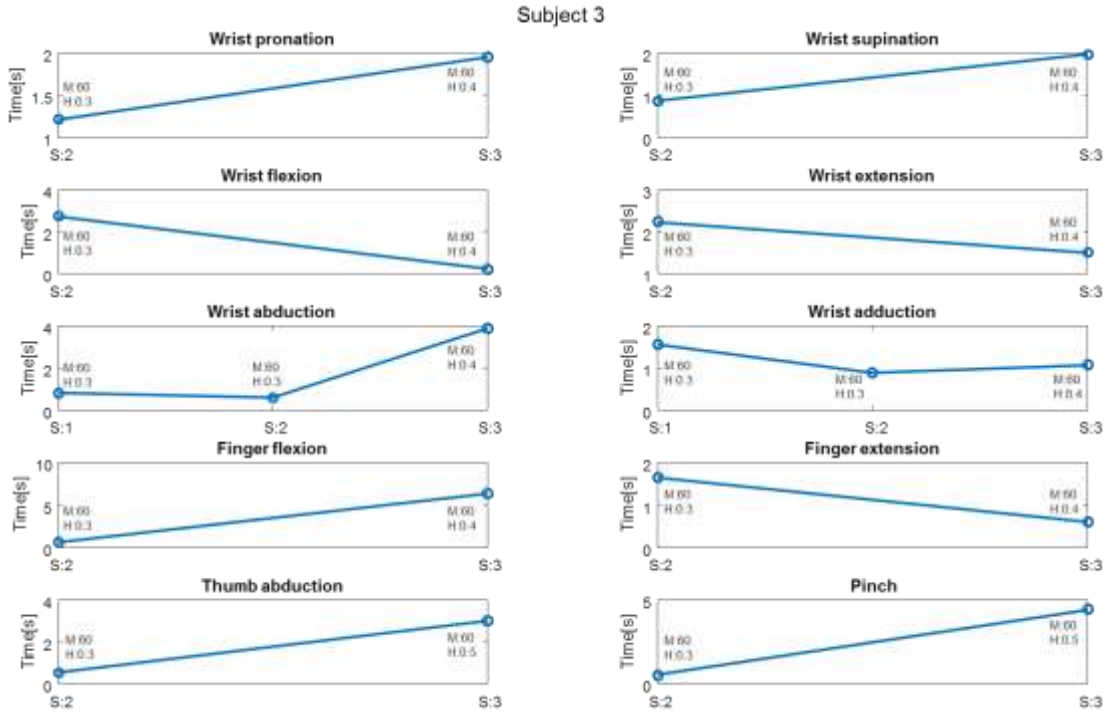

Figure 23. Mean values of the output value and related parameters across sections for patient 3.

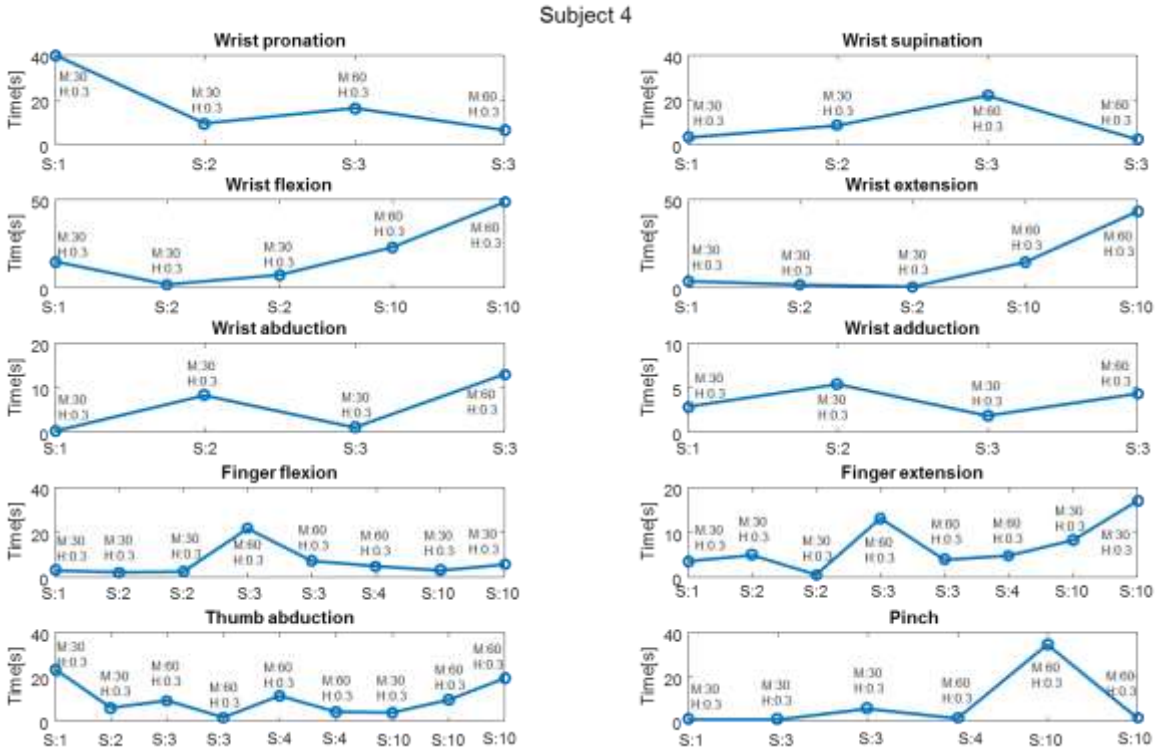

Figure 24. Mean values of the output value and related parameters across sections for patient 4.

It can be observed that each patient received a specific therapy: parameters have been usually adjusted across sessions, some movements have been performed twice or they have been completely omitted from a session. No trend can be detected according the therapy phase. Results of therapy sessions could be influenced by the variation of the exercise parameters. Therefore, instrumental data have been analyzed to evaluate the parameters' influence on patient performance. Following figures (Figure 25-Figure 27) show the distribution of the output variable separately for each parameter combination, they have been calculated only if the data set had a minimum required sample size.

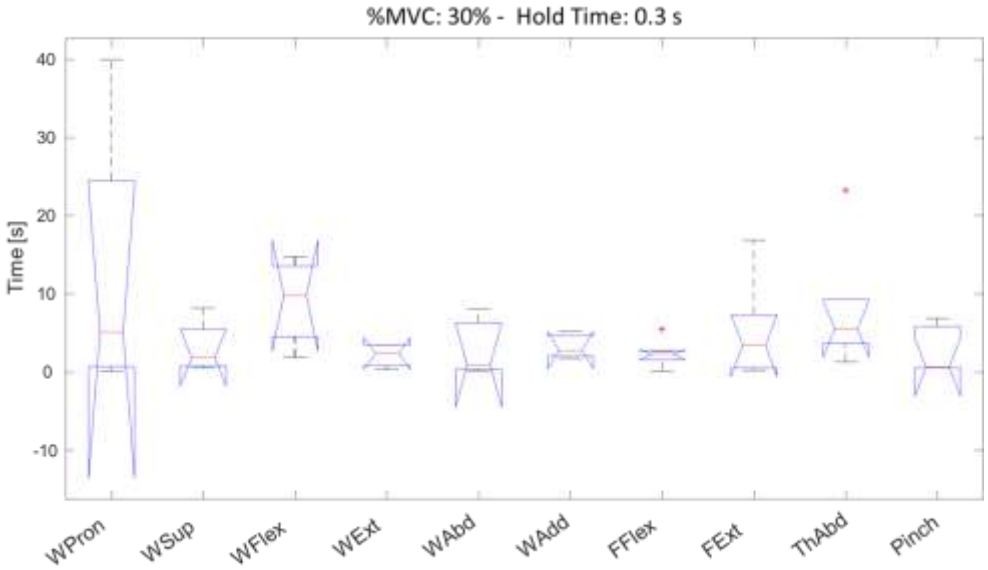

Figure 25. Boxplot showing the distribution of the output variable for each movement

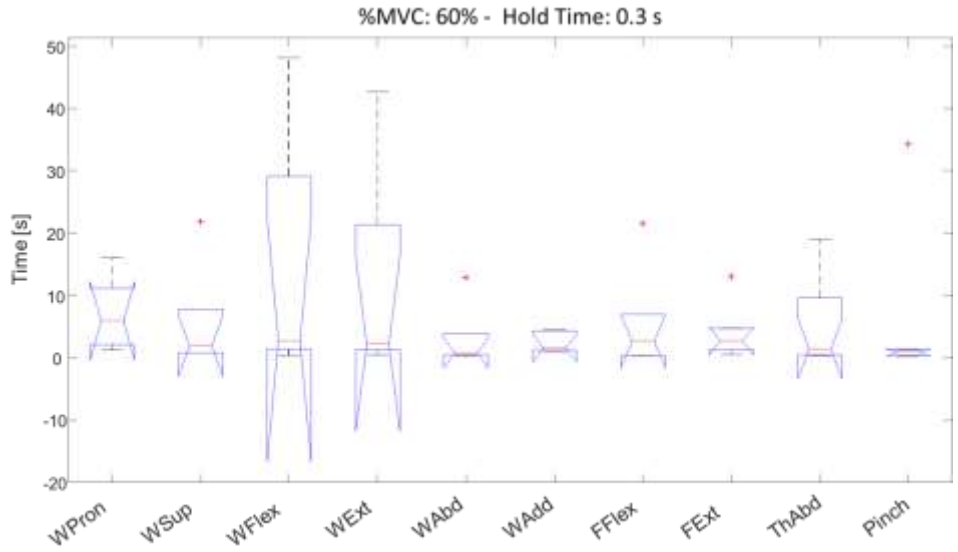

Figure 26. Boxplot showing the distribution of the output variable for each movement

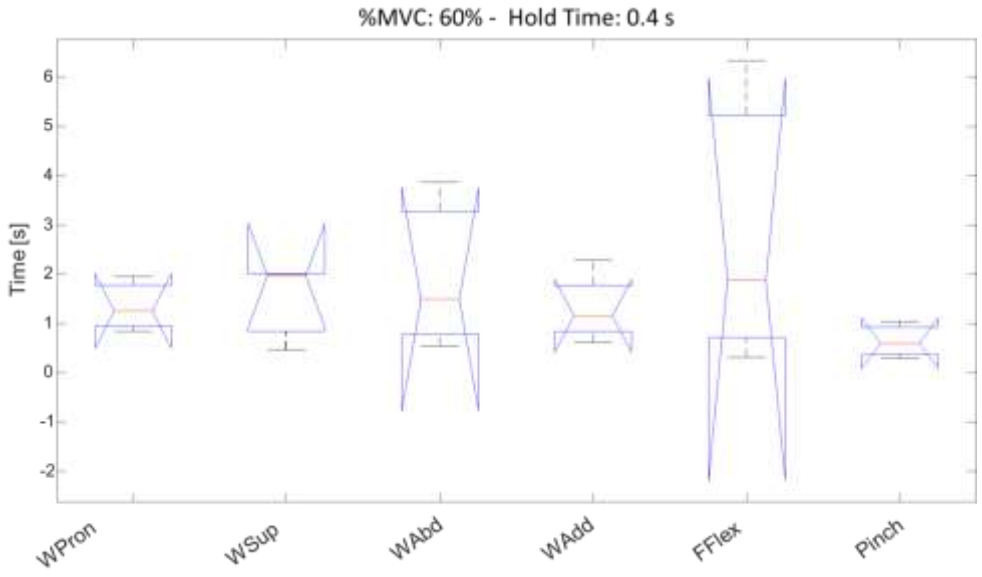

Figure 27. Boxplot showing the distribution of the output variable for each movement

Some observation can be made about the distribution of the median values (reported in Table XII) for the three parameter combinations: for both the first and the second combination Wrist abduction and Pinch show the lowest median values, while Wrist pronation and flexion show the highest values. The third combination of parameters determine a variation in the relation between movements and the movement with the lowest median value is Finger extension while Wrist supination and Finger flexion have the highest values.

Table XII. Numerical values of boxplot percentiles shown in Figure 25-Figure 27

Exercise Parameters - MVC: 30%; Duration of the contraction: 0.3 s										
Percentiles	**WPron**	**WSup**	**WFlex**	**WExt**	**WAbd**	**WAdd**	**FFlex**	**FExt**	**ThAbd**	**Pinch**
25th	0.70	0.82	4.54	0.87	0.36	2.05	1.61	0.60	3.67	0.59
50th	5.10	1.89	9.82	2.42	0.94	2.82	2.27	3.46	5.54	0.62
75th	24.49	5.47	13.62	3.46	6.33	4.69	2.78	7.30	9.31	5.82
Exercise Parameters - MVC: 60%; Duration of the contraction: 0.3 s										
Percentiles	**WPron**	**WSup**	**WFlex**	**WExt**	**WAbd**	**WAdd**	**FFlex**	**FExt**	**ThAbd**	**Pinch**
25th	2.15	0.84	1.34	1.30	0.48	1.21	0.32	1.28	0.49	0.32
50th	5.95	1.92	2.72	2.22	0.80	1.54	2.67	2.71	1.45	0.89
75th	11.17	7.77	29.10	21.33	3.87	4.34	7.02	4.72	9.56	1.31
Exercise Parameters - MVC: 60%; Duration of the contraction: 0.4 s										
Percentiles	**WPron**	**WSup**	**WFlex**	**WExt**	**WAbd**	**WAdd**	**FFlex**	**FExt**	**ThAbd**	**Pinch**
25th	0.94	0.84	/	/	0.78	0.83	0.71	0.37	/	/
50th	1.26	1.97	/	/	1.49	1.15	1.89	0.60	/	/
75th	1.78	2.01	/	/	3.28	1.77	5.22	0.93	/	/

The Kruskal-Wallis test has been applied to reveal if the output variable significantly differs for different movements. For all the combinations, the test doesn't reject the null hypothesis that movements samples are from identical distributions, this means that no movements show time values significantly different from the others.

The output variable has been also studied for each specific movement, in order to assess the influence of parameters variation on patient performance. Figure 28 shows the boxplots of time values for each combination.

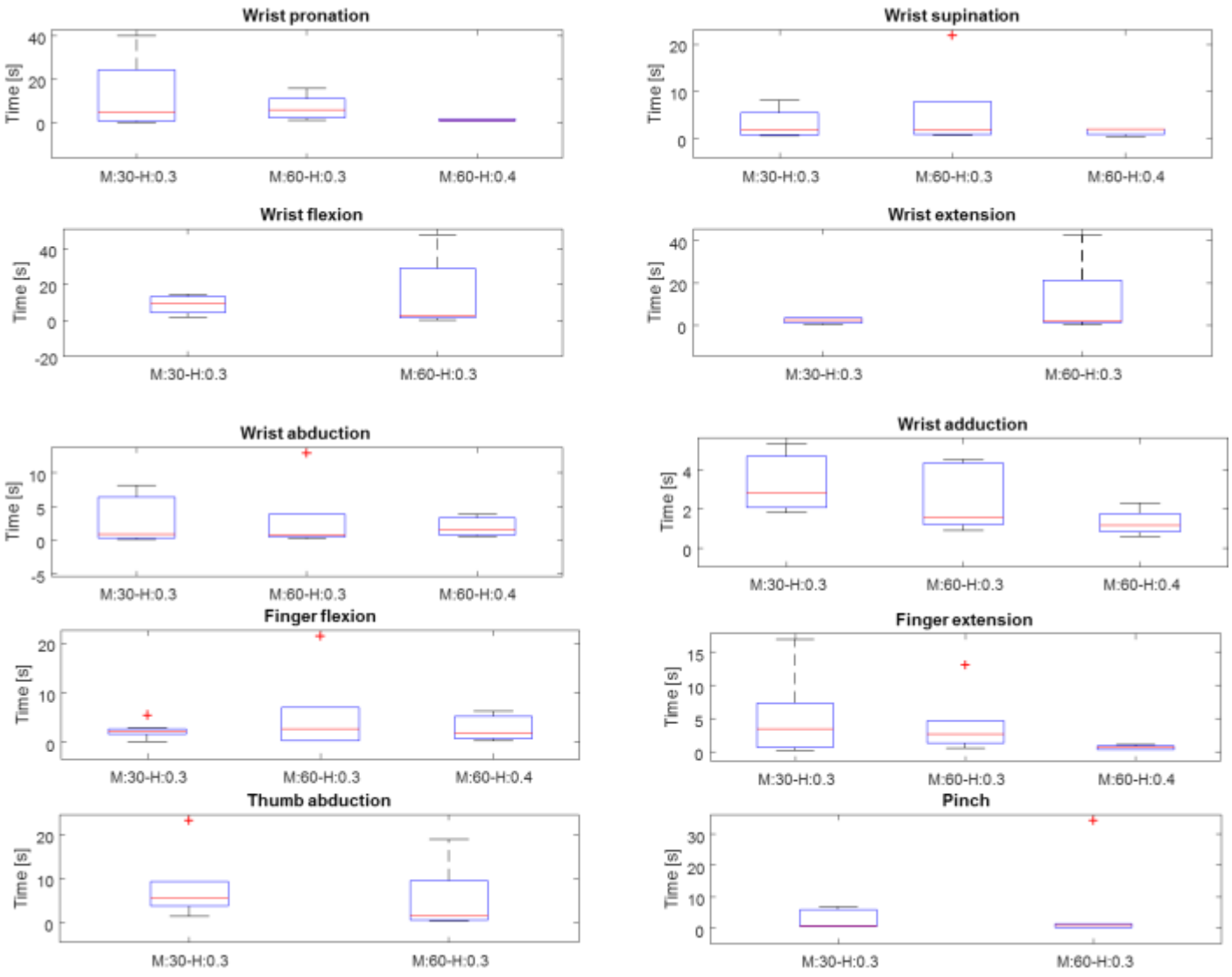

Figure 28. Boxplot of the output variable for each movement and parameter combination

The percent variation of the time values has been calculated when an exercise parameter has been modified from its initial value to its final value (the other parameter has been maintained constant). Results are shown in Table XIII.

Table XIII. Percentage variation of the output variable corresponding to a variation of an exercise parameter.

Percent variation of time values											
Variation	**WPron**	**WSup**	**WFlex**	**WExt**	**WAbd**	**WAdd**	**FFlex**	**FExt**	**ThAbd**	**Pinch**	**Mean**
%MVC	16.58	1.61	-72.34	-8.17	-14.74	-45.19	17.83	-21.55	-73.86	43.37	-15.65
Hold Time	-78.88	2.79	/	/	87.22	-25.28	-29.24	-77.76	/	/	-20.19

When the %MVC value is increased, time values increase for 4 movements. The variation of time values recorded when the duration of the required contraction was increased can be evaluated only for 6 movements: median values increase for 2 movements. The mean value of the percent variations is slightly negative in both cases, which means that a reduction of the output variable has been revealed. Also in this case, the Kruskal-Wallis test doesn't reveal any statistically significant difference between distributions recorded with different parameters.

Exercise: Ball

For exercise Ball, the time that the patient took to reach the target normalized to the target distance from the initial position of the marker has been considered as the output variable. Parameters that have been modified are the %MVC required to control the BF signal and the target dimension. The exercise has been performed using four combinations of parameters:

1. %MVC (M): 30% - Target dimension (T): 1
2. %MVC (M): 30% - Target dimension (T): 2
3. %MVC (M): 50% - Target dimension (T): 1
4. %MVC (M): 60% - Target dimension (T): 1

Following figures show the mean value of the output variable for each patient and movement, across therapy sessions.

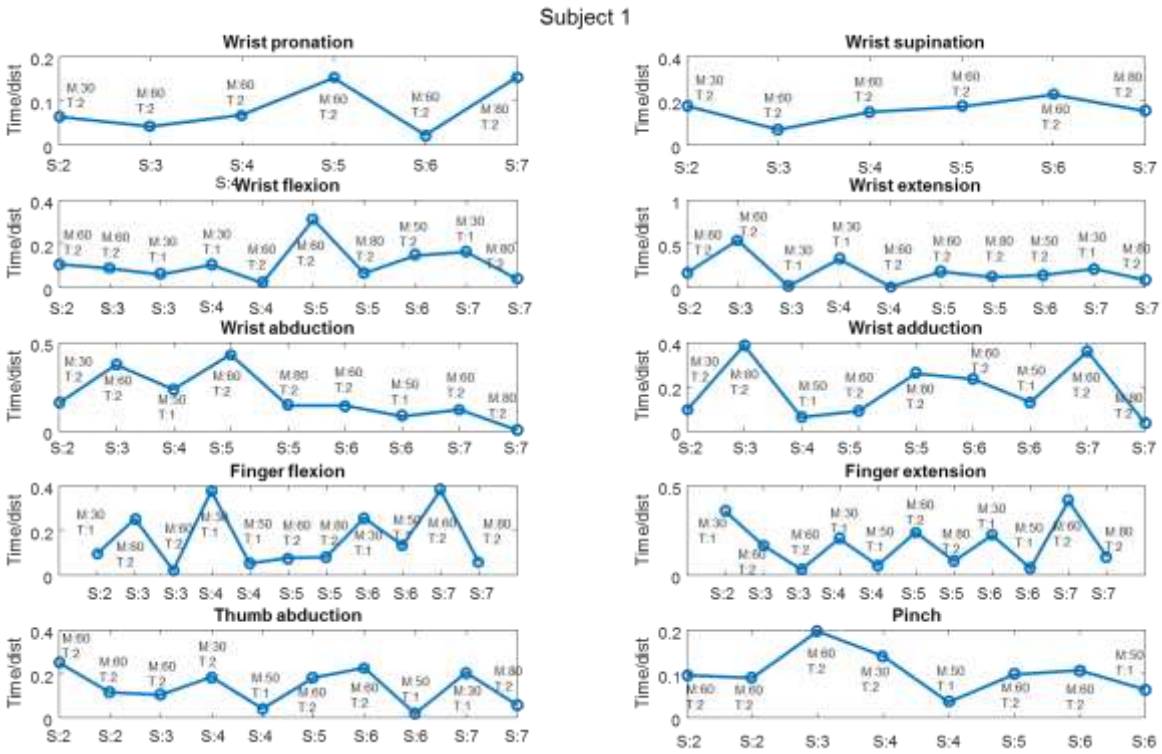

Figure 29. Mean values of the output value and related parameters across sections for patient 1.

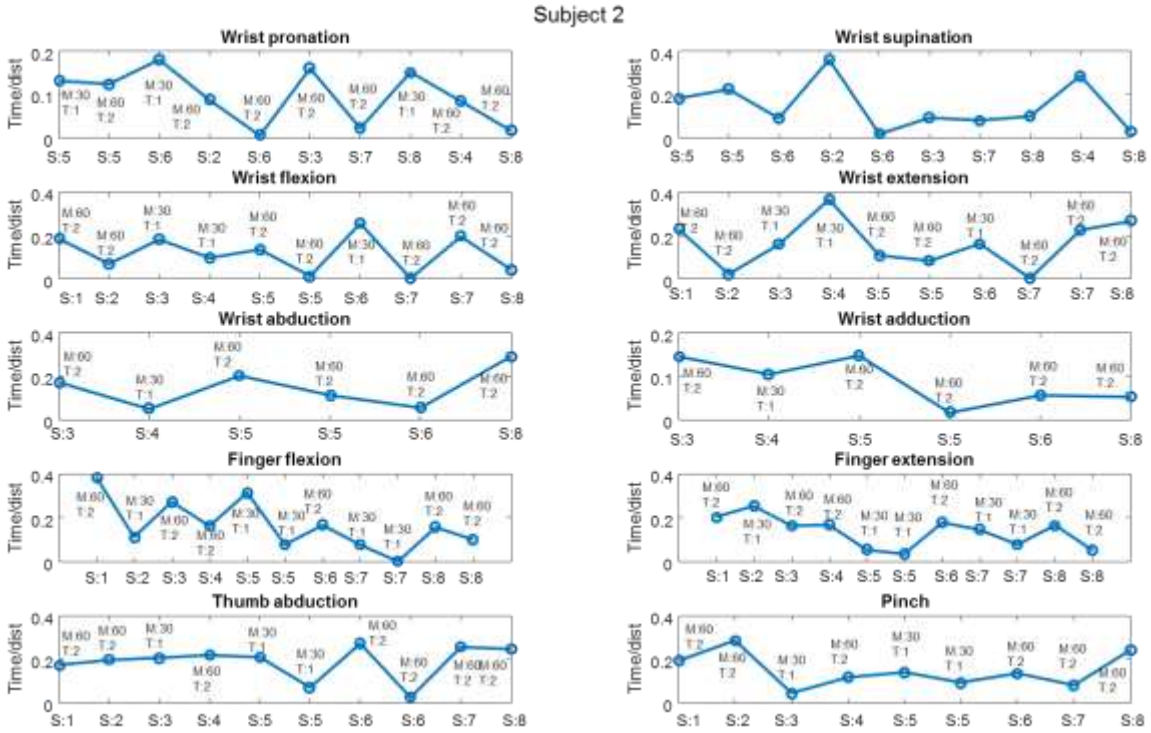

Figure 30. Mean values of the output value and related parameters across sections for patient 2.

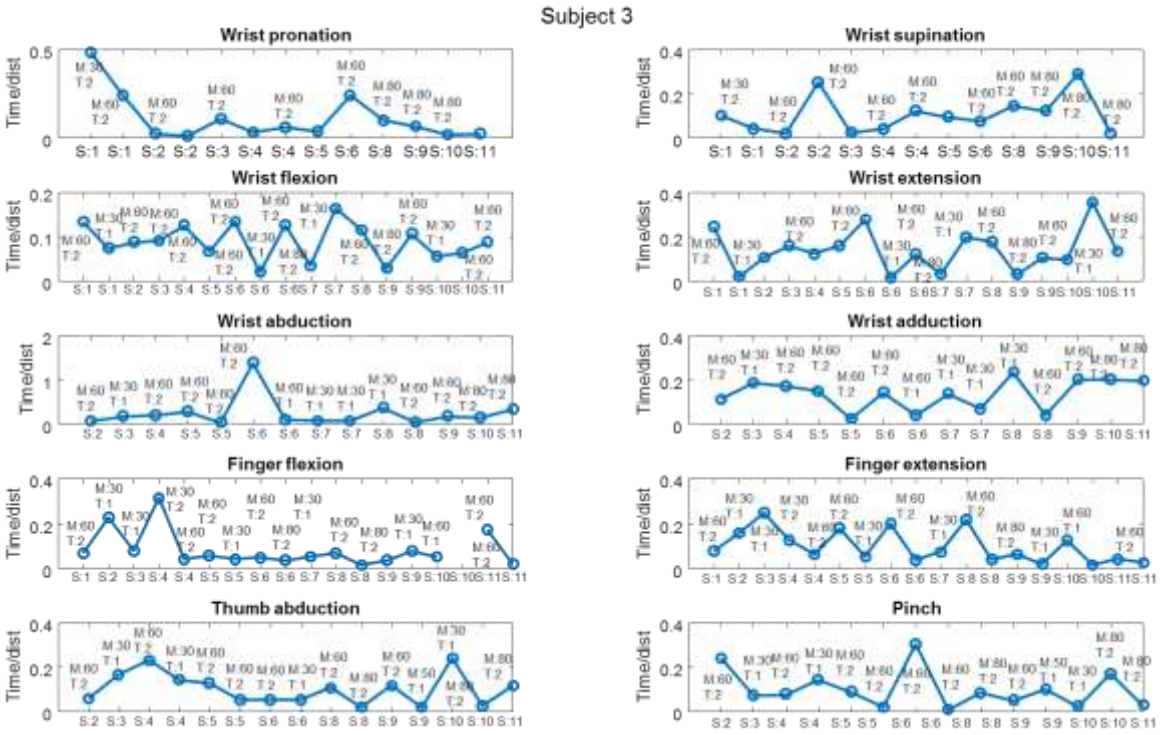

Figure 31. Mean values of the output value and related parameters across sections for patient 3.

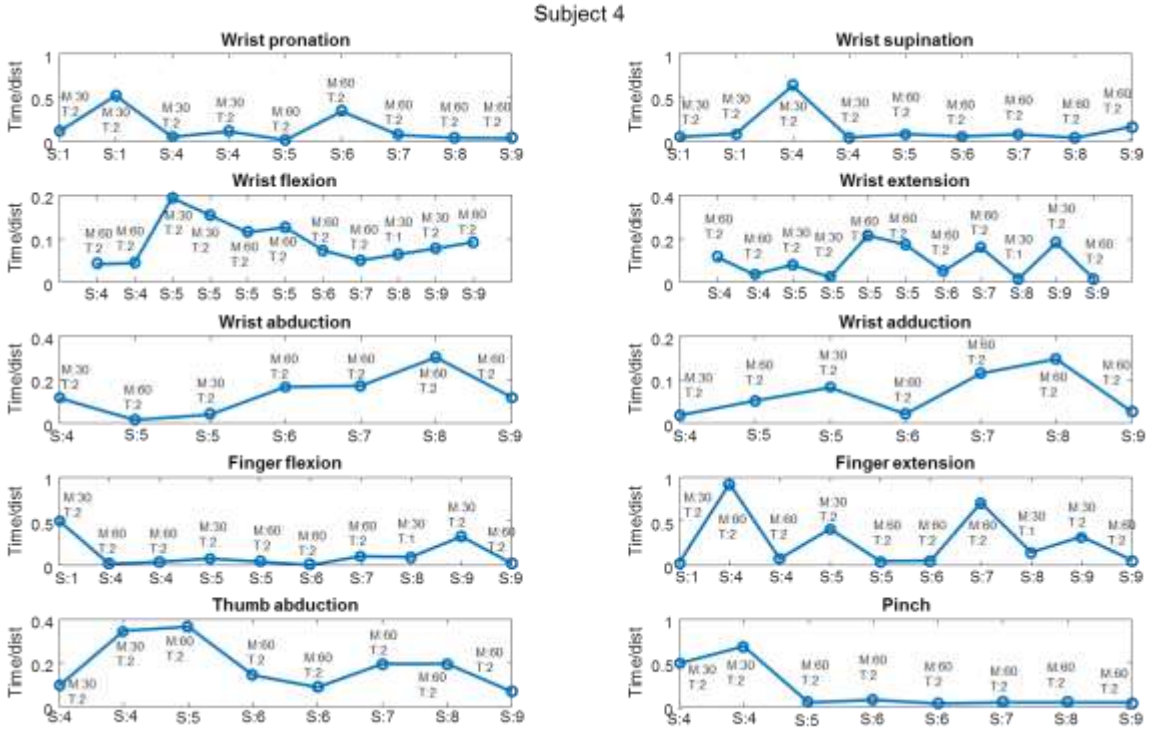

Figure 32. Mean values of the output value and related parameters across sections for patient 4.

Also in this case, figures highlight the variability of the therapy administered to the patients according their level and type of motor impairment.

For each performed movement, the distribution of the output variable has been evaluated according the exercise parameters. Following figures show the result of the study.

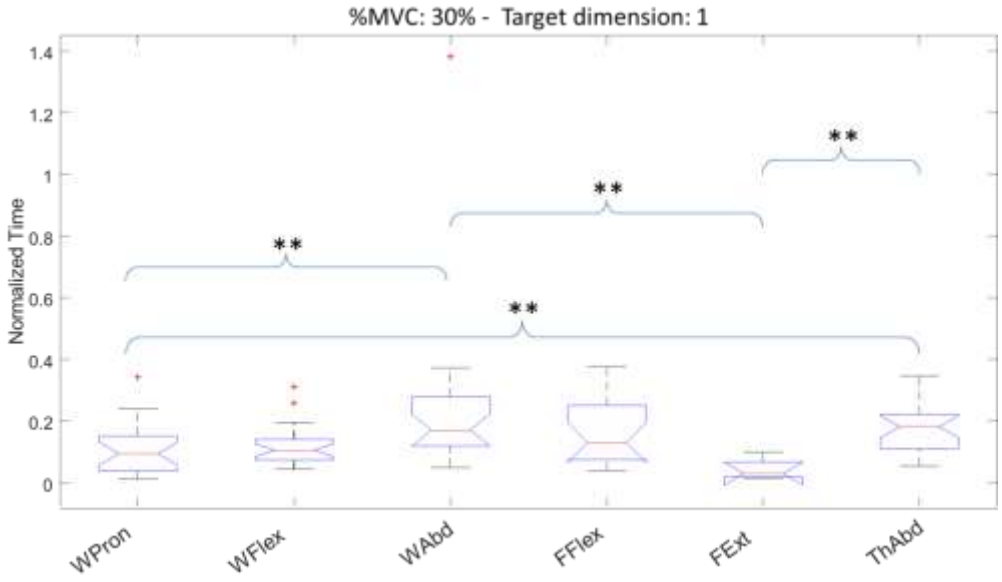

Figure 33. Boxplot showing the distribution of the output variable for each movement. ** ($p<0.01$)

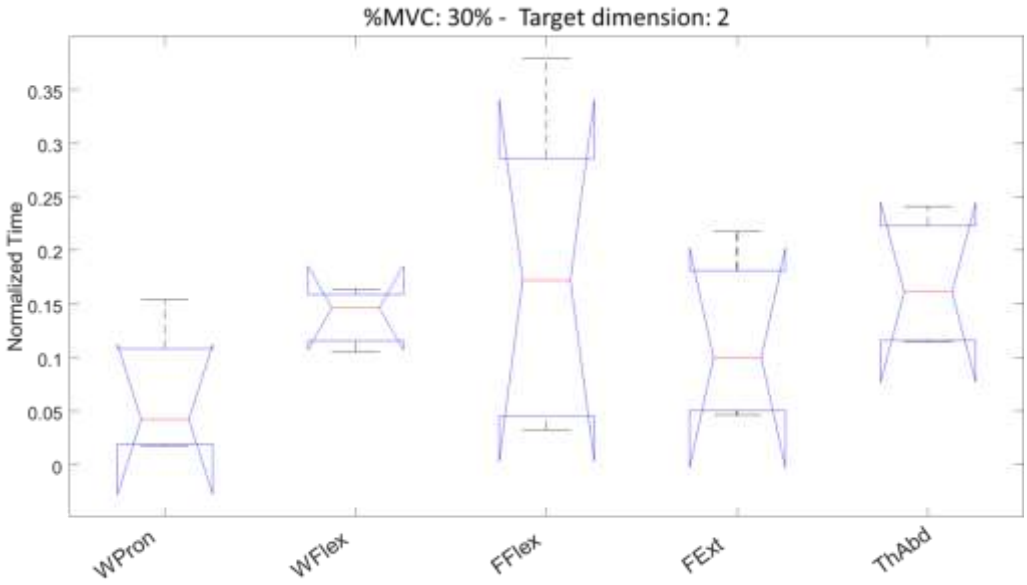

Figure 34. Boxplot showing the distribution of the output variable for each movement.

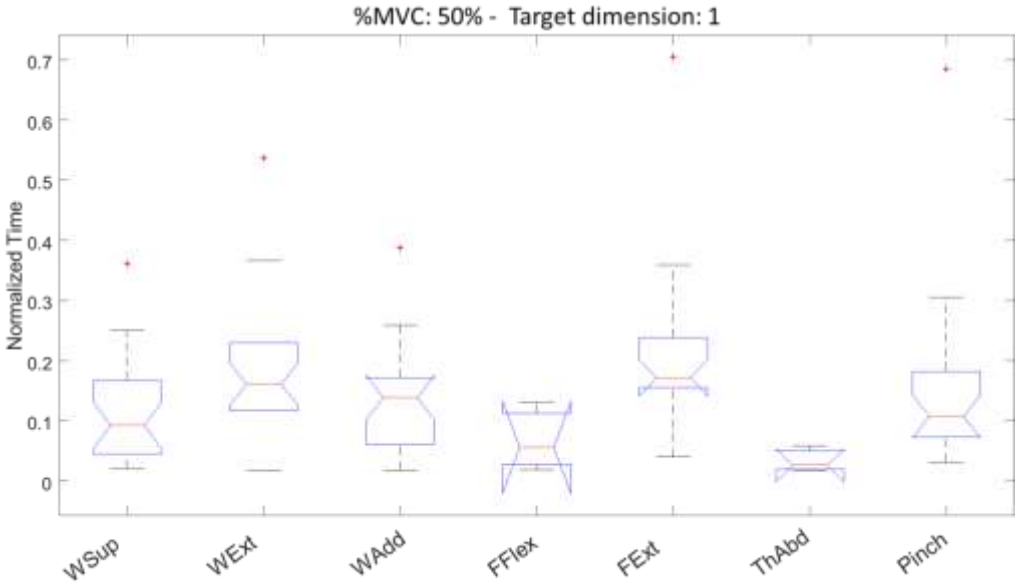

Figure 35. Boxplot showing the distribution of the output variable for each movement.

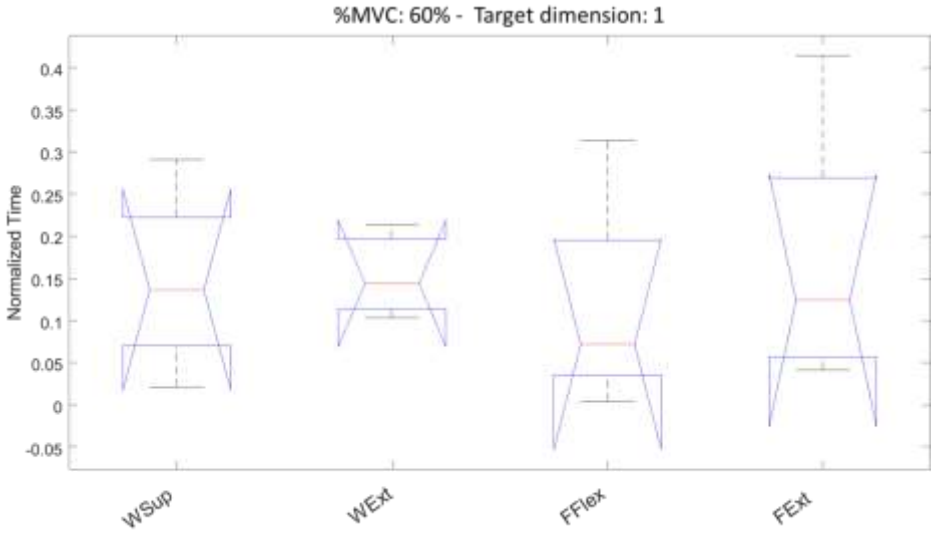

Figure 36. Boxplot showing the distribution of the output variable for each movement.

The Kruskal-Wallis test reveals significant differences between movements only for the first combination of the parameters. In this exercise, different subsets of movements have been performed for each combination of parameters. Moreover, no parameter combination has been applied to the complete movement set so a conclusion on the comparison between movements cannot be performed.

Movements are then analyzed to reveal the influence of parameters on task performance.

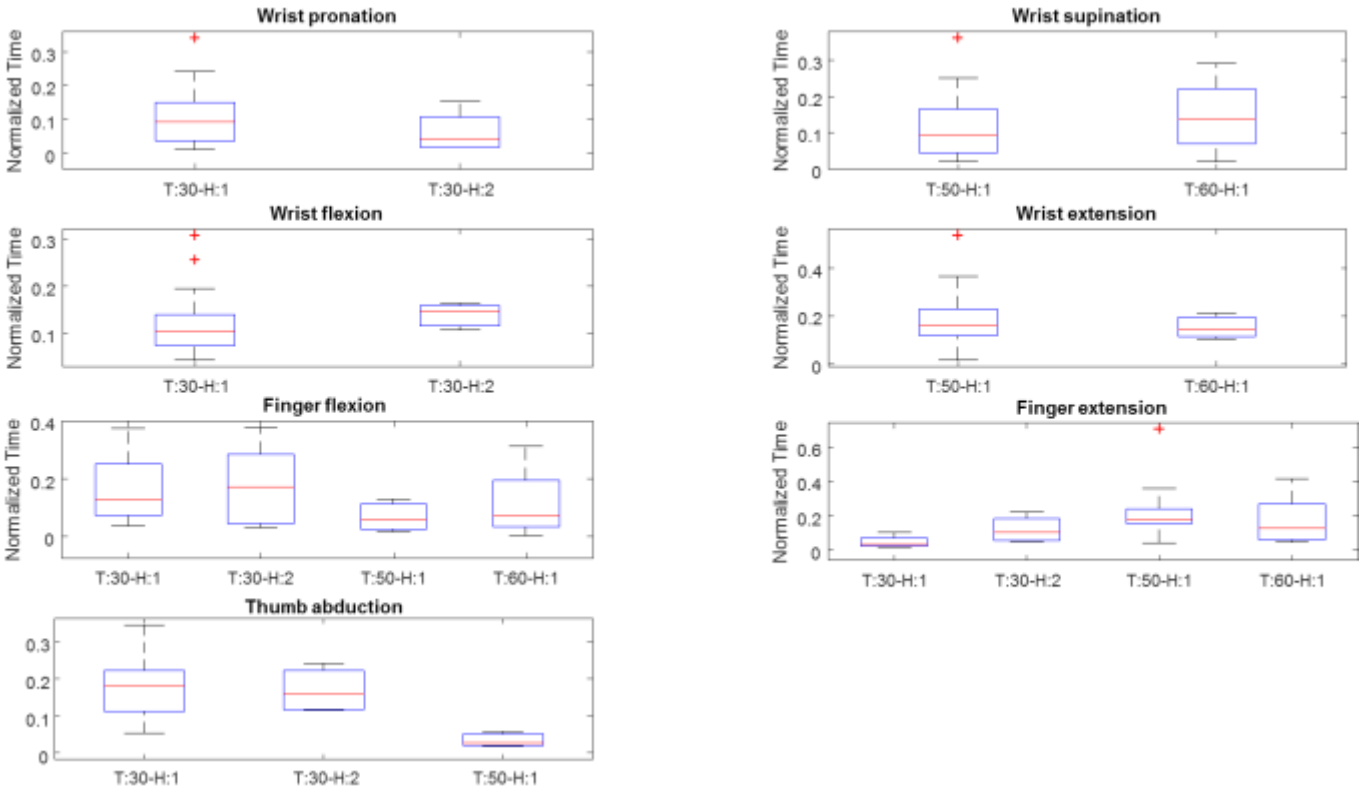

Figure 37. Boxplot of the output variable for each movement and parameter combination

The percent variation of the time values has been calculated when the %MVC has been modified from its initial value to its second and third values (target dimension has been maintained constant). Results are shown in Table XIV.

Table XIV. Percentage variation of the output variable corresponding to a variation of an exercise parameter

	Percent variation of output variable										
Variation	**WPron**	**WSup**	**WFlex**	**WExt**	**WAbd**	**WAdd**	**FFlex**	**FExt**	**ThAbd**	**Pinch**	**Mean**
MVC - I	/	/	/	/	/	/	-56.92	497.65	-85.84	/	118.30
MVC - II	/	47.76	/	-10.39	/	/	29.13	-27.72	/	/	9.70
Target dimension	-55.14	/	40.00	/	/	/	32.97	246.73	-11.58	/	50.60

Both the variation of the %MVC required to manage the control signal and the increase of the target dimension has the effect of increasing the speed of target reaching.

Fitts' law application

For exercise Ball, the results about variations of target dimension and exercise duration observed in the clinical trial, are also analyzed with reference to the Fitts' Law. Fitts' Law is a predictive model of

human movement primarily used in human–computer interaction and ergonomics. This scientific law predicts that the time required to rapidly move to a target area is a function of the ratio between the distance to the target and the width of the target [146]. This analysis is based on Fitts' law reviewed for the two-dimensional tasks by Scott MacKenzie and Buxton [147].

According to the Fitts' Law proposed for the two-dimensional tasks, the time (MT) to move and select a target of width W which lies at distance A is:

$$MT = a + b * \log_2(\mathrm{A} / \mathrm{W} + 1) \qquad (2)$$

where *a* and *b* are constants determined through linear regression, W corresponds to the region where an action terminates and the log term is the index of difficulty (ID). Figure 38 shows MT for each movement as a function of the ID.

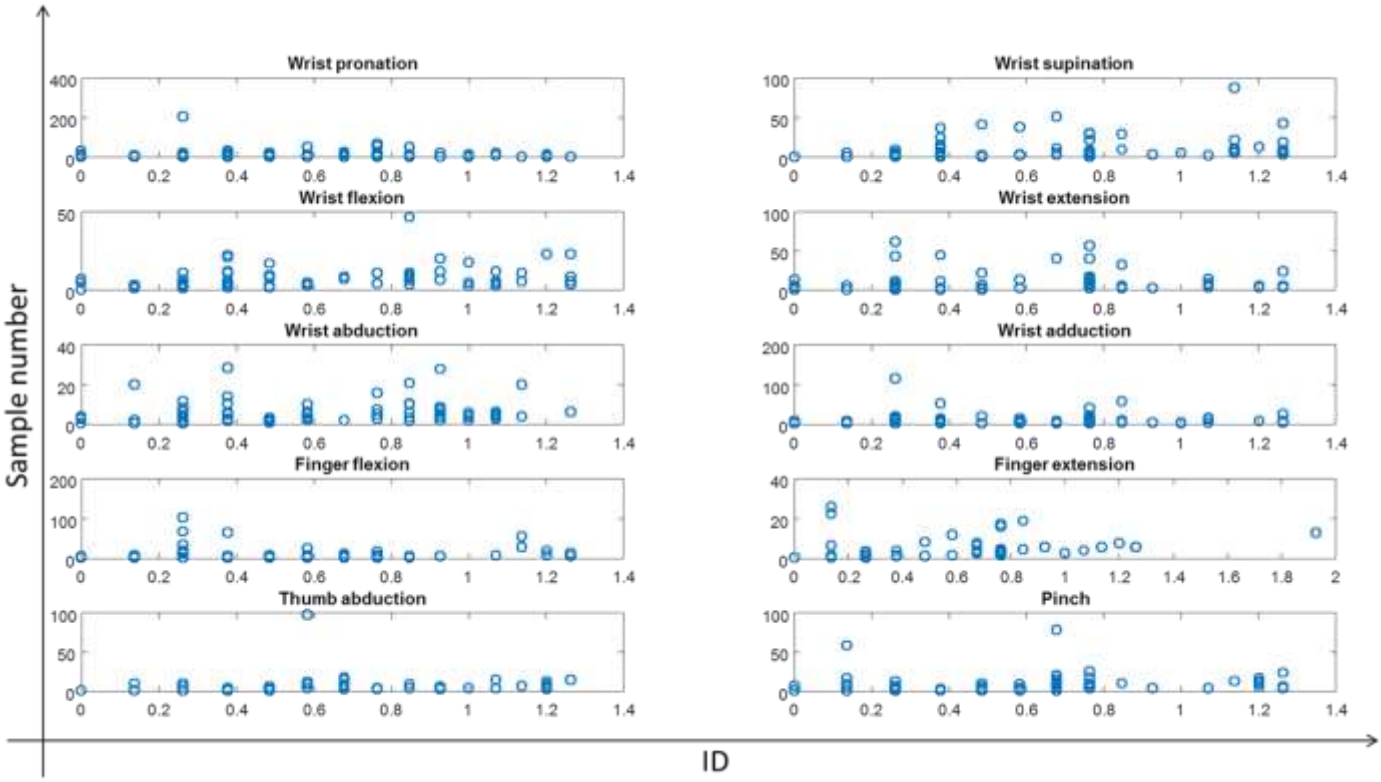

Figure 38. MT for each movement as a function of the ID

A linear regression is performed for the data of every movements, in order to determine the constants *a* and *b* of the model. Moreover, the performance parameters of the models are calculated and shown in Table XV.

Table XV. Performance parameters of Fitts' Law models

Movement	Wrist pronation	Wrist supination	Wrist flexion	Wrist extension	Wrist abduction
SSE	5.37E+05	1.44E+05	3.44E+04	1.23E+05	2.37E+04
R^2 [%]	0.5961	8.163	15.5	0.504	2.25
RMSE	21.26	13.11	6.918	13.06	5.705
Movement	**Wrist adduction**	**Finger flexion**	**Finger extension**	**Thumb abduction**	**pinch**
SSE	2.01E+05	2.07E+05	1.58E+04	9.22E+04	9.62E+04
R^2 [%]	0.1763	0.3663	4.469	1.088	5.609
RMSE	14.62	17.73	5.808	13.34	11.66

The root-mean-square error (RMSE) is acceptable with respect to the range of values of the MT. However, the sum of squared errors of prediction (SSE) tends to be large. Moreover, low R^2 values represent models that badly explain the variation in the response variable around its mean.

Exercise: Jump

The output variable of exercise Jump is the number of samples of error. The tested parameter is the obstacle width expressed in terms of sample number. Since a high number of obstacle widths has been employed, values have been grouped in four intervals:

1. Obstacle width (OW): 10-19;
2. Obstacle width (OW): 20-29;
3. Obstacle width (OW): 30-39;
4. Obstacle width (OW): >40.

The mean error number for each session is shown in following figures, separately for each patient.

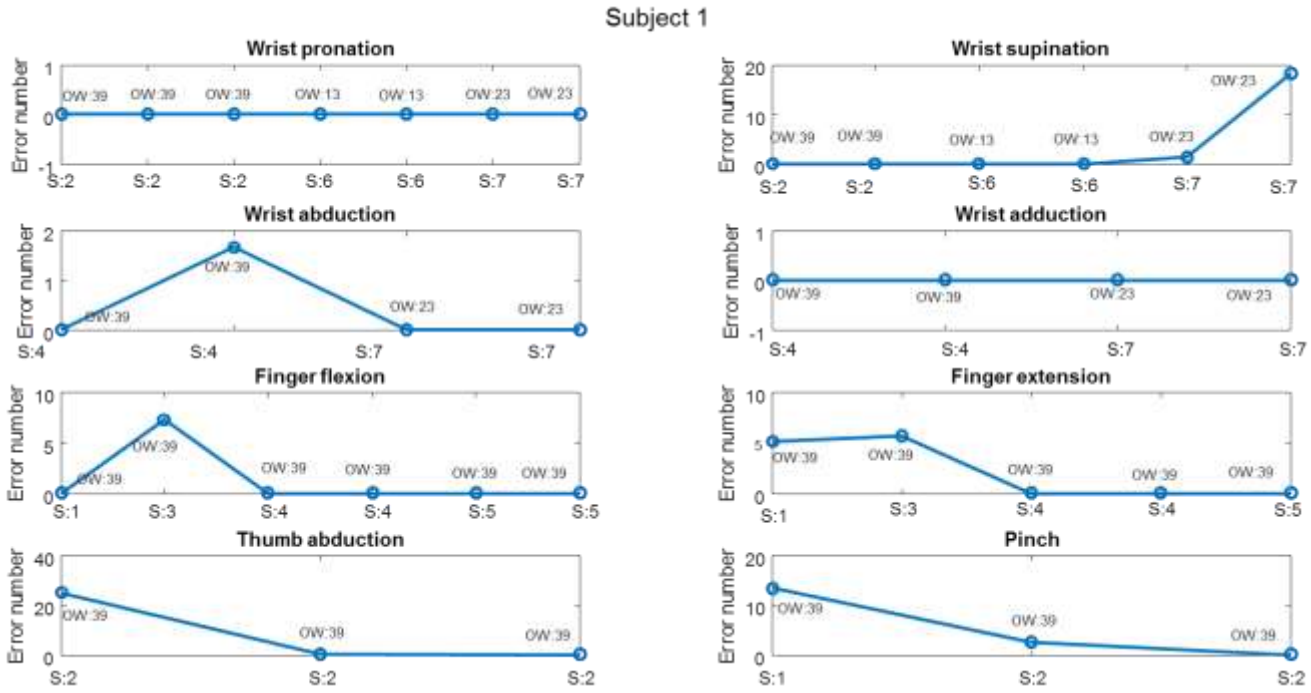

Figure 39. Mean values of the output value and related parameters across sections for patient 1

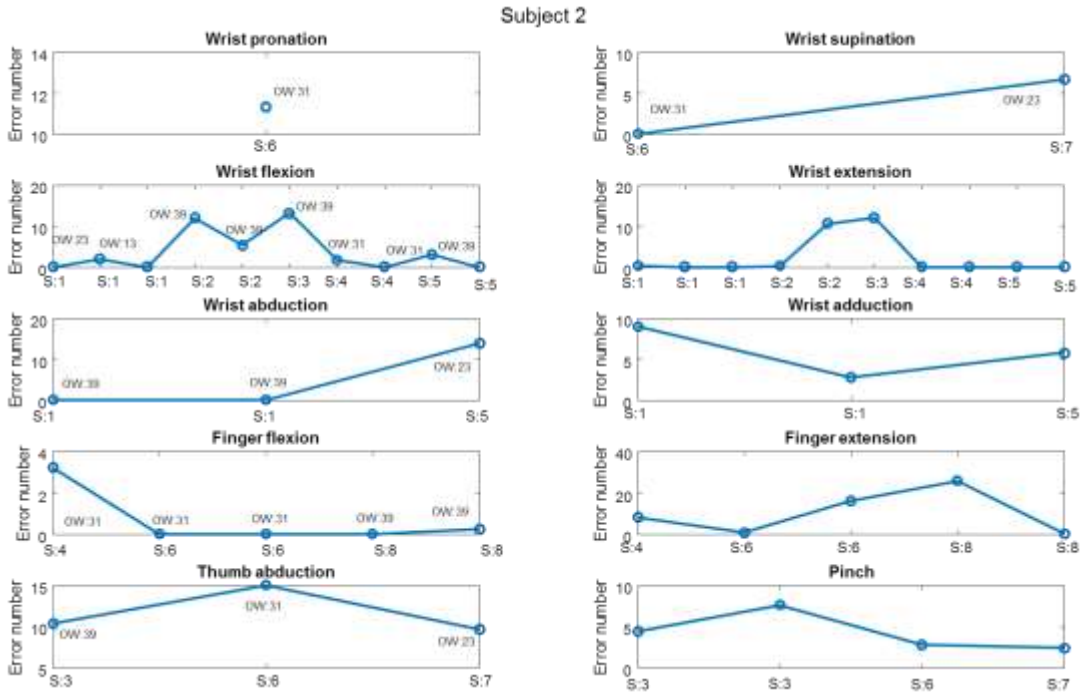

Figure 40. Mean values of the output value and related parameters across sections for patient 2

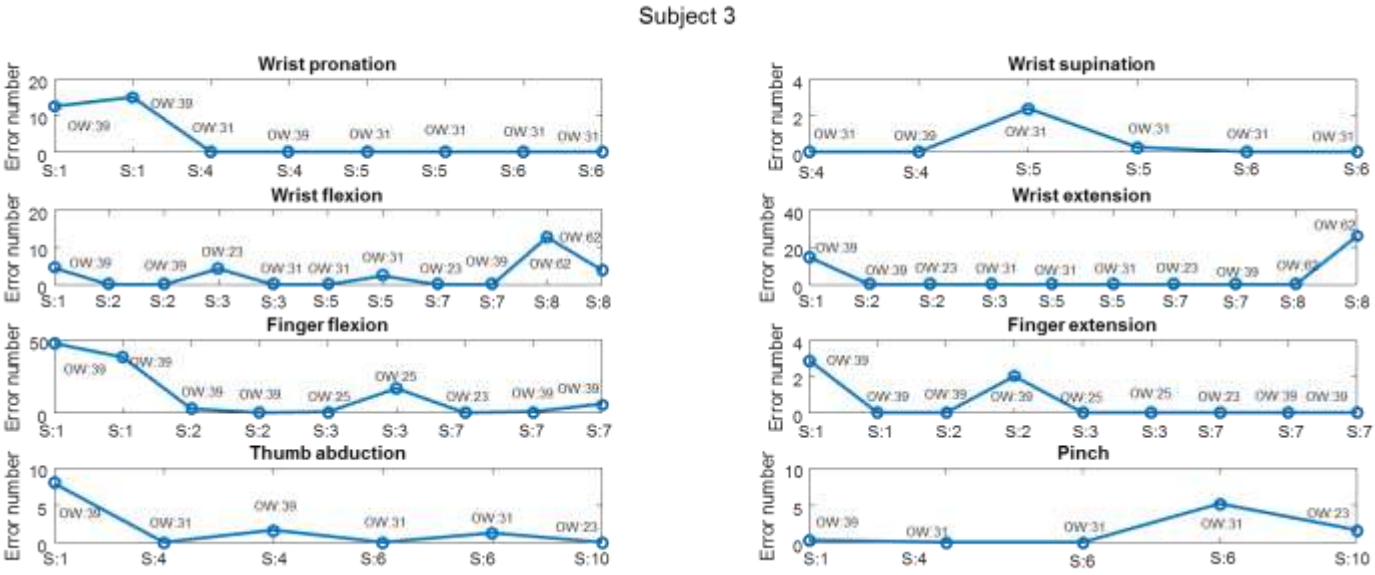

Figure 41. Mean values of the output value and related parameters across sections for patient 3

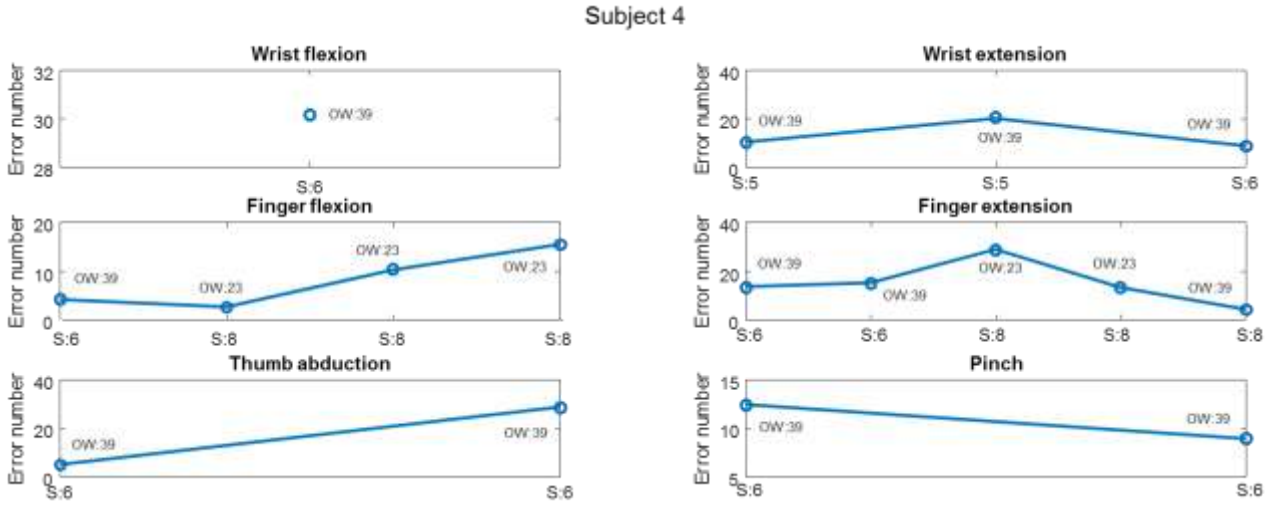

Figure 42. Mean values of the output value and related parameters across sections for patient 4.

Also in this case, therapies and parameters are highly patient-tailored. Some movements are included in the very late of the rehabilitation process and only the patient 2 performs this exercise on the entire set of movements.

Only the second and the third parameter combinations have a sufficient number of samples and have been analyzed from the point of view of the influence of parameters on the exercise

performance. Results of the comparison between movements performed with the same values of obstacle width are shown in the following figures.

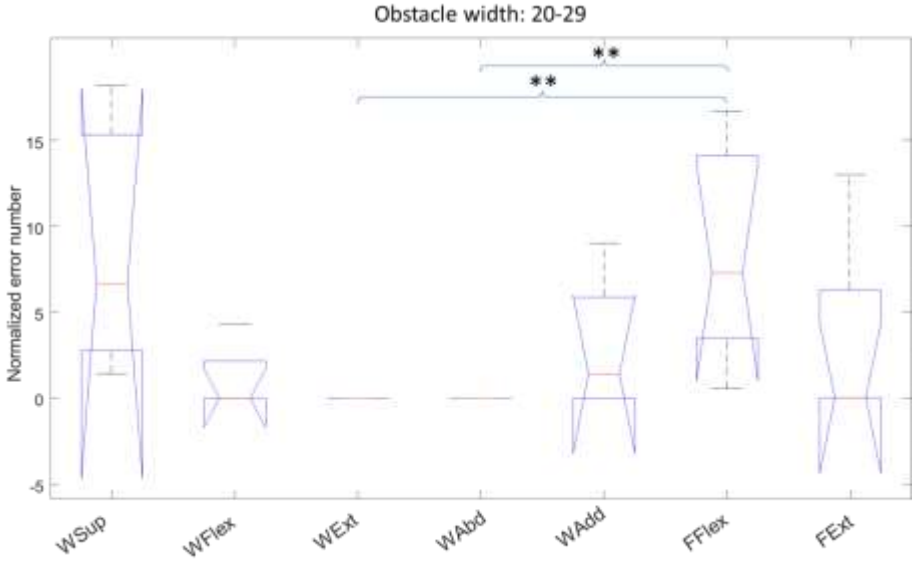

Figure 43. Boxplot showing the distribution of the output variable for each movement.

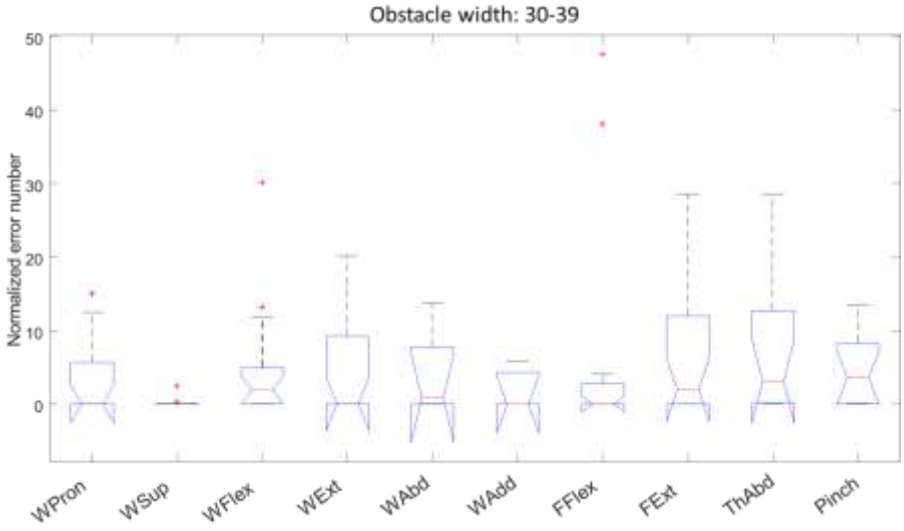

Figure 44. Boxplot showing the distribution of the output variable for each movement.

Wrist extension and abduction have been performed with no error when the obstacle width is in the range 20-29 samples and reveal a statistically significant difference with Finger flexion.

As shown in Table XVI, when the exercise has been performed with coarse movements of the wrist, the number of samples is generally lower with respect to the cases requiring movements

that involved fingers. An exception is Wrist supination when the obstacle width is between 20 and 29 samples.

Table XVI. Numerical values of boxplot percentiles shown in previous figures

Exercise Parameters - Obstacle width: 20-29										
Percentiles	**WPron**	**WSup**	**WFlex**	**WExt**	**WAbd**	**WAdd**	**FFlex**	**FExt**	**ThAbd**	**Pinch**
25th	/	2.75	0.00	0.00	0.00	0.00	3.47	0.00	/	/
50th	/	6.67	0.00	0.00	0.00	1.38	7.30	0.00	/	/
75th	/	15.32	2.15	0.00	0.00	5.88	14.10	6.25	/	/
Exercise Parameters - Obstacle width: 30-39										
Percentiles	**WPron**	**WSup**	**WFlex**	**WExt**	**WAbd**	**WAdd**	**FFlex**	**FExt**	**ThAbd**	**Pinch**
25th	0.00	0.00	0.00	0.00	0.00	0.00	0.00	0.00	0.20	0.14
50th	0.00	0.00	1.90	0.00	0.83	0.00	0.00	2.00	3.15	3.59
75th	5.65	0.06	4.95	9.22	7.73	4.35	2.83	12.03	12.69	8.24

Figure 45 shows the boxplots obtained for each movement.

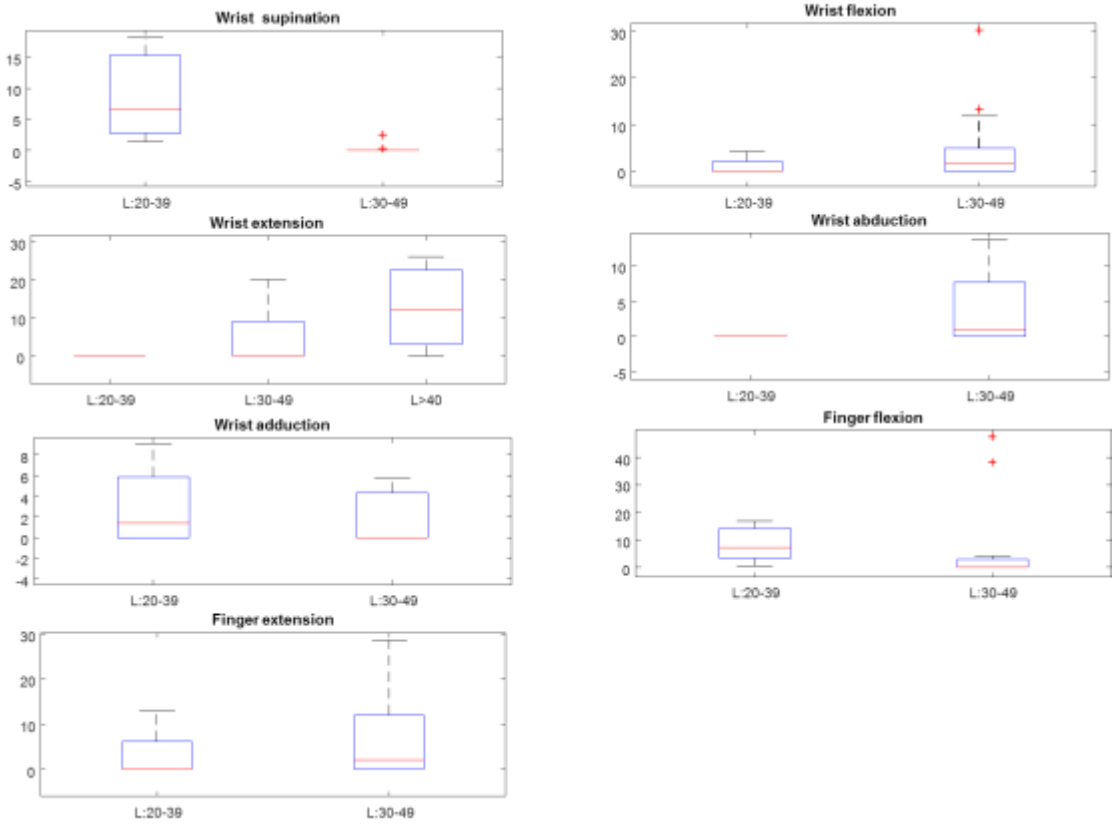

Figure 45. Boxplot of the output variable for each movement and parameter combination

The Kruskal-Wallis test doesn't reveal any statistically significant difference. Table XVII shows the variation of the output variable, it can be observed that the mean variation is null, which mean that globally, the variation of the obstacle width doesn't seem to influence the exercise performance.

Table XVII. Percentage variation of the output variable corresponding to a variation of an exercise parameter

Percent variation of output variable											
Variation	**WPron**	**WSup**	**WFlex**	**WExt**	**WAbd**	**WAdd**	**FFlex**	**FExt**	**ThAbd**	**Pinch**	**Mean**
Obstacle width	/	-100.00	100.00	0.00	100.00	-100.00	-100.00	100.00	/	/	0.00

Exercise: Arrow

In this exercise, the output variable is a Boolean whose value is 0 if the patient succeeded in reaching the target area, 1 otherwise. The parameters that have been modified and analyzed are the dimension of the target and the duration of the repetition.

The three combinations of these parameters are:

1. Target dimension (T): 2 - Repetition duration (D): 8 s;
2. Target dimension (T): 2 - Repetition duration (D): 10 s;
3. Target dimension (T): 3 - Repetition duration (D): 10 s;

Figure 46-Figure 49 show, for each patient, the administered therapy and the exercise parameters selected by the therapists.

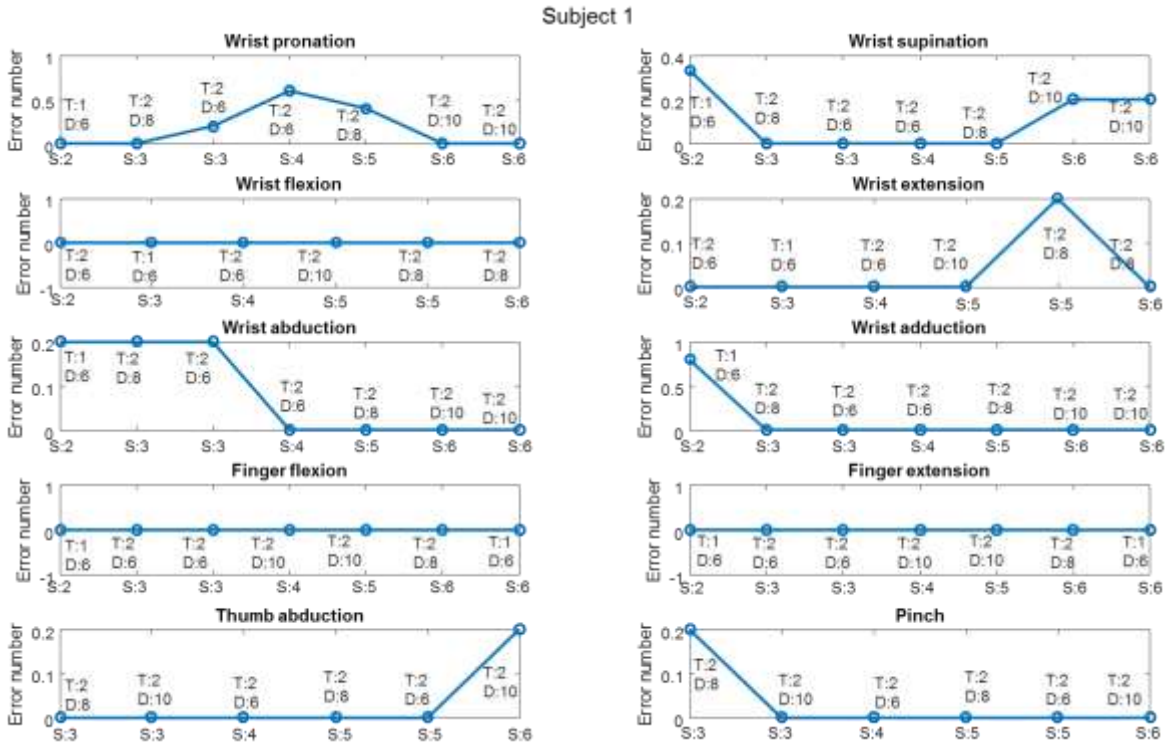

Figure 46. Mean values of the output value and related parameters across sections for patient 1

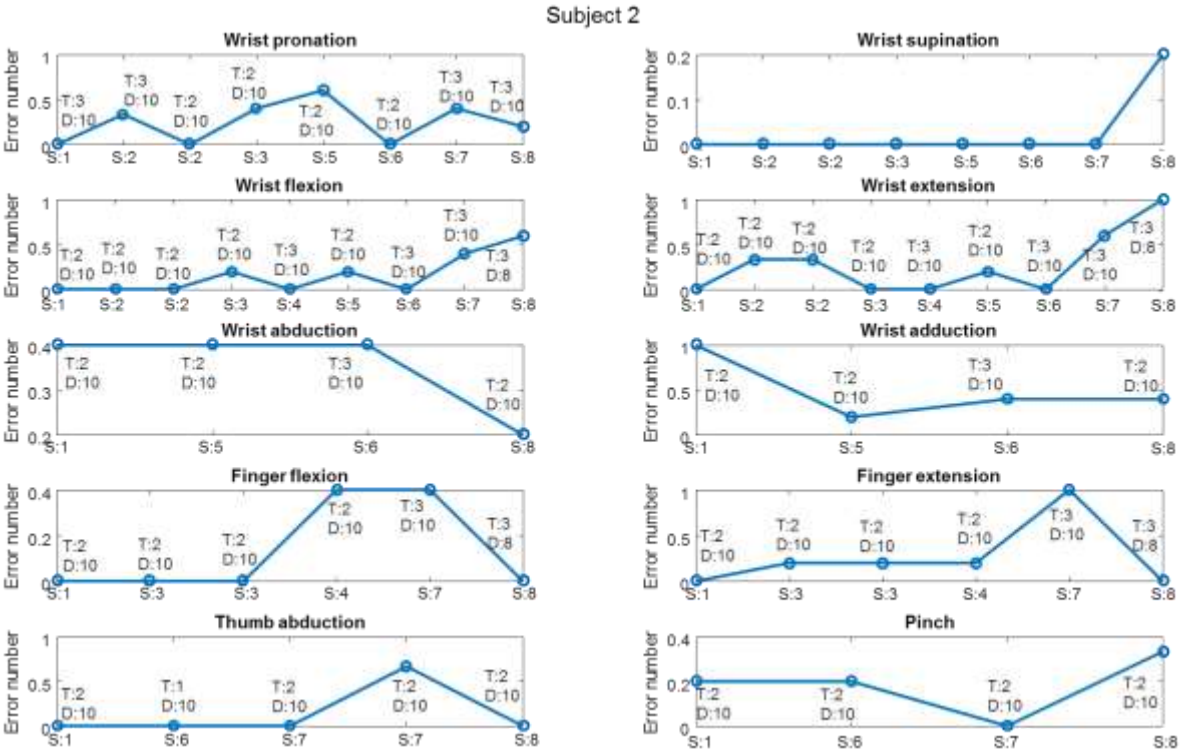

Figure 47. Mean values of the output value and related parameters across sections for patient 2

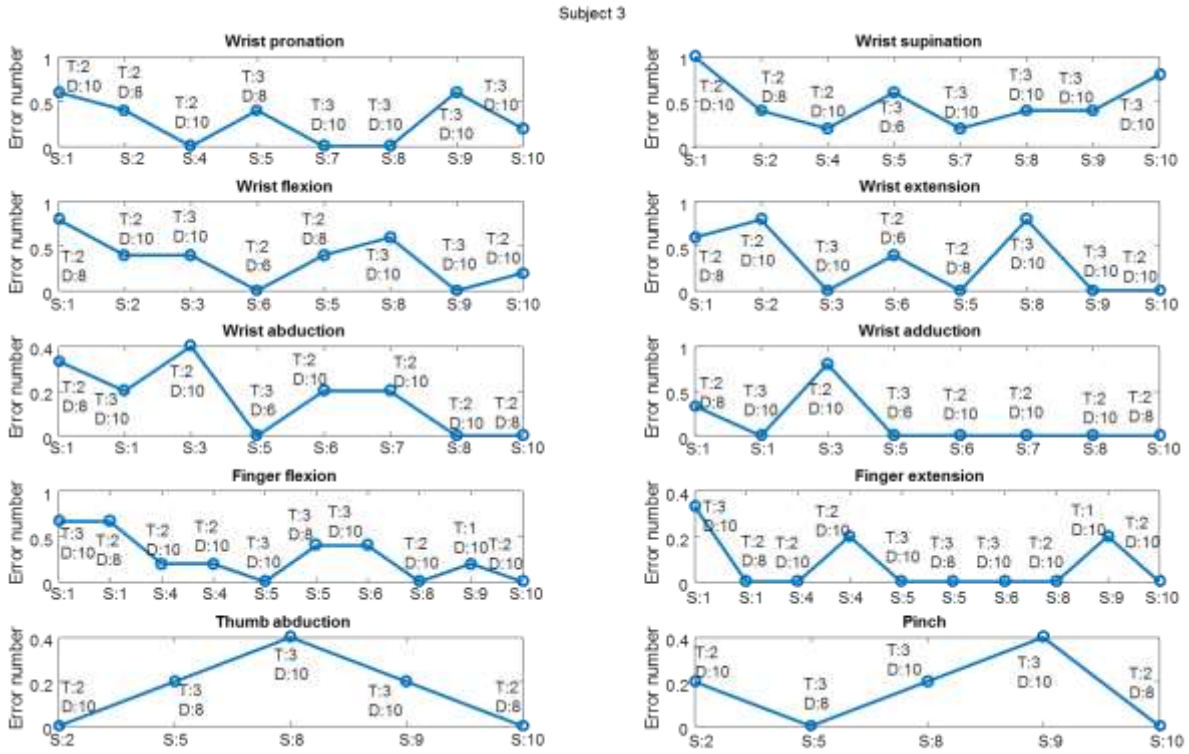

Figure 48. Mean values of the output value and related parameters across sections for patient 3

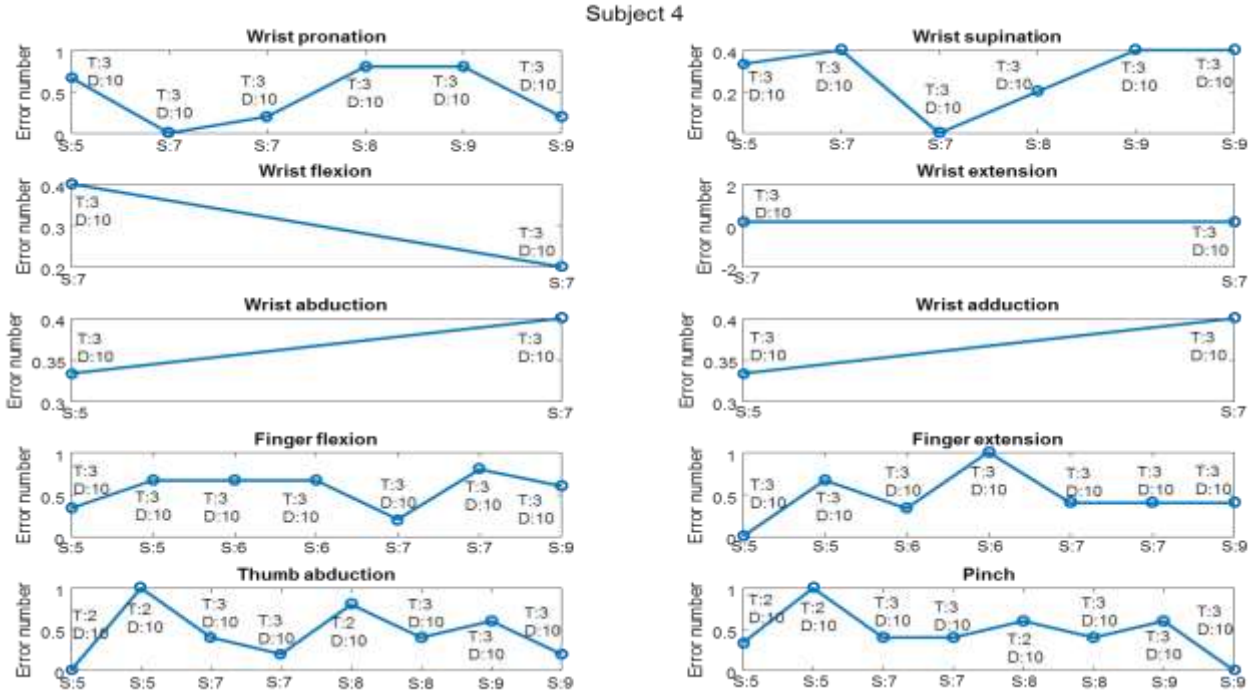

Figure 49. Mean values of the output value and related parameters across sections for patient 4

This exercise has been proposed with the entire set of movements to all patients. The repetition duration has been rarely set up to a value lower that 10 s while several values of the target dimension have been applied.

The output variable values for the movements are then compared separately for each parameter combination, with the aim of revealing if they significantly differ.

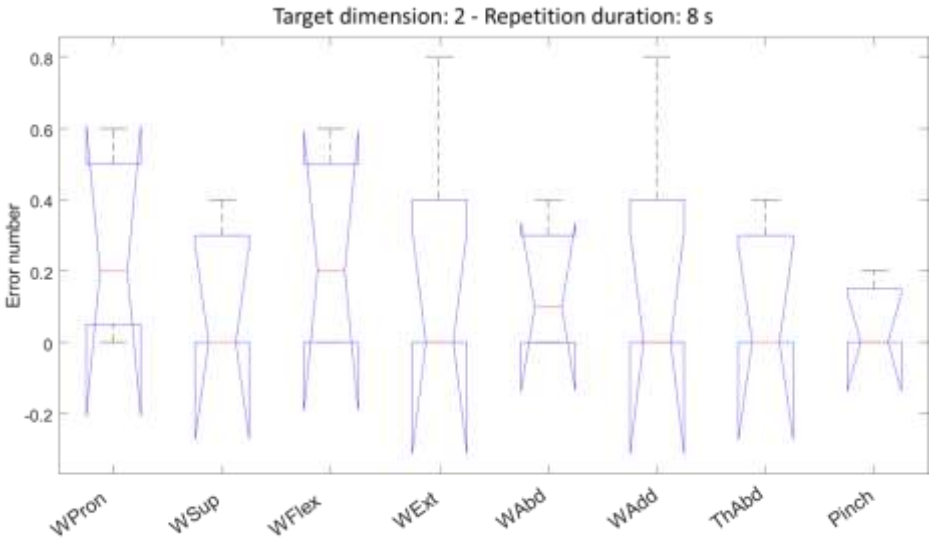

Figure 50. Boxplot showing the distribution of the output variable for each movement.

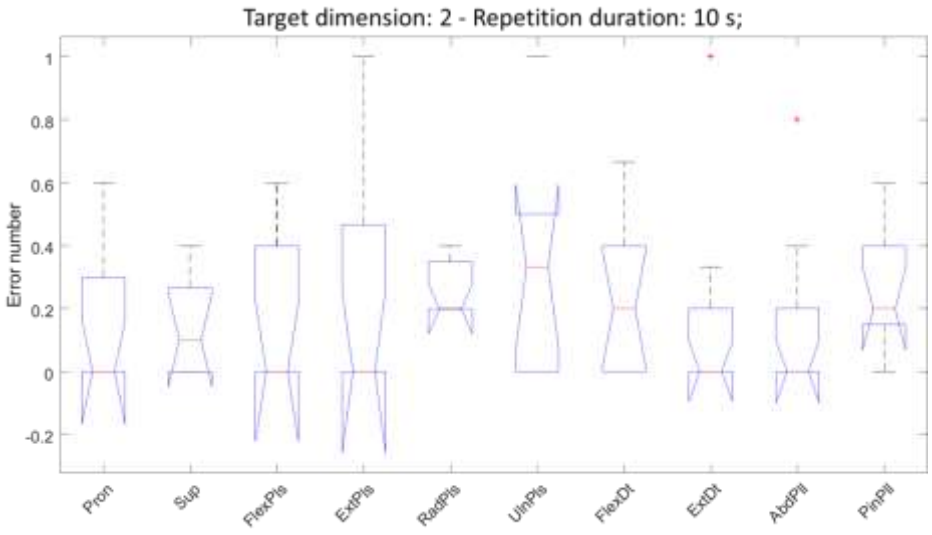

Figure 51. Boxplot showing the distribution of the output variable for each movement.

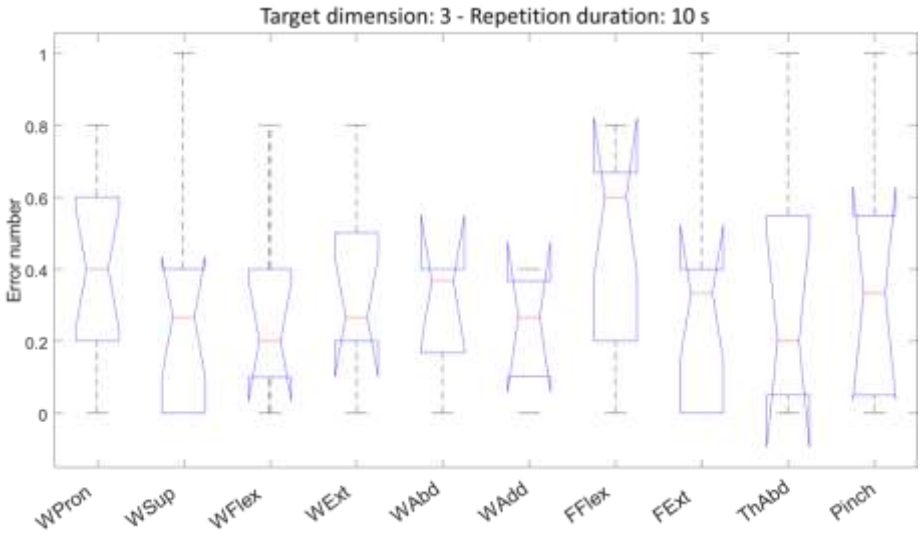

Figure 52. Boxplot showing the distribution of the output variable for each movement.

The Kruskal-Wallis test doesn't highlight any statistically significant difference between sets of movements performed with same parameters. Table XVIII shows numerical values of the output distributions. Wrist supination, extension and Thumb abduction reveal median error values lower than 0.1 for the first and second combination while the minimum median value for the third combination of parameters is 0.27.

Table XVIII. Numerical values of boxplot percentiles shown in previous figures

Exercise Parameters - Target dimension: 2; Duration: 8 s										
Percentiles	**WPron**	**WSup**	**WFlex**	**WExt**	**WAbd**	**WAdd**	**FFlex**	**FExt**	**ThAbd**	**Pinch**
25th	0.05	0.00	0.00	0.00	0.00	0.00	NaN	NaN	0.00	0.00
50th	0.20	0.00	0.20	0.00	0.10	0.00	NaN	NaN	0.00	0.00
75th	0.50	0.30	0.50	0.40	0.30	0.40	NaN	NaN	0.30	0.15
Exercise Parameters - Target dimension: 2; Duration: 10 s										
Percentiles	**WPron**	**WSup**	**WFlex**	**WExt**	**WAbd**	**WAdd**	**FFlex**	**FExt**	**ThAbd**	**Pinch**
25th	0.00	0.00	0.00	0.00	0.20	0.00	0.00	0.00	0.00	0.15
50th	0.00	0.10	0.00	0.00	0.20	0.33	0.20	0.00	0.00	0.20
75th	0.30	0.27	0.40	0.47	0.35	0.50	0.40	0.20	0.20	0.40
Exercise Parameters - Target dimension: 3; Duration: 10 s										
Percentiles	**WPron**	**WSup**	**WFlex**	**WExt**	**WAbd**	**WAdd**	**FFlex**	**FExt**	**ThAbd**	**Pinch**
25th	0.20	0.00	0.10	0.20	0.17	0.10	0.20	0.00	0.05	0.05
50th	0.40	0.27	0.20	0.27	0.37	0.27	0.60	0.33	0.20	0.33
75th	0.60	0.40	0.40	0.50	0.40	0.37	0.67	0.40	0.55	0.55

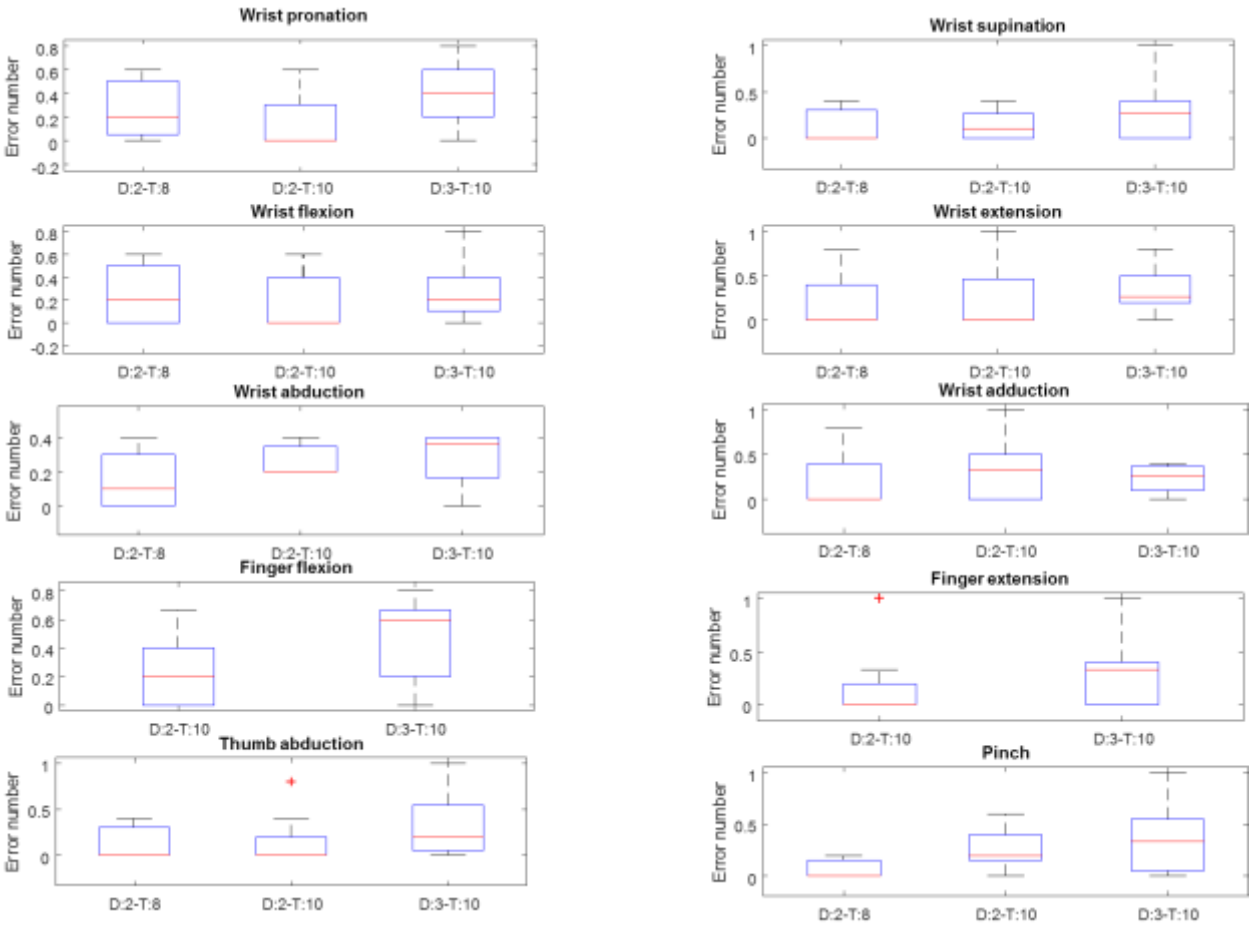

Figure 53. Boxplot of the output variable for each movement and parameter combination

Also in this case, no statistically significant difference has been revealed when movements are performed with each of the parameter combination.

The percent variation of the error number has been calculated. Table XIX show obtained results.

Table XIX. Percentage variation of the output variable corresponding to a variation of an exercise parameter

Percent variation of output variable											
Variation	**WPron**	**WSup**	**WFlex**	**WExt**	**WAbd**	**WAdd**	**FFlex**	**FExt**	**ThAbd**	**Pinch**	**Mean**
Target dimension	100.00	166.67	100.00	100.00	83.33	-20.00	200.00	100.00	100.00	66.67	103.33
Duration	-100.00	100.00	-100.00	0.00	100.00	100.00	/	/	0.00	100.00	25.00

It can be observed that the median values generally increase when both the parameters are increased, especially when the target dimension is modified from 2 to 3. In this case the mean value of variations is higher than 100%. The mean percent variation for the increase of the duration of a

task repetition is slightly positive, this means that, when the speed of the marker has been decreased, the error number moderately increased.

5.4.2.3 Conclusions

The comparison between the clinical outcome measured before the begin and at the end of the therapy reveals that parameters related to join pain and sensory function of the upper limb slightly decrease. Since the device and the protocol are not suitable for the treatment of sensory impairment or for the reduction of pain, these results are plausible. On the other hand, the increase of FMA-WH and BBT, suggests that the outcomes that are more specifically related with hand and finger motor functionalities, benefit from the EMG-BF therapy. NHPT decrease for patient P12 and remain the same for the other patients. The NHPT test requires fine dexterity of the thumb, a good tactile sensitivity and low tremor: the system and the rehabilitation protocol, as conceived for the clinical trial, are probably inefficient in the treatment of such a fine motor function. If these results will be confirmed by further evidence, the causes of this should be investigated and suitable improvements should be applied to the device: the EMG recording system could be further enhanced with the aim of better analyze signals produced during thumb and fingers movements, or the motion recognition strategy could be further developed for this purpose, or exercises focused on thumb and fingers could be proposed with higher frequency during the rehabilitation protocol.

One of the main requests of the rehabilitation field is related to the need of highly patient-specific therapies. Evidence from the instrumental data of the preliminary dataset shows an extensive use of this functionality. In fact, the protocols have been widely varied for different patients regarding the movements, the intensity and frequency of tasks, and the exercise level of challenge.

The comparison between exercise performance seems to reveal that no relevant difference exists between movements. Surprisingly, finger movements showed lower performance measures in only one case. These results are ascribable to the device control strategy: the calibration of the device is performed before every session and can be quickly repeated in case the patient or the therapist reveals anomalies in the control signal. This strategy is efficient in order to guarantee a stable control and the possibility of including in the protocol also highly impaired movements.

Exercise performance related to the variation of the intensity of the contraction requested to control the signal show interesting results for exercise Bar and for exercise Ball. In fact, it can be observed that an increase of the requested contraction within the 60% of the MVC, doesn't seem to increase the degree of difficulty of the exercise. On the contrary, an improvement of performance is highlighted. This means that the degree of controllability of the EMG-BF is a trade-off between a high sensibility of the device to the RMS signal variations, that can cause instability of the control signal and the comfortability of the patient who needs to control the signal with an MVC percentage that should be consistent with his/her degree of impairment. It could be of interest to investigate if this evidences is confirmed on a complete dataset and if a statistical significance is proved to exist. If these results are confirmed, a study about the cut-off value of the %MVC could be performed in order to reveal values that optimize the device controllability. This parameter could then be employed by the therapists to optimize the rehabilitation protocol in order to focus the therapy on EMG patterns reproducibility or on muscle reinforcement.

The analysis that has been performed with reference to the Fitts' Law on exercise Ball results, show that the Fitts' Law model is not suitable for the present experimental data: the experimental protocol included other exercises besides the exercise Ball and fatigue phenomena could alter the results. Moreover, the exercise has been performed with only two values of target width: more significant results could be obtained if the variation of the target width includes more values. Dedicated tests could be planned for the final design of the GUI, in order to further investigate this aspect.

Unfortunately, the longitudinal study is in the preliminary stages at the time of writing and the dataset is poor. Nevertheless, some interesting results have been revealed and it is expected that their consistence would increase when the complete dataset of enrolled patients will be analyzed.

6 Analysis of continuous movements: a comparison between temporal and spatial information

This chapter presents the research activity, not included in the clinical trial, that is more directly related to the EMG signal analysis.

Many studies highlighted the relevant role of the EMG signal in the quantitative assessment of motor impairment. The analysis of the muscular activity from an electrical point of view finds an important application to the cases of highly impaired patients who are unable to develop a movement or to produce a level of force that biomechanical sensors can reveal. These aspects strongly fostered the EMG signal study for application in the clinical and rehabilitation fields. This chapter presents a study that has been performed for this purpose and is focused on continuous movements of the hand and the wrist. The interpretation of EMG signals is based on the optimization of several parameters. Two relevant parameters are the spatial are the temporal information included in the EMG signal. In literature, the temporal information is mainly related to the length of the window employed to calculate the features of the EMG signal. The spatial information refers to the effect of electrode number, orientation, configuration and geometry on the analysis of sEMG signal. Recent focus on the analysis of continuous motions and on the interaction between sEMG temporal and spatial information reveals the importance of quantifying their respective discriminant powers in the analysis of continuous movements. The aim of the present work is to investigate the separate contributions of spatial and temporal information and quantitatively evaluate their relevance in the interpretation of the sEMG signals recorded during continuous movements. The spatial information was represented by RMS signals recorded on different electrodes while, differently from literature, the temporal information was expressed by the behavior of sEMG over time through RMS time series [148].

6.1 Experimental Setup and Protocol

The EMG signals were recorded using the portable EMG device employed in the clinical trial exposed in the present thesis (see Paragraph 5.1.1 for details) and same references have been used to position the electrode array (see Paragraph 5.2 – Experimental setup and protocol).

A group of 10 healthy volunteers (seven males and three females) aged between 26 and 35 years participated in the experiment and signed informed consent form. The study was in accordance with the Helsinki Declaration [112] and participant data have been treated according to the Organic Law of Protection of Personal Data. Subjects comfortably sat in front of a PC screen, with their elbow lying on the table, the forearm was perpendicular to the table to guarantee a comfortable rest position with no relevant muscular activity. Furthermore, the rest position allowed the execution of free wrist movements.

The experimental protocol comprised 14 wrist movements and the rest position. Specifically, the protocol included 4 movements (named single movements) activating different muscular areas: flexion, extension, supination and pronation. Each of the 4 movements was also performed in 2 temporal variants; in the first one (named double movement) the subject performed the same movement twice, returning in the rest position between two motion repetitions, in the second one (named maintained movement) the subject had to perform the movement and then maintain an isometric contraction in the target position. Finally, a rotation of the wrist (i.e. a continuous sequence of abduction, flexion, adduction, extension), was included. The wrist rotation was performed as a single movement and as a double movement (See Table XX).

Table XX. Movements included in the experimental protocol and labels

Mov. N°	Movement	Mov. Label	Variants	Var. Labels
0	Rest	Re		
1	Flexion	F	Single	S
2	Flexion	F	Double	D
3	Flexion	F	Maintained	M
4	Extension	E	Single	S
5	Extension	E	Double	D
6	Extension	E	Maintained	M
7	Supination	S	Single	S
8	Supination	S	Double	D
9	Supination	S	Maintained	M
10	Pronation	P	Single	S
11	Pronation	P	Double	D
12	Pronation	P	Maintained	M
13	Rotation	R	Single	S
14	Rotation	R	Double	D

The experimental protocol was selected to record a heterogeneous dataset about movements which differ both from a spatial and from a temporal point of view. For example, single flexion and single extension induce different activation maps for forearm muscles, but they have similar temporal profiles. On the contrary, single flexion and double flexion, involve the same muscles but the single flexion shows a single peak in the RMS signal, whereas the double flexion induces two peaks. The rotation of the wrist was introduced because its complex patterns involve a specific evolution of the muscular areas on the entire circumference covered by the electrode array over time.

A graphical interface (GUI) helped subjects to perform the protocol in the correct way and with the correct timing. The training phase was composed by 10 repetitions of all the movements. The testing phase consisted of 5 repetitions of a randomized sequence of the trained motions; the randomization was applied in order to avoid any adaptation effects. The GUI reproduced sounds in order to indicate timing and duration of the tasks; every repetition of a motion was performed with a predefined timing. Rest periods were introduced every 10 movements and additionally whenever the subject needed to avoid fatigue. The entire protocol lasted about 40 minutes.

6.2 Template making and matching (TMM)

Training repetitions were automatically segmented during the template making (training phase); the muscular activity was considered only when the RMS signal of at least 2 channels was higher than a threshold Sth equal to the 66° quantile of the signal. The quantile-based threshold improved the algorithm robustness to noise and its value was empirically determined for the experimental protocol. Whenever the threshold crossing was detected, the signal was segmented for W samples. The optimal value of W equal to 100 was empirically determined as the minimum time interval that guaranteed a uniform segmentation (W equal for all the movements), avoiding the overlap between two consecutive tasks. The window length W equal to 100 was applied to the entire protocol. The RMS signal on each channel was then normalized with respect to the maximum RMS value measured inside the window. Each template sample was then modelled as a gaussian variable X of parameters μ and σ using segmented data. Therefore, for each recording channel, each movement was represented as a series of W Gaussian variables.

For template matching (testing phase), a similarity measure between the templates and RMS signals recorded was calculated. The normalized RMS signals of the testing dataset were evaluated over a

sliding window (the testing window) of length W. To establish the equivalence between the testing window and the motion templates, the probability that every sample of the testing window belonged to each template was computed. To this purpose, for every sample of the testing window, the Complementary Cumulative Distribution Function (CCDF) was calculated with Equation 3.

$$F_X(x) = P(X > x) = \int_x^{+\infty} f_X(t)dt \qquad (3)$$

where $f_X(t)$ was the density function of X, X was the gaussian variable that model a template sample and x was the value of the testing sample. All the gaussian distributions were normalized to the standard normal (μ=0, σ=1) to reduce the computational power. CCDF values were then weighted according to the normalized RMS signal amplitude. The linear combination of the CCDF values (global CCDF) of all samples of the testing window was calculated for every movement.

The classification was performed in 2 steps:

1. Rest position vs. all: if the entire signal in the testing window was lower than Sth, the window was assigned to the rest position class.

2. Movement classification: windows that were not assigned to the rest position class were analyzed and classified. The testing window was assigned to the template that generated the highest global CCDF. However, if all the global CCDF values were lower than a minimum probability threshold Pth, the testing window was rejected and associated to the rest position. The Pth threshold was optimized over the training data of each subject in order to maximize the recognition performance.

Finally, the testing window was shifted by one sample and the new testing window was evaluated on the base of its global CCDF value. This procedure was repeated until the entire testing dataset was analyzed. Figure 54 shows the flow chart of the template making and matching process.

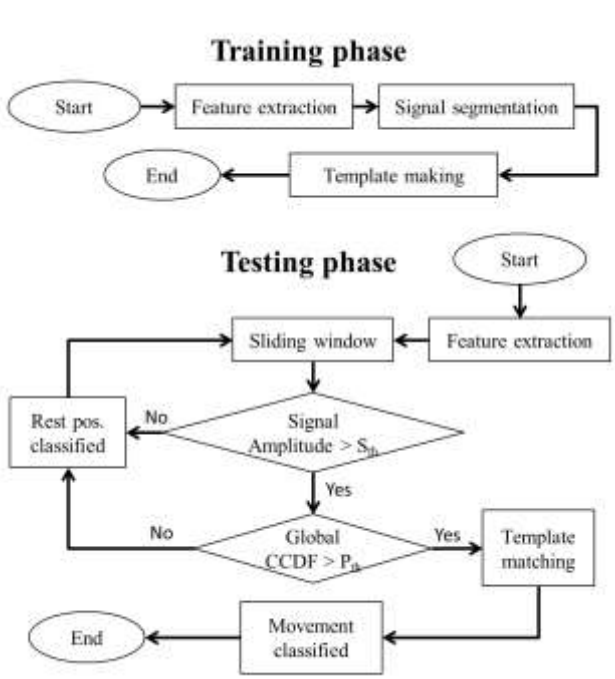

Figure 54. TMM Work Flow. During the training phase, RMS signals were segmented to identify movement repetitions and define templates. During the testing phase, signals were evaluated over a sliding window of length W. If the amplitude of the window signal was lower that the threshold Sth it was classified as Rest position. If it exceeded Sth, the linear combination of the Complementary Cumulative Distribution Function (CCDF) of all the window samples was calculated and compared with the threshold Pth. If the global CCDF didn't exceed Pth the window was classified as Rest Position, otherwise the template matching was performed, and the window was classified as the template associated with the highest CCDF.

6.2.1 TMM algorithm implementation

Since the aim of this work was to separately quantify the discriminant powers of the EMG temporal and spatial information for continuous motions, two different approaches to movement classification were considered and compared: the temporal approach and the spatial approach. Moreover, an additional approach was tested as a combination of both: the spatio-temporal approach. The spatio-temporal approach allowed the validation of the algorithm implemented and an evaluation of performance improvement when signals recorded on different electrodes were associated to RMS time series and vice-versa. Template making and matching was performed as described, but the data used to build templates and testing windows were different depending on the applied approach.

Temporal approach

In this technique the information of muscular activation areas was removed, thus a single signal calculated from all electrodes was applied as the input of the algorithm. Data window were averaged over the 4 channels with the highest average RMS value. The information related to the temporal variation of the RMS value was preserved, while the localization of the electrodes that contributed to the time series was neglected. Every time the segmentation window for template making moved or the testing window for template matching shifted, the selection of active channels was renewed and the averaging process was repeated. Thus, the input signal described the RMS time series generated when a specific movement was performed. Figure 55 details an example of training signals (red line) and template mean values (blue line) for wrist flexion (Figure 55.A) and extension (Figure 55.B) in the 3 temporal variants. It can be seen that RMS time series for movements performed with the same timings are not distinguishable.

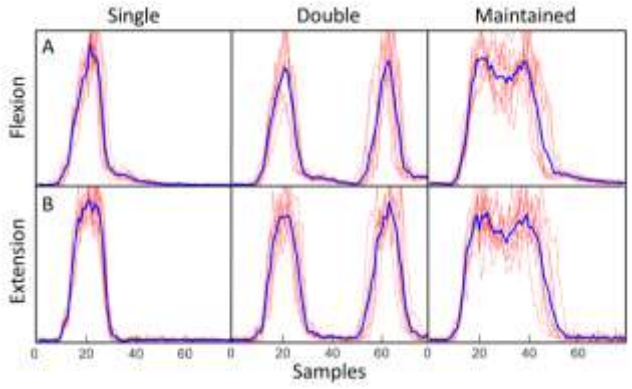

Figure 55. Examples of templates for wrist flexion (Figure 55.A) and extension (Figure 55.B) in single, double and maintained variants.

This test was performed in order to analyze the protocol while neglecting the muscles that were involved in the movements and to test the discriminant power of the only temporal information through the RMS time series. It could be expected that this method would completely fail in discriminating movements with same timings (see Figure 55) even if they differed in the muscles they activated (e.g. single flexion and single extension should induce the same temporal profile on different muscles).

Spatial approach

For this approach, the classification was solely based on spatial localization of muscular activation areas. The temporal information was removed averaging the RMS signals over the entire observation window. A subset of consecutive samples (from 20 samples to 50 samples, according to the movement duration) that exceeded the threshold Sth was identified separately for each channel. The RMS mean value of active samples was then calculated. The templates and the testing windows described the level of activation of each channel in terms of mean RMS amplitude for a specific movement. Radargraphs in Figure 56 represent training signals (red line) and template mean values (blue line) calculated with the spatial approach for wrist flexion and extension. The data length of each spoke is proportional to the normalized RMS amplitude on each channel (radargraph rays). In this case the 3 temporal variants are very similar while movements activating different muscles produce highly different templates.

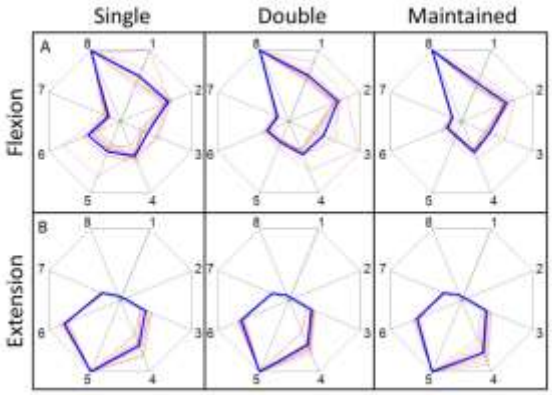

Figure 56. Radargraphs corresponding to templates for wrist flexion (Figure 56.A) and extension (Figure 56.B) in single, double and maintained variants. Each spoke represents a recording channel and the data length of each spoke is proportional to the normalized RMS amplitude.

This test should highlight that it was difficult to distinguish when a movement was performed once, twice or if it was maintained for a long time. On the contrary, this method should discriminate movements performed with different muscles (e.g. flexions from extensions) but confuse when the same motion was performed with different timings (e.g. single flexion vs. double flexion etc.).

Spatio-temporal approach

Considering the information from both the spatial and the temporal approaches, the input of the spatio-temporal approach was a matrix of size N · W, where N is the electrodes number equal to 8 and W is the window length equal to 100. Thus, a template was represented by the RMS time series on every channel. This approach was tested to validate the algorithm with a complete set of information and to compare recognition performance when the partial set was applied. The expectation was that this method discriminated both movements where different muscles were involved (i.e. flexion vs. extension vs. supination vs. pronation) and motions with different temporal profiles (e.g. single flexion from double flexion from maintained flexion). Moreover, high accuracy was expected for the recognition of wrist rotation, since this approach should be able to take into consideration both the dynamic spatial pattern, and timings of activation of all the muscles involved in the movement.

6.2.2 Evaluation of recognition performance

To evaluate classification performance the Confusion Matrix (CM) was computed. The CM is a matrix that easily allows the visualization of an algorithm performance. Each column of the matrix represents instances in an actual class (true class), while each row represents instances in a predicted class (output class). Three parameters were calculated from the CM: the Global Classification Accuracy for all approaches, the Local Classification Accuracy and the Output Percentage only for temporal and spatial approaches.

Global Classification Accuracy (GCA) - The GCA is a CM based measure of the classification performance of an algorithm. It is calculated as the ratio between the sum of instances in the principal diagonal and the sum of all instances. The expectation was that the CM of the spatio-temporal approach had a high GCA. The GCA of the spatio-temporal approach has been calculated in order to validate the TMM algorithm implemented. The temporal and the spatial approaches should have lower GCA values since they are not suitable to recognize respectively, spatial or temporal patterns.

Local Classification Accuracy (LCA) - According to previous considerations, it could be supposed that the spatial and the temporal approaches revealed some classification clusters. Therefore, in the CM calculated for the temporal approach the movements were ordered in the following way: all the single movements, then all the movements repeated twice and finally all the maintained movements. In fact, this approach should fail in discriminating motions that only differed in the muscles activated. On the contrary, the CM computed for the spatial approach was organized depending on the muscles activated: firstly all flexion movements, then all extension movements et cetera. The submatrix represented by each cluster was individuated. The LCA was calculated as the GCA of each submatrix. The LCA allows the quantification of the discriminant power of the type of information expressed by the input data on a specific subset of movements. The LCA was evaluated in comparison with the random guessing. In the case of the temporal approach, the expectation was a homogeneous classification rate of 20% for submatrices including 5 movements (single and double variations) and of 25% for the submatrix including 4 movements (maintained variation). For the spatial approach the expectation was that the recognition and the confusion of single, double and maintained versions of every movement should be homogeneously distributed with a rate of internal confusion comparable to the random guessing; 33% for submatrix of size 3x3 (submatrix for all the movements but the rotation) and 50% for the submatrix of size 2x2 (submatrix for the rotation).

Output Percentage (OP) - The OP was evaluated on the submatrices and calculated in 2 steps. Firstly, the sums of instances in each column of the submatrix (true classes) were calculated and normalized with respect to the number of actual instances pertaining each class. Then, the mean value of the sums was calculated. The OP value allowed the quantification of the correct instances in a specific submatrix. The ideal OP of all the submatrices for both the spatial and temporal approach is 100%. In fact, with the temporal approach the temporal variants should be clearly recognized from each other. On the contrary, the spatial approach should correctly discriminate the movements which generate different activation maps.

To assess the statistically significant difference between the approaches, the Friedman test was applied. If the Friedman test determined the difference, the conditions were compared pairwise using the Wilcoxon signed-rank tests. A level of $p<0.05$ was selected as the threshold for the statistical significance.

6.3 Results and discussion

For each approach, the movements in the CMs were ordered to highlight classification clusters. Different clusters are highlighted with different colors. See Table XX for labels used in CM. Following figures show the CMs obtained for the tested approaches that allowed the evaluation of the discriminant power separately for the spatial and the temporal information.

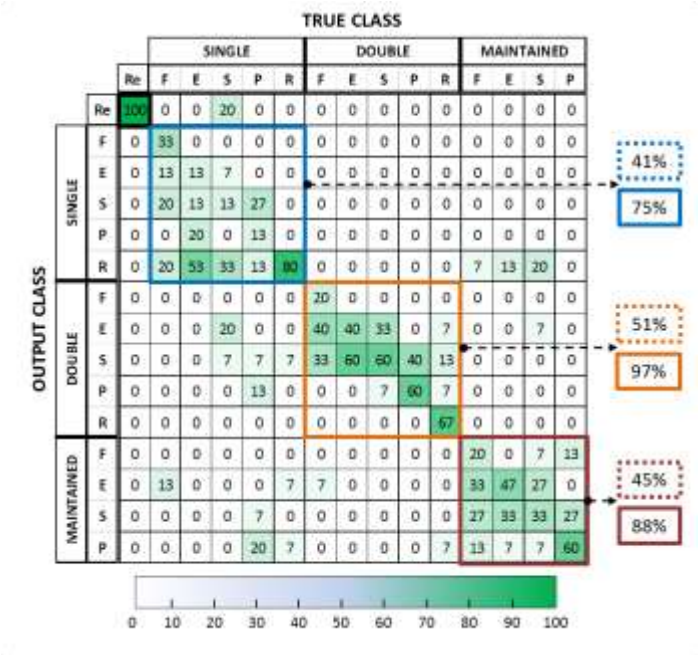

CM 1.Confusion Matrix [%] of the temporal approach, LCA (dashed line) and OP (continuous line) of submatrices grouping movements with similar timings.

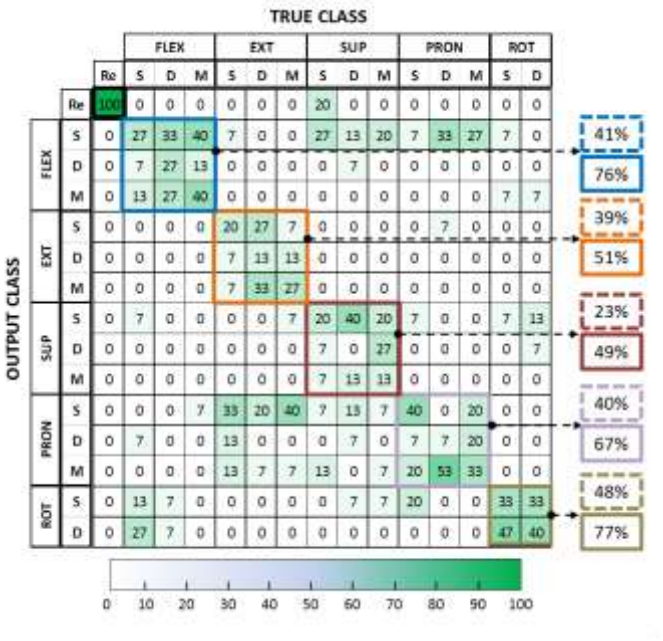

CM 2.Confusion Matrix [%] of the spatial approach, LCA (dashed line) and OP (continuous line) of submatrix grouping movements involving same muscular areas.

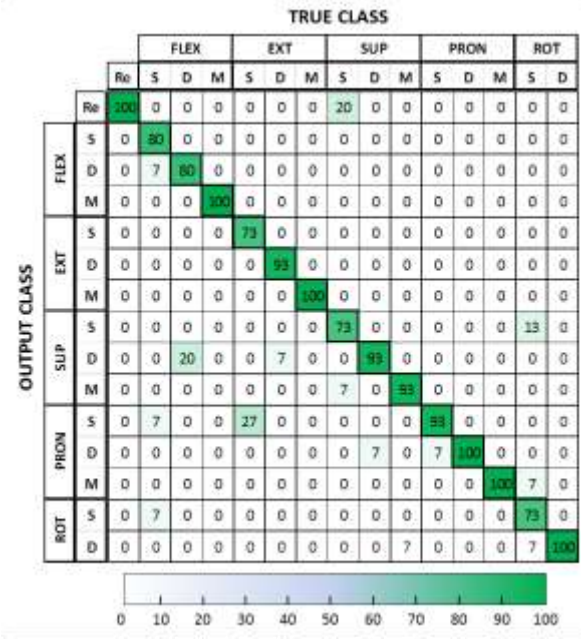

CM 3.Confusion Matrix [%] of the spatio-temporal approach.

CM1 show results obtained for the temporal approach. The GCA of 44±26% and the OP of 87% are in line with expectations and reveal that the only temporal patterns are not sufficient to correctly discriminate the set that include movements which differ only in the muscles they activate. Nevertheless, the LCA of the temporal submatrices overtake expectations. In fact, LCA values are

respectively 41% for single movements, 51% for double movements and 45% for maintained movements. These values are about twofold ($\chi2 = 30$, $p \ll 0.001$) with respect to 20% (single and double variations) and 25% (maintained variation). This suggests that the movements of the protocol performed with similar timings but activating different muscles, have specific RMS temporal patterns which contributed to distinguish one from each other. This is in line with previous studies [149], [150] and suggests that the specificity of temporal patterns is also relevant for EMG feature time series regardless the position of the recording electrodes.

CM2 represent the confusion matrix obtained with the spatial approach. The results reveal a mean GCA value of 29±22%. This approach shows no statistical differences with random guessing ($\chi2 = 0.08$, $p = 0.8$) with a mean LCA of 38% that was few lower than the expected value of 41.5%, with a minimum of 23% for the supination and a maximum of 48% for the rotation. Moreover, the mean OP value of 64% is calculated, it is considerably lower than the ideal value of 100%. In fact, it can be observed that the pronation and the maintained pronation, are often wrongly recognized and confused with the 3 temporal variants of the extension, while the flexion is often misclassified as supination and pronation movements. It indicates that the contribution of the temporal information for the recognition of movements of the protocol is not limited to the capability to distinguish temporal variants of the same movement, but also helps to more accurately discriminate different movements with close activation areas.

The spatio-temporal approach allows the validation of the algorithm implemented. It can be seen that the CM3 is highly diagonal with a GCA of 90±10.5%, this suggests that the algorithm implemented is efficient when applied to the experimental protocol. This result is comparable with the results obtained with the TMM applied to handwriting recognition with a maximum of 6 pair of electrodes positioned on the forearm muscles [151][152]. This approach allows the discrimination of both the movements that are different for muscles involved and movements that are performed with same muscles but with different timings. Moreover, the wrist rotation (single and double variations) has classification accuracy values comparable with the other movements of the protocol.

The statistical difference between the tested approaches was verified ($p<<0.01$).

6.4 Conclusion

This study provided a TMM algorithm and an experimental protocol with the aim of fully separating the contributions of spatial and temporal information for continuous movement analysis. The proposed algorithm showed congruent results for the three approaches tested and demonstrated the significance of the temporal information of the EMG signal for discriminating continuous movements, both when they only differ in the muscular areas they activate and when they are performed with different timings. Moreover, the results for the spatio-temporal approach could also have relevance in other fields such as rehabilitation, sports and recognition of Sign Language gestures.

Findings of the present study are promising and suggest that the EMG temporal information for continuous motions analysis should have a major attention. Latest requests in the rehabilitation field include task-oriented (instead of impairment-oriented) therapies and tools to quantitative monitor the recovery progress of patients. This goal demands instruments that enhance information related to the kinematics of the movement and approaches that allow the analysis of muscular patterns. An approach that tracks the temporal relation between the activation of the muscles involved in the movement could provide an important support to this study. The spatio-temporal approach proposed in the present study appears suitable for these applications, since it provides an activation map of the muscular areas and information about their evolution during the movement execution.

Further work will be done to test the algorithm on a more challenging experimental protocol including a set of complex movements. Dynamic Time Warping could be introduced as a preprocessing step to find an optimal alignment between time series and improve results. Finally, the robustness of the method will be tested using other features (e.g. MAV, IEMG, WL, AAC) and other distance measures between the templates and testing sample sequences.

7 Thesis conclusions

Technological solutions have shown great potentialities in motor rehabilitation applications. The present research was motivated by the aim of developing and validating an EMG-BF device in the context of post-stroke motor rehabilitation of the hand. The development of the device has been preceded by an extensive literature review on rehabilitation technologies. Moreover, the consultations of the therapists of the Cerebrovascular Disease Unit of the San Camillo Hospital (Venezia, Italy) supported all the evolution phases of the system. The device was portable, lightweight and suitable for a wide variety of forearm diameters. EMG signals were processed and transmitted via Bluetooth to a host PC, where a GUI displayed the BF and supported therapists and patients during the rehabilitation sessions.

A clinical trial has been planned and successfully submitted to the Health Department. The study included two phases: a cross-sectional study performed in order to reveal the clinical characteristics of patients who are able to control the device and a longitudinal study, for the evaluation of the clinical effect and safety of a rehabilitation therapy performed with the device. Preliminary results of the cross-sectional study highlighted a correlation between the patient clinical picture and the dexterity in successfully managing the control signal. Moreover, a significant relation has been found between clinical outcomes and the data recorded with the device during the exercises, i.e. the RMS of the EMG signal and the time that the patients need to complete the proposed tasks. The evidence confirms the feasibility of the technological solution in a clinical context and gives some quantitative results about the reliability of the performance parameters that can be extracted. The longitudinal study is in the early stages, but the related data analysis revealed some relevant aspects. In fact, clinical measures specifically related to the functionality of the hand and fingers improved, suggesting the efficacy of the therapy. Measures that have been selected in order to assess the patient performance, revealed the efficacy of the device calibration strategy: exercises performed with fingers movements such as thumb abduction and pinch, revealed degrees of difficulty that were comparable with wrist movements. Therapies administered were highly patient-tailored, showing that the device satisfied this aspect of the therapy-related criteria requested for technological

solutions. The system should be integrated with a tool for EMG post-processing. Results of the analysis on patient motor patterns could be additional parameters included in performance reports. From this perspective, Chapter 6 investigated the aspects related to the analysis of continuous motions of the wrist and highlighted the relevance of the temporal information in the interpretation of this type of movements.

Summarizing, the present thesis evolved from a research environment to a clinical context, through a productive collaboration with the therapists and patients and through the starting of a clinical trial. The tested device is one of the first technologies that shows both a level of comfortability as high as commercial devices and the technical characteristics requested for an effective EMG analysis, even on finger movements. Moreover, an efficient approach for the analysis of continuous movements performed during the therapy has been identified.

A comprehensive data analysis will be done when the trial will be concluded, and results will be used for further improvements of the system and to plan a randomized control study. From a broader perspective, the EMG-BF device could be tested in other motor rehabilitation fields (e.g. orthopedic rehabilitation) and in telerehabilitation applications.

8 References

[1] M. Nordin and H. V. Frankel, *Basic Biomechanics of the Muscoloskeletal System*, 3th ed. 2001.

[2] R. M. Enoka, "Neuromechanics of human movement," *Human Kinetics*, vol. 4th Editio, no. Book, Whole. p. 549, 2008.

[3] E. R. Kandel, J. H. Schwartz, and T. M. Jessell, *Principles of Neural Science*, 4th ed. The McGraw-Hill Companies, 2000.

[4] A. F. Huxley and R. Niedergerke, "Structural changes in muscle during contraction; interference microscopy of living muscle fibres," *Nature*, vol. 173, no. 4412, pp. 971–973, 1954.

[5] B. Katz, "The Electrical Properties of the Muscle Fibre Membrane," *Proc. R. Soc. B Biol. Sci.*, vol. 135, no. 881, pp. 506–534, 1948.

[6] D. Dumitru, *Electrodiagnostic medicine*. Hanley and Belfus, 1995.

[7] H. Lodish, A. Berk, S. L. Zipursky, P. Matsudaira, D. Baltimore, and J. Darnell, "Molecular Properties of Voltage-Gated Ion Channels," in *Molecular Cell Biology*, 4th ed., W. H. Freeman, Ed. New York, 2000.

[8] H. Lodish, A. Berk, S. L. Zipursky, P. Matsudaira, D. Baltimore, and J. Darnell, "The Action Potential and Conduction of Electric Impulses," in *Molecular Cell Biology*, 4th ed., W. H. Freeman, Ed. New York, 2000.

[9] R. Merletti and P. (Philip A. . Parker, *Electromyography : physiology, engineering, [1] Merletti R, Parker P (Philip A. Electromyography : physiology, engineering, and noninvasive applications. 2004.and noninvasive applications*. 2004.

[10] M. Graziano, "the Organization of Behavioral Repertoire in Motor Cortex," *Annu. Rev. Neurosci.*, vol. 29, no. 1, pp. 105–134, 2006.

[11] J. Donoghue and J. Sanes, "Motor areas of the cerebral cortex," *J. Clin. Neurohysiology*, 1994.

[12] C. Sherrington, *The Integrative Action of the Nervous System*. New Haven: Yale Univ. Press, 1906.

[13] K. W. Horch and D. Gurpreet, Eds., *Neuroprosthetics-Theory and Practice (Series on Bioengineering & Biomedical Engineering - Vol. 2)*. World Scientific Publishing Company, 2004.

[14] C. N. Prudente, R. Stilla, C. M. Buetefisch, S. Singh, E. J. Hess, X. Hu, K. Sathian, and H. A. Jinnah, “Neural Substrates for Head Movements in Humans: A Functional Magnetic Resonance Imaging Study,” *J. Neurosci.*, vol. 35, no. 24, pp. 9163–9172, 2015.

[15] W. Penfield and T. Rasmussen, “The Cerebral Cortex of Man. A Clinical Study of Localization of Function.pdf,” *Academic Medicine*, vol. 25. p. 375, 1950.

[16] K. Barrett, H. Brooks, S. Boitano, S. Barman, and G. D. Schott, “Penfield’s homunculus: a note on cerebral cartography.,” *Ganong’s Rev. Med. Physiol.*, vol. 56, no. 4, pp. 329–333, 1993.

[17] E. Henneman, G. Somjen, and D. O. Carpenter, “Functional significance of cell size in spinal motoneurons,” *J. Neurophysiol.*, vol. 28, 1965.

[18] L. Stark, “A Linear Stochastic Model of the Single Motor Unit,” *Biol. Cybern.*, vol. 18, 1982.

[19] C. J. de Luca, R. S. LeFever, M. P. McCue, and A. P. Xenakis, “Behaviour of human motor units in different muscles during linearly varying contractions,” *J. Physiol.*, vol. 329, pp. 113–128, 1982.

[20] J. Moore, G. Zouridakis, and F. Kreith, *BIOMEDICAL TECHNOLOGY and DEVICES*. CRC PRESS, 2004.

[21] J. Basmajian and C. J. De Luca, “Description and Analysis of the EMG Signal,” *Muscles alive their Funct. Reveal. by Electromyogr.*, pp. 65–100, 1985.

[22] G. Birò and L. Partridge, “Analysis of multiunit spike records.,” *J Appl Physiol. .*, vol. 30, no. 4, pp. 521–6, 1971.

[23] C. J. De Luca and E. J. van Dyk, “Derivation of some parameters of myoelectric signals recorded during sustained constant force isometric contractions,” *Biophys. J.*, vol. 15, no. 12, pp. 1167–1180, 1975.

[24] M. B. I. Reaz, M. S. Hussain, and F. Mohd-Yasin, “Techniques of EMG signal analysis: detection, processing, classification and applications (Correction),” *Biol. Proced. Online*, vol. 8, no. 1, pp. 163–163, 2006.

[25] B. Y. D. E. Goldman, “IN MEMBRANES (From the Department of] Physiology , College of Physicians and Surgeons , Columbia University , New York),” pp. 37–60, 1943.

[26] M. R. Neuman, *Medical Instrumentation*. Webster, J.G., 1978.

[27] J. Y. Baek, J. H. An, J. M. Choi, K. S. Park, and S. H. Lee, “Flexible polymeric dry electrodes for the long-term monitoring of ECG,” *Sensors Actuators, A Phys.*, vol. 143, no. 2, pp. 423–429, 2008.

[28] C. Gondran, E. Siebert, P. Fabry, E. Novakov, and P. Y. Gumery, “Non-polarisable dry electrode

based on NASICON ceramic," *Med. Biol. Eng. Comput.*, vol. 33, no. 3, pp. 452–457, 1995.

[29] R. Merletti and P. J. Parker, *Electromyography: Physiology, Engineering, and Non-Invasive Applications*. 2004.

[30] S. Blok, J., J. van Asselt, V. Dijk, and D. Stegeman, "On an optimal pastless electrode to skin interface in surface EMG," in *The state of the art on sensors and sensor placement procedures for surface electromyography: A proposal for sensor placement procedures*, Enschede: Roessingh Research and development, 1997, pp. 71–76.

[31] D. Farina, N. Jiang, H. Rehbaum, A. Holobar, B. Graimann, H. Dietl, and O. C. Aszmann, "The extraction of neural information from the surface EMG for the control of upper-limb prostheses: Emerging avenues and challenges," *IEEE Trans. Neural Syst. Rehabil. Eng.*, vol. 22, no. 4, pp. 797–809, 2014.

[32] A. Stango, F. Negro, and D. Farina, "Spatial Correlation of High Density EMG Signals Provides Features Robust to Electrode Number and Shift in Pattern Recognition for Myocontrol," *IEEE Trans. Neural Syst. Rehabil. Eng.*, vol. 23, no. 2, pp. 189–198, 2015.

[33] Y. Geng, X. Zhang, Y.-T. Zhang, and G. Li, "A novel channel selection method for multiple motion classification using high-density electromyography.," *Biomed. Eng. Online*, vol. 13, no. 1, p. 102, 2014.

[34] Z. Fu, A. Y. Bani Hashim, Z. Jamaludin, and I. S. Mohamad, "Design of a low cost EMG amplifier with discreet op-amps for machine control," *ARPN J. Eng. Appl. Sci.*, vol. 11, no. 5, pp. 3345–3349, 2016.

[35] M. M. Shobaki, N. A. Malik, S. Khan, A. Nurashikin, S. Haider, S. Larbani, A. Arshad, and R. Tasnim, "High Quality Acquisition of Surface Electromyography – Conditioning Circuit Design," *IOP Conf. Ser. Mater. Sci. Eng.*, vol. 53, p. 12027, 2013.

[36] A. C. Metting van Rijn, A. Peper, and C. A. Grimbergen, "High-quality recording of bioelectric events - Part 1 Interference reduction, theory and practice," *Medical & Biological Engineering & Computing*, vol. 28, no. 5. pp. 389–397, 1990.

[37] F. N. Guerrero, E. M. Spinelli, and M. A. Haberman, "Analysis and Simple Circuit Design of Double Differential EMG Active Electrode," *IEEE Trans. Biomed. Circuits Syst.*, vol. 10, no. 3, pp. 787–795, 2016.

[38] C. Levkov, G. Mihov, R. Ivanov, I. Daskalov, I. Christov, and I. Dotsinsky, "Removal of power-line

interference from the ECG: a review of the subtraction procedure," *Biomed. Eng. Online*, vol. 4, no. 1, p. 50, 2005.

[39] M. Golabbakhsh, "ECG and power line noise removal from respiratory EMG signal using adaptive filters," *Majlesi J. Electr. …*, vol. 5, no. 4, pp. 28–33, 2011.

[40] D. T. Mewett, H. Nazeran, and K. J. Reynolds, "Removing power line noise from recorded EMG," *Annu. Reports Res. React. Institute, Kyoto Univ.*, vol. 3, pp. 2190–2193, 2001.

[41] R. L. Sacco, S. E. Kasner, J. P. Broderick, L. R. Caplan, J. J. Connors, A. Culebras, M. S. V Elkind, M. G. George, A. D. Hamdan, R. T. Higashida, B. L. Hoh, L. S. Janis, C. S. Kase, D. O. Kleindorfer, J. M. Lee, M. E. Moseley, E. D. Peterson, T. N. Turan, A. L. Valderrama, and H. V. Vinters, "An updated definition of stroke for the 21st century: A statement for healthcare professionals from the American heart association/American stroke association," *Stroke*, vol. 44, no. 7, pp. 2064–2089, 2013.

[42] Y. Béjot, H. Bailly, J. Durier, and M. Giroud, "Epidemiology of stroke in Europe and trends for the 21st century," *Press. Medicale*, vol. 45, no. 12, pp. e391–e398, 2016.

[43] S. S. Rathore, A. R. Hinn, L. S. Cooper, H. A. Tyroler, and W. D. Rosamond, "Characterization of incident stroke signs and symptoms findings from the atherosclerosis risk in communities study," *Stroke*, vol. 33, no. 11, pp. 2718–2721, 2002.

[44] A. P. Sangole and M. F. Levin, "A new perspective in the understanding of hand dysfunction following neurological injury.," *Top. Stroke Rehabil.*, vol. 14, no. 3, pp. 80–94, 2007.

[45] R. S. Johansson and J. R. Flanagan, "Coding and use of tactile signals from the fingertips in object manipulation tasks.," *Nat. Rev. Neurosci.*, vol. 10, no. 5, pp. 345–59, 2009.

[46] World Health Organization, "Towards a Common Language for Functioning , Disability and Health ICF," *Int. Classif.*, vol. 1149, pp. 1–22, 2002.

[47] M. H. Rabadi, "Review of the randomized clinical stroke rehabilitation trials in 2009.," *Med. Sci. Monit.*, vol. 17, no. 2, p. RA25-43, 2011.

[48] Y. Hara, "Brain Plasticity and Rehabilitation in Stroke Patients," *J. Nippon Med. Sch.*, vol. 82, no. 1, pp. 4–13, 2015.

[49] S. H. Jang, "Motor function-related maladaptive plasticity in stroke: A review," *NeuroRehabilitation*, vol. 32, no. 2, pp. 311–316, 2013.

[50] J. W. Krakauer, "Motor learning: its relevance to stroke recovery and neurorehabilitation.,"

Curr. Opin. Neurol., vol. 19, no. 1, pp. 84–90, 2006.

[51] T. H. Murphy and D. Corbett, “Plasticity during stroke recovery: from synapse to behaviour,” *Nat. Rev. Neurosci.*, vol. 10, no. 12, pp. 861–872, 2009.

[52] S. M. Hatem, G. Saussez, M. Della Faille, V. Prist, X. Zhang, D. Dispa, and Y. Bleyenheuft, “Rehabilitation of Motor Function after Stroke: A Multiple Systematic Review Focused on Techniques to Stimulate Upper Extremity Recovery.,” *Front. Hum. Neurosci.*, vol. 10, no. September, p. 442, 2016.

[53] F. M. Ivey, S. J. Prior, C. E. Hafer-macko, L. I. Katzel, R. F. Macko, and A. S. Ryan, “Strength Training for Skeletal Muscle Endurance after Stroke,” *J. Stroke Cerebrovasc. Dis.*, no. 18, pp. 1–8, 2016.

[54] C. Patten, J. Lexell, and H. E. Brown, “Weakness and strength training in persons with poststroke hemiplegia: rationale, method, and efficacy.,” *J. Rehabil. Res. Dev.*, vol. 41, no. 3A, pp. 293–312, 2004.

[55] S. P. Swinnen, N. Dounskaia, and J. Duysens, “Patterns of bimanual interference reveal movement encoding within a radial egocentric reference frame.,” *J. Cogn. Neurosci.*, vol. 14, no. 3, pp. 463–471, 2002.

[56] G. F. Wittenberg, R. Chen, K. Ishii, K. O. Bushara, E. Taub, L. H. Gerber, M. Hallett, and L. G. Cohen, “Constraint-Induced Therapy in Stroke: Magnetic-Stimulation Motor Maps and Cerebral Activation,” *Neurorehabil. Neural Repair*, vol. 17, no. 1, pp. 48–57, 2003.

[57] J. D. Schaechter, “Motor rehabilitation and brain plasticity after hemiparetic stroke,” *Prog. Neurobiol.*, vol. 73, no. 1, pp. 61–72, 2004.

[58] G. Kwakkel, J. M. Veerbeek, E. E. H. Van Wegen, and S. L. Wolf, “Constraint-induced movement therapy after stroke,” *Lancet Neurol.*, vol. 14, no. 2, pp. 224–234, 2015.

[59] S. L. Small, G. Buccino, and A. Solodkin, “The mirror neuron system and treatment of stroke,” *Dev. Psychobiol.*, vol. 54, no. 3, pp. 293–310, 2012.

[60] M. P. Veldman, N. A. Maffiuletti, M. Hallett, I. Zijdewind, and T. Hortobágyi, “Direct and crossed effects of somatosensory stimulation on neuronal excitability and motor performance in humans,” *Neurosci. Biobehav. Rev.*, vol. 47, pp. 22–35, 2014.

[61] O. Schuhfried, R. Crevenna, V. Fialka-Moser, and T. Paternostro-Sluga, “Non-invasive neuromuscular electrical stimulation in patients with central nervous system lesions: An

educational review," *J. Rehabil. Med.*, vol. 44, no. 2, pp. 99–105, 2012.

[62] F. C. Hummel and L. G. Cohen, "Non-invasive brain stimulation: a new strategy to improve neurorehabilitation after stroke?," *Lancet Neurol.*, vol. 5, no. 8, pp. 708–712, 2006.

[63] C. Kuo and G. Hu, "Post-stroke Spasticity: A Review of Epidemiology, Pathophysiology and Treatments," *Int. J. Gerontol.*, vol. 12, no. 4, pp. 280–284, 2018.

[64] H. I. Berends, J. M. Nijlant, K. L. Movig, M. J. Van Putten, M. J. Jannink, and M. J. Ijzerman, "The clinical use of drugs influencing neurotransmitters in the brain to promote motor recovery after stroke; a cochrane systematic review.," *Eur.J.Phys.Rehabil.Med.*, vol. 45, 2009.

[65] K. H. Cho and W. Song, "Robot-Assisted Reach Training for Improving Upper Extremity Function of Chronic Stroke," pp. 149–155, 2015.

[66] A. a a Timmermans, A. I. F. Spooren, H. Kingma, and H. a M. Seelen, "Influence of task-oriented training content on skilled arm-hand performance in stroke: A systematic review.," *Neurorehabil. Neural Repair*, vol. 24, pp. 858–870, 2010.

[67] R. P. S. van Peppen, G. Kwakkel, S. Wood-Dauphinee, H. J. M. Hendriks, P. J. van der Wees, and J. Dekker, "The impact of physical therapy on functional outcomes after stroke: What's the evidence?," *Clin. Rehabiliitation*, vol. 18, no. 8, pp. 833–862, 2004.

[68] L. Legg, P. Langhorne, P. Duncan, A. Gershkoff, L. Glasmann, E. Hui, J. L, J. Leonardi-Bee, P. Logan, T. Meade, R. de Vet, J. Stoker-Yates, K. Tilling, M. Walker, and C. Wolfe, "Rehabilitation therapy services for stroke patients living at home: systematic review of randomised trials," *Lancet*, vol. 363, no. 9406, pp. 352–356, 2004.

[69] L. Brewer R., Bambi; McDowell K., Sharon; W orthen-Chaudlrai C., "Poststroke Upper Extremity Rehabilitation: A Review of Robotic Systems and Clinical Results.," *Top Stroke Rehabil.*, vol. 14, no. 6, pp. 22–44, 2007.

[70] K. R. Lohse, C. G. E. Hilderman, K. L. Cheung, S. Tatla, and H. F. M. Van Der Loos, "Virtual reality therapy for adults post-stroke: A systematic review and meta-analysis exploring virtual environments and commercial games in therapy," *PLoS One*, vol. 9, no. 3, 2014.

[71] K. Brütsch, T. Schuler, A. Koenig, L. Zimmerli, S. (-Koeneke), L. Lünenburger, R. Riener, L. Jäncke, and A. Meyer-Heim, "Influence of virtual reality soccer game on walking performance in robotic assisted gait training for children," *J. Neuroeng. Rehabil.*, vol. 7, no. 1, p. 15, 2010.

[72] S. R. Wood, N. Murillo, P. Bach-y-Rita, R. S. Leder, J. T. Marks, and S. J. Page, "Motivating,

Game-Based Stroke Rehabilitation: A Brief Report," *Top. Stroke Rehabil.*, vol. 10, no. 2, pp. 134–140, 2003.

[73] M. J. Fu, J. Knutson, J. Chae, and C. Science, "HHS Public Access," vol. 26, no. 4, pp. 747–757, 2016.

[74] M. Kamkarhaghighi, P. Mirza-babaei, and K. El-Khatib, "Game-Based Stroke Rehabilitation," in *Recent Advances in Technologies for Inclusive Well-Being*, Springer, Ed. 2017, pp. 147–162.

[75] R. Magill, *Motor learning and control: Concepts and applications*, 7th ed. New York: McGraw-Hill, 2003.

[76] D. Sharma, M. F. Ck, F. Khan, and R. A. Gaowgzeh, "Effectiveness of knowledge of result and knowledge of performance in the learning of a skilled motor activity by healthy young adults," no. May, 2016.

[77] D. Sharma, "Knowledge of Result Versus Knowledge of Performance in Learning Motor Skilled Activity for Upper Limb in Recovery Stage of Stroke – A Randomized Experimental Study Randomized Experimental Study," no. September, pp. 3–6, 2016.

[78] A. a a Timmermans, H. a M. Seelen, R. D. Willmann, and H. Kingma, "Technology-assisted training of arm-hand skills in stroke: concepts on reacquisition of motor control and therapist guidelines for rehabilitation technology design.," *J. Neuroeng. Rehabil.*, vol. 6, no. figure 1, p. 1, 2009.

[79] O. M. Giggins, U. M. Persson, and B. Caulfield, "Biofeedback in rehabilitation.," *J. Neuroeng. Rehabil.*, vol. 10, no. 1, p. 60, 2013.

[80] M. Dozza, L. Chiari, and F. B. Horak, "Audio-biofeedback improves balance in patients with bilateral vestibular loss," *Arch. Phys. Med. Rehabil.*, vol. 86, no. 7, pp. 1401–1403, 2005.

[81] P. P. Breen, A. Nisar, and G. Ólaighin, "Evaluation of a single accelerometer based biofeedback system for real-time correction of neck posture in computer users," *Proc. 31st Annu. Int. Conf. IEEE Eng. Med. Biol. Soc. Eng. Futur. Biomed. EMBC 2009*, pp. 7269–7272, 2009.

[82] J. R. Davis, M. G. Carpenter, R. Tschanz, S. Meyes, D. Debrunner, J. Burger, and J. H. J. Allum, "Trunk sway reductions in young and older adults using multi-modal biofeedback," *Gait Posture*, vol. 31, no. 4, pp. 465–472, 2010.

[83] L. L. Verhoeff, C. G. C. Horlings, L. J. F. Janssen, S. A. Bridenbaugh, and J. H. J. Allum, "Effects of biofeedback on trunk sway during dual tasking in the healthy young and elderly," *Gait Posture*,

vol. 30, no. 1, pp. 76–81, 2009.

[84] T. A. Kuiken, H. Amir, and R. A. Scheidt, “Computerized biofeedback knee goniometer: Acceptance and effect on exercise behavior in post-total knee arthroplasty rehabilitation,” *Arch. Phys. Med. Rehabil.*, vol. 85, no. 6, pp. 1026–1030, 2004.

[85] B. Kim, W. Gong, and S. Lee, “The Effect of Push-up Plus Exercise with Visual Biofeedback on The Activity of Shoulder Stabilizer Muscles for Winged Scapula,” *J. Phys. Ther. Sci.*, vol. 22, no. 4, pp. 355–358, 2010.

[86] S. E. Sihvonen, S. Sipilä, and P. A. Era, “Changes in Postural Balance in Frail Elderly Women during a 4-Week Visual Feedback Training: A Randomized Controlled Trial,” *Gerontology*, vol. 50, no. 2, pp. 87–95, 2004.

[87] V. Hatzitaki, I. G. Amiridis, T. Nikodelis, and S. Spiliopoulou, “Direction-induced effects of visually guided weight-shifting training on standing balance in the elderly,” *Gerontology*, vol. 55, no. 2, pp. 145–152, 2009.

[88] J. Moreland and M. a Thomson, “Efficacy of electromyographic biofeedback compared with conventional physical therapy for upper-extremity function in patients following stroke: a research overview and meta-analysis.,” *Phys. Ther.*, vol. 74, no. 6, pp. 534-43–7, 1994.

[89] L. Bradley, P. Services, B. B. Hart, S. Mandana, and S. General, “Electromyographic biofeedback for gait training after stro k e,” *Clin. Rehabil.*, vol. 12, no. 98, pp. 11–22, 1998.

[90] J. L. Crow, N. B. LINCOLN, N. F.M., and de W. W., “The effectiveness of EMG biofeedback in the treatment of arm function after stroke,” *J. Advert. Res.*, vol. 11, 1989.

[91] S. L. Wolf and S. A. Binder-MacLeod, “Electromyographic biofeedback applications to the hemiplegic patient. Changes in lower extremity neuromuscular and functional status.,” *Phys. Ther.*, vol. 63, no. 9, pp. 1404–13, 1983.

[92] Y. M. J. Inglis J., Donald M.W., Monga T.N., Sproule M., “Electromyographic biofeedback and physical therapy of the hemiplegic upper limb,” *Arch Phys Med Rehabil*, vol. 65, 1984.

[93] van der M. J. Mulder T., Hulstijn W., “EMG feedback and the restoration of motor control. A controlled group study of 12 hemiparetic,” *Am J Phys Med*, vol. 65, 1986.

[94] B.-M. S. A. Wolf S.L., “Electromyographic biofeedback applications to the hemiplegic patient. Changes in upper extremity neuromuscular and functional status,” *Phys Ther*, vol. 63, 1983.

[95] B. D. Burnside I.G., Tobias H.S., “Electromyographic feedback in the remobilization of stroke

patients: a controlled trial.," *Arch Phys Med Rehabil*, vol. 63, 1982.

[96] S. L. Wolf and S. A. Binder-MacLeod, "Electromyographic biofeedback applications to the hemiplegic patient. Changes in lower extremity neuromuscular and functional status.," *Phys. Ther.*, vol. 63, 1983.

[97] N. C. Hurd W.W., Pegram V., "Comparison of actual and simulated EMG biofeedback in the treatment of hemiplegic patients," *Am J Phys Med*, vol. 59, 1980.

[98] T. K. Basmajian JV, Kukulka CG, Narayan MG, "Biofeedback treatment of foot-drop after stroke compared with standard rehabilitation technique: effects on voluntary control and strength," *Arch Phys Med Rehabil*, vol. 56, 1975.

[99] H. S. L. Cozean C.D., Pease W.S., "Biofeedback and functional electric stimulation in stroke rehabilitation.," *Arch Phys Med Rehabil*, vol. 69, 1988.

[100] JU-HONG KIM, "The effects of training using EMG biofeedback on stroke patients upper extremity functions," *J. Phys. Ther. Sci.*, pp. 1085–1088, 2017.

[101] Bhs. A. Julie D. Moreland, MSc, Mary Ann Thomson, MSc, Angela R. FUOCO, "Electromyographic biofeedback to improve lower extremity function after stroke: a meta-analysis," *Arch Phys Med Rehabil*, vol. 79, no. 2, pp. 134–140, 1992.

[102] H. D. Kimmel, "The Relevance of Experimental Studies to Clinical Applications of Biofeedback t," vol. 6, no. 2, pp. 263–271, 1981.

[103] P. Parker, K. Englehart, and B. Hudgins, "Myoelectric signal processing for control of powered limb prostheses," *J. Electromyogr. Kinesiol.*, vol. 16, pp. 541–548, 2006.

[104] K. M. Sibley, A. Tang, D. Brooks, D. a Brown, and W. E. McIlroy, "Feasibility of adapted aerobic cycle ergometry tasks to encourage paretic limb use after stroke: a case series.," *J. Neurol. Phys. Ther.*, vol. 32, no. 2, pp. 80–7, 2008.

[105] D. Barbosa, C. P. Santos, and M. Martins, "The Application of Cycling and Cycling Combined with Feedback in the Rehabilitation of Stroke Patients : A Review," *J. Stroke Cerebrovasc. Dis.*, vol. 24, no. 2, pp. 253–273, 2015.

[106] J. Jonsdottir, D. Cattaneo, M. Recalcati, A. Regola, M. Rabuffetti, M. Ferrarin, and A. Casiraghi, "Task-Oriented Biofeedback to Improve Gait in Individuals With Chronic Stroke: Motor Learning Approach," *Neurorehabil. Neural Repair*, vol. 24, no. 5, pp. 478–485, 2010.

[107] R. I. G. Inal, N. S. Unit, M. Education, N. S. Program, and M. Education, "O RIG INAL R ES E A R C

H Neuropediatrics postgraduate students ’ learning process through hidden curriculum at Universidad Nacional de Colombia,” vol. 64, no. 3, pp. 453–458, 2016.

[108] A. Pascual-Leone, “NIH Public Access,” *IEEE Trans Neural Syst Rehabil Eng*, vol. 13, no. 3, pp. 325–334, 2005.

[109] P. Lum, D. Reinkensmeyer, R. Mahoney, W. Z. Rymer, and C. Burgar, “and Challenges to Clinical Acceptance,” vol. 8, no. 4, pp. 40–53, 2002.

[110] A. Hochstenbach-Waelen and H. a M. Seelen, “Embracing change: practical and theoretical considerations for successful implementation of technology assisting upper limb training in stroke.,” *J. Neuroeng. Rehabil.*, vol. 9, no. 1, p. 52, 2012.

[111] L. E. Kahn, M. L. Zygman, W. Z. Rymer, and D. J. Reinkensmeyer, “Robot-assisted reaching exercise promotes arm movement recovery in chronic hemiparetic stroke: a randomized controlled pilot study.,” *J. Neuroeng. Rehabil.*, vol. 3, p. 12, 2006.

[112] M. Saif, “World Medical Association Declaration of Helsinki: ethical principles for medical research involving human subjects.” 2000.

[113] S. Muceli, N. Jiang, and D. Farina, “Extracting signals robust to electrode number and shift for online simultaneous and proportional myoelectric control by factorization algorithms,” *IEEE Trans. Neural Syst. Rehabil. Eng.*, vol. 22, no. 3, pp. 623–633, 2014.

[114] G. Li, A. E. Schultz, and T. A. Kuiken, “Quantifying pattern recognition- based myoelectric control of multifunctional transradial prostheses,” *IEEE Trans. Neural Syst. Rehabil. Eng.*, vol. 18, no. 2, pp. 185–192, 2010.

[115] A. J. Young, L. J. Hargrove, and T. A. Kuiken, “Improving myoelectric pattern recognition robustness to electrode shift by changing interelectrode distance and electrode configuration,” *IEEE Trans. Biomed. Eng.*, vol. 59, no. 3, pp. 645–652, 2012.

[116] K. Nagata, K. Ando, S. Nakano, H. Nakajima, M. Yamada, and K. Magatani, “Development of the human interface equipment based on surface EMG employing channel selection method.,” in *Conference proceedings : ... Annual International Conference of the IEEE Engineering in Medicine and Biology Society. IEEE Engineering in Medicine and Biology Society. Conference*, 2006, vol. 1, pp. 6193–6196.

[117] R. Menon, G. Di Caterina, H. Lakany, L. Petropoulakis, B. Conway, and J. Soraghan, “Study on interaction between temporal and spatial information in classification of EMG signals in

myoelectric prostheses," *IEEE Trans. Neural Syst. Rehabil. Eng.*, vol. 4320, no. c, pp. 1–1, 2017.

[118] K. L. Moore, A. F. Dalley, and A. M. R. Agur, *Upper Limb - Clinically Oriented Anatomy*, 6th ed. Philadelphia, 2010.

[119] D. Farina, R. Merletti, and R. M. Enoka, "The extraction of neural strategies from the surface EMG: an update," *J. Appl. Physiol.*, vol. 117, no. 11, pp. 1215–1230, 2014.

[120] A. Fugl-Meyer, L. Jääskö, I. Leyman, S. Olsson, and S. Steglind, "The post-stroke hemiplegic patient. A method for evaluation of physical performance.," *Scand J Rehabil Med.*, vol. 7, no. 1, pp. 13–31, 1975.

[121] B. R. and M. Smith, "Interrater reliability of a modified ashworth scale of muscle spasticity," *Phys. Ther.*, vol. 67, no. 2, pp. 206–207, 1987.

[122] A. Thibaut, C. Chatelle, E. Ziegler, M.-A. Bruno, S. Laureys, and O. Gosseries, "Spasticity after stroke: Physiology, assessment and treatment," *Brain Inj.*, vol. 27, no. 10, pp. 1093–1105, 2013.

[123] M. F. Levin, J. Desrosiers, D. Beauchemin, N. Bergeron, and A. Rochette, "Development and Validation of a Compensations Used for Reaching in Patients With Hemiparesis :," *Phys Ther*, vol. 84, no. 1, pp. 8–22, 2004.

[124] V. Mathiowetz, G. Volland, N. Kashman, and K. Weber, "Adult norms for the box and block test of manual dexterity.," *Am. J. Occup. Ther.*, vol. 39, no. 6, pp. 386–391, 1985.

[125] R. Bohannon and M. Smith, "Interrater reliability of a modified ashworth scale of muscle spasticity.," *Phys. Ther.*, vol. 67, no. 2, pp. 206–207, 1987.

[126] S. J. Page, G. D. Fulk, and P. Boyne, "Clinically Important Differences for the Upper-Extremity Fugl-Meyer Scale in People With Minimal to Moderate Impairment Due to Chronic Stroke," *Phys. Ther.*, vol. 92, no. 6, pp. 791–798, 2012.

[127] H. Huang, S. L. Wolf, and J. He, "Recent developments in biofeedback for neuromotor rehabilitation.," *J. Neuroeng. Rehabil.*, vol. 3, no. 1, p. 11, 2006.

[128] C. Bütefisch, H. Hummelsheim, P. Denzler, and K. H. Mauritz, "Repetitive training of isolated movements improves the outcome of motor rehabilitation of the centrally paretic hand," *J. Neurol. Sci.*, vol. 130, no. 1, pp. 59–68, 1995.

[129] A. J. Butler, "REPETITIVE TASK PRACTICE: A CRITICAL REVIEW OF CONSTRAIN," vol. 8, no. 6, pp. 325–338, 2013.

[130] G. Kwakkel, R. C. Wagenaar, J. W. R. Twisk, G. J. Lankhorst, and J. C. Koetsier, "Intensity of leg

and arm training after primary middle cerebral artery stroke: a randomised trial," *Lancet*, vol. 354, pp. 191–196, 1999.

[131] K. Laver, S. George, S. Thomas, J. Deutsch, and M. Crotty, "Cochrane review: virtual reality for stroke rehabilitation.," *Eur J Phys Rehabil Med.*, vol. 48, no. 3, pp. 523–30, 2012.

[132] K. Laver, S. George, S. Thomas, J. E. Deutsch, and M. Crotty, "Virtual Reality for Stroke Rehabilitation," *Cochrane Collab.*, no. 2, pp. 1–110, 2015.

[133] G. Gensini, A. Carolei, S. Ricci, T. Mazzoli, C. Padiglioni, L. Patoia, S. Quaglini, and G. Reboldi, *SPREAD – Stroke Prevention and Educational Awareness Diffusion Ictus cerebrale: Linee guida italiane di prevenzione e trattamento*, 8th ed. 2016.

[134] S. F. Keith RA, Granger CV, Hamilton BB, "The functional independence measure: a new tool for rehabilitation.," *Adv Clin Rehabil.*, vol. 1, pp. 6–18, 1987.

[135] B. Röhrig, J.-B. du Prel, D. Wachtlin, R. Kwiecien, and M. Blettner, "Fallzahlplanung in klinischen Studien," *Dtsch Arztebl Int*, vol. 107, no. 31–32, pp. 552–556, 2010.

[136] P. Sale, S. Mazzoleni, V. Lombardi, D. Galafate, M. P. Massimiani, F. Posteraro, C. Damiani, and M. Franceschini, "Recovery of hand function with robot-assisted therapy in acute stroke patients," *Int. J. Rehabil. Res.*, vol. 37, no. 3, pp. 236–242, 2014.

[137] A. Turolla, M. Dam, L. Ventura, P. Tonin, M. Agostini, C. Zucconi, P. Kiper, A. Cagnin, and L. Piron, "Virtual reality for the rehabilitation of the upper limb motor function after stroke: a prospective controlled trial," *J. Neuroeng. Rehabil.*, vol. 10, no. 1, p. 85, 2013.

[138] A. Vukomanovic, A. Djurovic, and Z. Brdareski, "Diagnostic accuracy of the A-test and cutoff points for assessing outcomes and planning acute and post-acute rehabilitation of patients surgically treated for hip fractures and osteoarthritis," *Vojnosanit. Pregl.*, vol. 73, no. 12, pp. 1139–1148, 2016.

[139] V. C. K. Cheung, L. Piron, M. Agostini, S. Silvoni, A. Turolla, and E. Bizzi, "Stability of muscle synergies for voluntary actions after cortical stroke in humans," *Proc. Natl. Acad. Sci.*, vol. 106, no. 46, pp. 19563–19568, 2009.

[140] J. Roh, W. Z. Rymer, E. J. Perreault, S. B. Yoo, and R. F. Beer, "Alterations in upper limb muscle synergy structure in chronic stroke survivors," *J. Neurophysiol.*, vol. 109, no. 3, pp. 768–781, 2013.

[141] S. S. Fitts, M. C. Hammond, G. H. Kraft, and P. B. Nutter, "Quantification of gaps in the EMG

interference pattern in chronic hemiparesis," *Electroencephalogr. Clin. Neurophysiol.*, vol. 73, no. 3, pp. 225–232, 1989.

[142] R. L. Hammond MC, Fitts SS, Kraft GH, Nutter PB, Trotter MJ, "Co-contraction in the hemiparetic forearm: quantitative EMG evaluation," *Arch Phys Med Rehabil*, vol. 69, pp. 348–351, 1988.

[143] J.-O. Dyer, E. Maupas, S. de Andrade Melo, D. Bourbonnais, and R. Forget, "Abnormal coactivation of knee and ankle extensors is related to changes in heteronymous spinal pathways after stroke," *J. Neuroeng. Rehabil.*, vol. 8, no. 1, p. 41, 2011.

[144] Y. Li, X. Zhang, Y. Gong, Y. Cheng, X. Gao, and X. Chen, "Motor function evaluation of hemiplegic upper-extremities using data fusion from wearable inertial and surface EMG sensors," *Sensors (Switzerland)*, vol. 17, no. 3, 2017.

[145] S. Li, C. Zhuang, C. M. Niu, Y. Bao, Q. Xie, and N. Lan, "Evaluation of functional correlation of task-specific muscle synergies with motor performance in patients poststroke," *Front. Neurol.*, vol. 8, no. JUL, 2017.

[146] P. M. Fitt, "THE INFORMATION CAPACITY OF THE HUMAN MOTOR," *J. Exp. Psychol.*, vol. 47, no. 6, 1954.

[147] I. S. Mackenzie, W. Bu, and F. Law, "EXTENDING FITTS ' LAW TO TWO-DIMENSIONAL TASKS," pp. 219–226, 1992.

[148] M. Di Girolamo, A. Favetto, M. Paleari, N. Celadon, and P. Ariano, "A comparison of sEMG temporal and spatial information in the analysis of continuous movements," *Informatics Med. Unlocked*, vol. 9, 2017.

[149] M. Flanders, "Temporal patterns of muscle activation for arm movements in three-dimensional space," *J. Neurosci.*, vol. 11, no. 9, pp. 2680–2693, 1991.

[150] M. D. Klein Breteler, K. J. Simura, and M. Flanders, "Timing of muscle activation in a hand movement sequence," *Cereb. Cortex*, vol. 17, no. 4, pp. 803–815, 2007.

[151] G. Huang, D. Zhang, X. Zheng, and X. Zhu, "An EMG-based handwriting recognition through dynamic time warping.," in *Conference proceedings : Annual International Conference of the IEEE Engineering in Medicine and Biology Society. IEEE Engineering in Medicine and Biology Society.*, 2010, pp. 4902–4905.

[152] M. Linderman, M. A. Lebedev, and J. S. Erlichman, "Recognition of Handwriting from

Electromyography," vol. 4, no. 8, pp. 2–9, 2009.